Molokai Fishpond Tidal Circulation Study

by

R.C. Ertekin [1], H. Sundararaghavan [2] and A.T.F.M. (Sander) van Stiphout[3]

Department of Ocean Engineering
School of Ocean and Earth Science and Technology
University of Hawaii at Manoa
2540 Dole Street, Holmes Hall 402
Honolulu, HI 96822

OE Report No.: UHMOE - 96203
Sea Grant Report No.: UNIHI-SEAGRANT-TR-96-03

August, 1996

Final Report submitted to the University of Hawaii Sea Grant College Program
Project No. NA36RG0507-R/EL-7PD, February - July, 1996.

[1]Professor and Principal Investigator
[2]Graduate Teaching Assistant and Ph.D. Student
[3]Graduate Research Assistant and Ph.D. Student

Table of Contents

Summary

Recently, there has been a growing interest in the restoration of Hawaiian fishponds, especially the ones along the southern coast of the island of Molokai. This project has two goals: (1) survey of potential sites for restoration and (2) study the circulation characteristics of a candidate fishpond to identify likely sources of poor circulation that lead to significant accumulation of silt in the fishpond. One of the fishponds, namely One Alii fishpond, currently being used by homesteaders, was surveyed to obtain the geometry and water depth in and out of the fishpond and the tidal elevations. These data were used in the numerical tidal-circulation simulations. Fishpond circulation was simulated numerically by solving the tidal equations in conjunction with a finite- element method. Computer codes are used for the hydrodynamic studies. In these studies, two models were investigated: i) One Alii fishpond with one makaha (sluice gate) and ii) One Alii fishpond with two makahas. The numerical simulations indicate that there is significant improvement in the fishpond circulation with two makahas. The methodology developed here can be used to study the circulation characteristics of any fishpond, however, a number of improvements must be made and also the method must be verified with direct observational data that need to be collected especially for the current structure within the fishpond. Once the verifications are done, it would be possible to apply the present numerical method to other fishponds and make recommendations on ways to reduce sediment accumulation which has been the cause of one of the stumbling blocks in the economic viability of fishponds.

Acknowledgement

This publication is funded in part by a grant/cooperative agreement from the National Oceanic and Atmospheric Administration, project #R/EL-7PD which is sponsored by the University of Hawaii Sea Grant College Program, SOEST, under Institutional Grant No. NA35TG0507 from NOAA office of Sea Grant, Department of Commerce. The views expressed herein are those of the authors and do not necessarily reflect the views of NOAA of any of its sub-agencies. Report No. UNIHI-SEAGRANT-TR-96-03. We are very grateful to Dr. Robert D. Howerton of Sea Grant Extension Service, for assisting us during our visits to Molokai. We are also very thankful to Mr. Dean N. Fujii, the Executive Director of the Molokai Community Development Corporation, for his help and sharing with us his knowledge and experience on fishponds. Thanks are also due to Mr. Pascal G.P. Ferier, a Ph.D Student in OE department, for his help during the second site visit, to Prof. L. Minerbi of Department of Urban and Regional Planning of UHM for providing several references of great importance, and to Mr. Craig Tasaka, Planning Program Manager of GIS, Office of the Governor, for providing us with the aerial photographs of the southern coast of Molokai. And finally, this project would not have been possible without the continued encouragement and enthusiasm of Drs. Chuck E. Helsley and Rose Pfund of the UH Sea Grant College Program who also reviewed and commented on an earlier version of this report.

Chapter 1

Introduction

Recently, there has been a growing interest in the restoration of Hawaiian fishponds, especially the ones along the southern coast of the island of Molokai. Most of the fishponds are not being utilized because of their poor conditions and the problems associated with obtaining permits, and also because the importance of the utilization of marine resources has not received much attention. Fishponds are unique to the Hawaiian Islands and thus they are very important national historical assets. But perhaps more importantly, they can be a significant source of food and, therefore, contribute to the economical well being of the Hawaiian people. This project is motivated by the possibility of the revitalization of the fishponds on the island of Molokai and, hopefully, will contribute to the future federal and state efforts by presenting a technique to simulate fishpond circulation by using numerical methods. Recommendations can then be made on the restoration of fishpond walls and sluice gates (or makaha in Hawaiian) to improve circulation within a given fishpond.

There have been very few studies on fishponds on the island of Molokai or other Hawaiian Islands. These few works include Summers (1971) and Minerbi et al. (1993) which concentrated mostly on the historical aspects of fishponds and their conditions, with recommendations for their restorations and uses and as such they are valuable references. However, no references in the literature could be found on the circulation characteristics of fishponds.

The circulation of a fishpond is very much dependent on the wall geometry and number of locations of the makahas. If the circulation is weak within the fishpond, water movement will not be sufficient to inhibit silt accumulation which in turn significantly reduces the efficiency of fishpond operations. In some cases, accumulation of silt has even lead to the abandonment of a fishpond because of the high cost of silt removal. Thus, the simulation of fishpond circulation, using numerical methods, can be a critical analytical tool in the

restoration of fishponds.

Two site visits were made to Molokai to determine the conditions of selected fishponds. These site visits and our observations are discussed in .

During the second site visit in April 1996, several measurements were made to gather data on water depth, tidal elevation and fishpond geometry of One Alii fishpond. These data were used in the numerical simulations that will be described in subsequent chapters of this report.

The hydrodynamic model used in the circulation simulations is described in Chapter 3. The model is based on continuity and momentum equations for a viscous fluid where the viscous effects are incorporated empirically through various coefficients. This is common in circulation studies. Furthermore, the governing equations of the problem are made such that the unknown velocity components are depth averaged. The theoretical model is completed by identifying the boundary conditions on the boundaries of the computational region which include the walls of the fishpond. Chapter 3 also includes a brief introduction to the numerical method used to solve the established initial-boundary-value problem, namely the finite-element method which utilizes the Galerkin method.

The finite-element method used in this study requires the generation of six-noded triangular elements to describe the computational region. The element or grid generation and the accuracy of the numerical techniques are discussed in Chapter 4. The results, conclusions and recommendations and references are given in Chapters 5, 6, and 7, respectively.

Chapter 2

Molokai site visits

1 Site visit of November 1, 1995

Drs. Fai Cheung, Cengiz Ertekin and Mark Merrifield of the OE department traveled to Molokai on November 1, 1995 to visit several fishponds. Dr. Robert D. Howerton, the Sea Grant agent for Maui County, was our host. He took us to six fishponds that are located on the southern coast of Molokai.

The fishponds we visited and their physical conditions, based on our limited inspection, are as follows (this section is based on Ertekin and Merrifield, 1995):

1) One Alii fishpond (also known as Alii fishpond):

This fishpond is sheltered by a wide fringing reef. It is being utilized; however, there are only a few users. The fishpond is owned by the state. According to Dr. Howerton, there are concerns about mangrove infestation, however, the complaints may not be justified since there are arguments for the benefits of the presence of mangrove around fishponds as a nursery for fish. The sluice gate should be strengthened and a new sluice gate may be needed to reduce sediment accumulation which appears to be a problem for this fishpond. There also are problems with obtaining water quality permits from DOH for the users. Currently, two fenced areas inside the fishpond are used to grow mullet. This fishpond is close to being operational in terms of overall structure, however, it appears that circulation within the fishpond is weak and that sedimentation would be an ongoing problem. This is site number 135 on the Molokai map given in Summers (1971). See Fig. 34 of the same reference for the geometry of this fishpond.

2) Kanoa fishpond:

This fishpond is site number 137 on the Molokai map of Summers (1971). It is a very large fishpond (50 acres) with a badly damaged wall, 872 m (2,860 ft) long. Trade wind conditions are very good resulting in desirable circulation inside the fishpond. There is no mangrove around the perimeter of the fishpond. Walls must be repaired and new sluice gates must be constructed. It appears that this fishpond is ideal for numerical and laboratory studies of environmental conditions inside the fishpond. The fishpond is inactive. Given the poor condition of the outer wall, this fishpond would be very expensive to reestablish.

3) Keawanui fishpond:

This is site number 163 on the Molokai map of Summers (1971). See also Figs. 1,45 and 48 of the same reference. This fishpond belongs to the Bishop Estate and is located near a school for troubled kids. It is in good condition but there is no activity. Federal funds have been secured by the state to build a hatchery near the school. It appears that Oceanic Institute may build the hatchery and operate it. This fishpond is inside a harbor, however, water quality appeared to be good. There may be an opportunity to cooperate with Bishop Estate to make this fishpond active after studying the conditions and restoring the wall and sluice gate if necessary (it was too distant to see details from our observation point). If the school is closed (this is under discussion) the buildings may be used for fishpond related activities. This appeared to be a good site for further studies.

4) Ualapue fishpond:

This is site number 185 on the Molokai map of Summers (1971). See also Fig. 45 of the same reference. This is a state-owned fishpond. This fishpond is active (1 or 2 fenced in fish pens) with several users. Poaching has been a problem around the area. The wall and the sluice gates were recently repaired by the state and are in excellent condition. There are hatchery tanks which have never been used and abandoned currently. This fishpond is an excellent candidate for a study. Sedimentation did not appear to be a major problem although the bottom must be surveyed. It is well exposed to the Trades. Wave action on the outer wall was minimal during our visit.

5) Kahinapohaku fishpond:

This is a privately owned fishpond. It is designated as a "demonstration fishpond" by the state because no circulation problems were apparent. Strong swell was present outside the fishpond. There are plans to restore it. It is easily accessible (next to the highway) but small (only 4 acres). Only foundation stones remain at present. Trash dumping is a problem here. The fishpond is inactive. Considerable work is required to restore the wall. See Fig. 67 of Summers (1971).

6) Nameless fishpond/trap:

This is site number 233 on the Molokai map of Summers (1971). It had been used as a fishtrap rather than a fishpond. Rocks are available nearby for easy repairs of the wall. Good circulation was observed inside the fishpond. This site is designated as a "demonstration fishpond" by the state. The fishpond is inactive. The wall is in bad shape and would have to be fortified to withstand moderate wave action.

This site visit resulted in the determination of a number of tasks to be done before a full fledged study of fishponds can be initiated. Some of these are:

- Obtain information on the availability of environmental data for Molokai: Tidal elevations, Wind statistics, Wave statistics Obtain information on seafloor bathymetry at the south coast of Molokai
- Determine: locations, sizes, wall, and sluice gate geometric data, sediment characteristics, physical conditions of fishponds on Molokai
- Determine social/cultural restrictions on the scope of such a study
- Contact the agencies in charge of the permit process to determine related problems
- Contact current users to determine what the real-life problems associated with fishponds are and identify potential users of the fishponds
- Study the circulation characteristics of one candidate fishpond using computer modeling in which sluice gate locations are varied

Note that most of the information given in this section is preliminary and must be confirmed by using other sources as necessary. This brief report is a result of a one day trip and most information was gathered during our discussions with Dr. R.D. Howerton.

The recent work of Farber (1996) addresses the permit related problems extensively and therefore, these problems will not be discussed in this study. The reader is referred to Farber (1996) for accounts of the fishpond restoration movement and obstacles to restoration, such as the high cost of obtaining the required ten (10) different permits from federal, state and county agencies. Kubato's (1996) article also sheds light into the red tape that stalls Molokai fishpond revival. Some other factors that have stalled the development of fishponds during the territorial and state government eras can be found in an earlier article of Kikuchi (1976).

2 Site visit of April 3-4, 1996

Sander van Stiphout and Pascal Ferier traveled to Molokai on April 3, 1996 to visit several fishponds. On April 4, measurements were conducted in One Alii fishpond. During the visit, they were guided around by Dr. R.D. Howerton (Sea Grant Extension Service, Maui County) and Mr. D.N. Fujii (Molokai Community Development Corporation). Pictures, slides and a 15-minute video presentation support this report. The description of the fishponds is an addition to earlier reports of site visits (see Minerbi et al., 1993, and Ertekin and Merrifield, 1995–Section 2.1 above). The reader is also referred to the fishpond maps in Minerbi et al. (1993).

The following fishponds were visited on April 3, 1996:

1) Keawanui fishpond (see site 163, Fig. 1a, from Summers, 1971):

This fishpond belongs to Bishop Estate. It is located near a Kamehameha School facility which may be closed in the near future. There are two makahas. There is also a gap in the wall, near the peninsula, due to the damage by wave action, see Fig. 1b. The gap has an approximate width of a 30 m (100 ft). The wall is free from mangroves but mangroves are encroaching on the landward side of the fishpond, see Fig. 1c. The peninsula appears to be a silted area inside the fishpond because the wall continues on the outer side of the peninsula. This part of the wall is enforced with cement. Evidence of erosion is visible on the nearby mountains. The run-off from the mountains might, therefore, be considerable.

2) Ualapue fishpond (see site 185, Fig. 2a, from Summers, 1971):

The fishpond is owned by the state. It is in excellent condition and is being used, see Fig. 2b. The wall is fully above water during the high tide. The width of the two makahas is 2 meters (6.6 ft), see Fig. 2c. There are some mangroves in the eastern part of the fishpond; they do not appear to be a problem however, see Fig. 2d. Siltation also does not appear to be a problem. There are two nursery tanks which are not in use, see Fig. 2e. Poaching has been a problem around the area.

3) Niaupala fishpond (see site 192, Fig. 3a, from Summers, 1971)

The fishpond is located right off the main road. It was in use until 1984. Since then the pond has been abandoned. This has resulted in parts of the wall (especially the south-west part) being submerged during the high tide, see Fig. 3b. About a quarter of the wall is covered with mangroves, see Fig. 3c. This fishpond is a good example to what happens to the condition of a fishpond when it is neglected for a number of years. 4) One Alii fishpond (see site 135, Fig. 4a, from Summers, 1971):

The fishpond is of the loko kuapa type and has two makahas. It is interesting to note that the southern makaha that is open now was closed in 1937 as seen in Fig. 4a. Both makahas have a width of 2.5 m (8.2 ft). Total area of the fishpond is about 27 acres. The wall length is about 823 m (2,700 ft), wall thickness or width is 1.2 m (4 ft), and wall height is about 1.4 m (4.5 ft). Three quarters of the wall are covered with mangroves, see Fig. 4b. A lot of mangroves grow in the eastern part of the fishpond, decreasing the total area of the fishpond considerably, see Fig. 4c. The fishpond is silted in heavily. There is a fenced area inside the fishpond which can be used as a nursery, but it seemed that the fishpond is used irregularly, see Fig. 4d. The area in and around the makaha on the western side of the fishpond is very shallow because either some people placed rocks in the makaha for unknown reasons or it was broken by wave action, see Fig. 4e. It appears that the western makaha which is closed now was open during the site visit of Brewer (1993). This makaha seen in Fig. 4a is, therefore, closed at low tide and barely allows water passage during high tide. It is speculated that, when the western makaha was broken, the southern makaha was built after 1957 (see the reference to Dunn, J.M., 1957 in Summers, 1971) and before 1975 since the aerial photographs cited in Minerbi et al. (1993) show two makahas. Also, Manoa Mapworks (1984) indicates (see Photograph 1-263: Section 13) two makahas. Figure 4f shows the location of One Alii fishpond as seen from a NOAA airplane in September 1993. The fishpond is leased to Hawaiian Home Lands by the state and is managed by homesteaders, living near the fishpond. Mr. Dean E. Fujii, the Executive Director of the Molokai Community Development Corporation, is very interested in cooperating with us and hopes that the results of our research will motivate the homesteaders to work in the fishpond more regularly. Among the fishponds visited both in November, 1995 and April, 1996, it was decided that One Alii fishpond is the most convenient one to survey and study circulation characteristics. The written permission of the management of One Alii fishpond which allowed us to work in the fishpond was obtained earlier.

In the survey measurements described in the next section, our goal was to obtain the water depth variation in and outside the fishpond, the fishpond geometry and the tidal elevation which are needed in simulating the circulation patterns inside the fishpond by means of a computer model.

	X-Coordinate	Y-Coordinate
Inside the Fishpond	19.3 m (63.3 ft)	-1.1 m (-3.6 ft)
Outside the Fishpond	-18.7 m (-61.4 ft)	-11.2 m (36.7 ft)

Table 2.1: Locations of tide measurements

3 Measurements

On April 4, 1996, one of the needed parameters for the computer modeling, namely the bathymetry of One Alii fishpond and surrounding waters, was obtained. To determine the position inside the fishpond, markers are placed along the wall of the fishpond. Marker #1 is assumed to be at position (x,y)=(0,0). The distance between the first and the second marker was measured first. The angle in-between the north direction and Marker #2 was also measured. The position of Marker #2 is now determined. By knowing the position of two markers, the position of the other markers can be determined. The angles in-between the north direction and the two markers were measured to determine the coordinates of each subsequent survey point. To measure these angles, a datascope was used. The same method was used to determine the locations inside and outside the fishpond.

To correct the measured waterdepths, the tide was measured inside and outside the fishpond at the locations given in Table 1.

In Fig. 4a, the origin of the X and Y axes is shown. The water depths were measured every 15 minutes from 10:30 a.m. until 6:00 p.m. (see Figs. 5 and 6) both inside and outside the fishpond. To compare the tide inside the fishpond with the tide outside the fishpond, the mean waterdepths inside and outside the fishpond were determined. This value was subtracted from the measured waterdepths (see Fig. 7). The differences at low and high tide seen in Fig. 7 might be a result of measuring errors. The phase lag of one hour is remarkable. Trade winds came in from the south-east direction that day, instead of the common trade winds from the east.

To verify the tidal information, the prediction of the tide for April 4, 1996, obtained from National Weather Service (1996), is shown in Fig. 8. In Fig. 9, the tidal information from Fig. 8 was adjusted by subtracting the mean tidal elevation (in-between 10:00 a.m. and 6:00 p.m.) from the actual tidal elevation. This was done to compare the predicted tide to the measured tide which is shown in Fig. 7. When comparing the results shown in Figs. 7 and 9, it is clear that our measurements were higher than the predicted high water elevation. The predicted tide also decreased the measured phase lag to about 30 minutes.

	X-Coordinate	Y-Coordinate
Makaha on the west side of the fishpond	-1.2 m (-3.9 ft)	-34.0 m (-111.6 ft)
Makaha on the south side of the fishpond	114.0 m (374 ft)	-172.8 m (567 ft)

Table 2.2: Locations of makahas of One Alii fishpond

The measured waterdepths inside as well as outside the fishpond were corrected, using the information in Fig. 7. These corrected waterdepths give a good representation of the bathymetry inside as well as outside the fishpond. A contour plot of the waterdepths around the fishpond can be found in Fig. 10. A close up of the bathymetry near the southern makaha is shown in Fig. 11. The waterdepths in the plots are in meters. The positions where the makahas are located are given in Table 2. The locations shown in Table 2 refer to the center of each makaha on the inner side of the fishpond. The width of each makaha is 2.5 m (8.2 ft).

The waterdepths outside the fishpond gradually increase from 0.65 m (2.1 ft), near the makaha on the western side of the fishpond (see Fig. 10), to 1.1 m (3.6 ft), near the makaha on the southern side of the fishpond, to 1.72 m (5.6 ft), approximately 370.0 m (1,214 ft) from the shore (approximately 190.0 m (623.4 ft) from the southern makaha).

Chapter 3

Hydrodynamic model

To simulate the circulation in the fishpond, a computer program developed by Sundararaghavan (1992) was used. The computer program was developed originally to simulate the wastewater transport from the Sand island outfall on the south shore of the island of Oahu. The model includes the simulation of a two- dimensional depth averaged shallow water flow and the transport phenomena. The numerical method uses an Eulerian-Lagrangian approach, in which the convection equation is solved by using the method of characteristics. The model uses semi-implicit finite differences to represent the time derivatives and is stable and computationally efficient.

Numerical calculations of circulation patterns are often performed to analyze different situations and, to a certain extent, to obtain a better understanding of what is happening in a particular location. Such problems are inherently three-dimensional and are quite complex. In the present model, a depth averaged approach is used to formulate the problem using the finite-element method (FEM). Since, in shallow waters, the flow variation over the depth is often less significant, the vertically averaged equations and variables should describe the physical situation adequately. However, in deeper waters, which intercept the top of the thermocline, it is no longer possible to use a depth-averaged approach and a two- or multilayer model is required. In such a situation, the three-dimensional Navier-Stokes equations are solved by using a coordinate transformation along the vertical direction.

1 Theory

The water flow is described by the conservation equations of mass (or continuity) and momentum. A two-dimensional formulation will be considered in the plan view. The governing equations are given as follows.

Equation of continuity:

$$\frac{\partial \eta}{\partial t} + \frac{\partial \{u(h+\eta)\}}{\partial x} + \frac{\partial \{v(h+\eta)\}}{\partial y} = 0 \tag{3.1}$$

Equations of motion:

$$\frac{\partial u}{\partial t} + u\frac{\partial u}{\partial x} + v\frac{\partial u}{\partial y} - fv - E_x\frac{\partial^2 u}{\partial x^2} - E_y\frac{\partial^2 u}{\partial y^2} + \frac{1}{\rho(h+\eta)})(\tau_x{}^b - \tau_x{}^s) + g\frac{\partial \eta}{\partial x} = 0 \tag{3.2}$$

$$\frac{\partial v}{\partial t} + u\frac{\partial v}{\partial x} + v\frac{\partial v}{\partial y} - fu - E_x\frac{\partial^2 v}{\partial x^2} - E_y\frac{\partial^2 v}{\partial y^2} + \frac{1}{\rho(h+\eta)}(\tau_y{}^b - \tau_y{}^s) + g\frac{\partial \eta}{\partial y} = 0 \tag{3.3}$$

where $h = h(x, y)$ is the variable bottom depth, $\eta = \eta(x, y, t)$ is the water elevation, f is the Coriolis parameter, ρ is the mass density of water, $\tau_x^s, \tau_y^s, \tau_x^b, \tau_y^b$ are the surface (superscript s) and bottom (superscript b) shear stresses components, respectively, $u = u(x, y, t)$ and $v = v(x, y, t)$ are the depth averaged water particle velocity components in the x and y directions, respectively, and E_x and E_y are the eddy dispersion coefficients in x and y directions, respectively. The Coriolis term is not considered in this study because of the small spatial scale used in the calculations.

The bottom and surface shear stresses are given by:

$$\tau_x^b = C_f \rho u \sqrt{(u^2 + v^2)} \tag{3.4}$$

$$\tau_y^b = C_f \rho v \sqrt{(u^2 + v^2)} \tag{3.5}$$

$$\tau_x^s = \rho_{air} C_D U_{10} \sqrt{U_{10}^2 + V_{10}^2}, \quad \tau_y^s = \rho_{air} C_D V_{10} \sqrt{U_{10}^2 + V_{10}^2} \tag{3.6}$$

where

$$C_f = \frac{g}{C^2} \; : \; Chezy \tag{3.7}$$

and ρ_{air} is the air density, U_{10} and V_{10} are the wind speeds at 10 m (32.8 ft) above the surface, in x and y directions, respectively, C_D is the wind drag coefficient which is given

as an empirical function of U_{10} or V_{10} , C_f is the bottom friction coefficient which can be obtained from , for example, the empirically determined Chezy coefficient, C, given in 3.7, and g is the gravitational acceleration. Other empirically determined friction coefficients such as the ones based on Manning or Darcy-Weisbach equations can also be used. Surface wind stresses are not considered in this study and left to future work.

The problem to be solved is in the time domain, so all the initial and boundary conditions must be given. That is $\eta = \eta_0(x, y)$ for all (x, y) and $(u, v) = (u_0(x, y)\ ,\ v_0(x, y))$ for all (x, y) at time t=0. On the land boundaries, the velocities can be specified as equal to zero. On the entrance boundary where the tide is specified, either the surface elevation or the normal velocity can be specified. If the surface elevation is specified, as in the case here, the velocities are then calculated at the entrance boundary. This is discussed further in Chapter 4.

2 Finite-Element Method

The system of equations described above generally is solved by approximate methods such as the finite- element method. Traditionally, the FEM has utilized the calculus of variations in problem formulation. This entails the determination of a functional related to the appropriate physical process and the subsequent minimization of that functional. For this system of equations, a functional is not known. In the computer program, Eqs. 3.1 to 3.3 are therefore formulated using weighted residual methods.

The weighted residual method can be summarized as follows. First, as a trial, a set of functions with arbitrary coefficients is assumed to be the approximate solution. Then, the problem is solved for the coefficients such that the trial solution satisfies the governing equations to its best, i.e., the error in the approximation is minimized. Consider the general partial differential equation $L\phi = 0$, where L operates on ϕ. To solve this equation, is approximated by:

$$\phi^a(x, y) \ = \ \sum_{j=1}^{m} N_j(x, y)\phi_j \tag{3.8}$$

where m is the number of element nodes and N_j is the shape function. Substituting the approximate solution into differential equation yields

$$L\phi^a(x, y) \ = \ R(x, y, \phi_j) \ \neq \ 0 \tag{3.9}$$

where R is a residual. Thus, the problem is to determine the coefficients which minimize the residual. The Galerkin method is adopted in the model used in this study. In this technique, the weighted average of the residual is forced to zero. The weighing functions are those chosen to approximate the trial solution, which are the shape functions themselves. This can be expressed as:

$$\oint\oint_{A_e} N_i(x,y)R(x,y,\phi_j)\ dA\ =\ 0 \tag{3.10}$$

where A_e is the area of an element.

The approximate solution, satisfying the minimization of the residual condition to give a best fit solution, can be expressed as

$$k^{(e)}\{\phi\}^{(e)}\ =\ \{p^{(e)}\} \tag{3.11}$$

where $k^{(e)}$ and $\{p^{(e)}\}$are the element characteristic matrix and vector, respectively, and $\{\phi^{(e)}\}$ is the vector of nodal displacements of element e. By simply adding all the element equations together, the system of equations for the entire domain is established. This is based on the requirement of continuity at the element nodes. i.e., at the nodes where the elements are connected, the values of the variables should be the same for all the elements joined at that node. It should be noted that the assembly process does not introduce any spurious contributions if we choose interpolation functions that ensure continuity of not only the variables at the element boundaries, but also those of their derivatives, up to one order less than the highest order derivative appearing in the system equations. Thus,

$$[K] = \sum_{e=1}^{N_m} k^{(e)} \tag{3.12}$$

$$\{P\} = \sum_{e=1}^{N_m} \{p^{(e)}\}$$

where K and $\{P\}$ are the assembled system characteristic matrix and vectors and Nm is the total number of elements.

It can be seen that contribution at a particular node comes from only those elements that share the node. This results in a system characteristic matrix that is both banded and sparse. If the system is linear, the unknowns can directly be solved for by standard techniques, such as Gaussian elimination. If they are non- linear, they can be solved by

iterative methods. It is noted that the numerical model used in this study is nonlinear in space and linear in time. Also, the time-stepping scheme used here results in a time invariant system matrix. Therefore, an LLT decomposition of the system of equations could have been used here where the decomposition is done only once rather than at every time step to obtain the decomposed matrix. The system of equations was solved at every time step using this decomposed matrix and, therefore, the solution method is very efficient.

The computer program uses quadratic triangular elements. The quadratic elements offer a number of advantages over the linear elements. First, the second-order polynomial provides a higher accuracy, facilitating the use of larger elements compared with the linear elements. This, in turn, results in more efficient computations. The second advantage is that the elements can be curved to fit irregular boundaries. This feature, however, has not been included in this program and left as part of a future study.

Chapter 4

Computations

1 Grid generation and bathymetry

When the bathymetry inside and outside the fishpond is measured, a number of actions need to be taken to simulate the circulation in the fishpond. First of all, the bathymetry, in this case the bathymetry of One Alii fishpond, was digitized to prepare the input data for the grid generation program. The gridgeneration program used is called TRIGRID (1995) which is based on the work of Henry and Walters (1993). A triangular mesh was generated by TRIGRID. The mesh had to be refined near the makahas to describe the boundaries properly and to obtain accurate results when running the program. There is a trade off between the time-step size and the minimum distance between the two nodes, and this is described by the Courant number. For numerical stability reasons, the Courant number has to be smaller than 1.0. As a result, when refining the mesh in a certain area, the time-step has to decrease. The Courant number is defined as follows (see for example, Roache, 1972):

$$C_R \;=\; \frac{c_g \Delta t}{\Delta x} \;\leq\; 1 \tag{4.1}$$

in which cg is the group velocity, defined for shallow-water (or long) waves as

$$c_g \;=\; \sqrt{gd} \tag{4.2}$$

where Δt is the time-step, Δx is the minimum distance between two nodes and d is the mean waterdepth (see also Kashiyama and Okada, 1992).

The area ends about 180.0 m (590.5 ft) offshore of the southern makaha. The distance from the west border of the mesh to the west side of the fishpond is about 100.0 m (328.1

ft). The distance from the east border of the mesh to the east side of the fishpond is also about 100.0 m (328.1 ft).

The FEM model requires quadratic triangular elements with six instead of the usual three nodes. Each of the three extra nodes are located in-between the two already existing nodes. The option to create quadratic triangular nodes was not included in the mesh generation program TRIGRID. A computer program was written to create these new nodes and to write the data in the correct format, required by the FEM model. The boundary conditions for this specific case were defined as well. Another computer program was written to reduce the bandwidth by renumbering the nodes. The reason for not including these programs in the FEM model was to give the user the opportunity to check the data outside the program.

One Alii fishpond has two makahas. In reality, the one on the west side of the fishpond is almost completely closed by rocks. To determine a way to increase the circulation in the fishpond, two models or cases were examined. One is the case of One Alii fishpond with one makaha which is on the south side of the fishpond. The second case has two makahas. In that case, the fairly closed makaha on the west side of the fishpond was opened up in the computer program input.

To run these cases, the bathymetry had to be slightly adjusted because any sudden changes in the water depth, as in the case of One Alii fishpond near the southern makaha, caused numerical problems since the slope of the fishpond floor becomes very large at those points. In Fig. 12, a contour plot of the bathymetry inside and outside the fishpond is shown. The same bathymetry was used in both makaha models. The bathymetry near the southern makaha was made smoother (see Fig. 13). Also the minimum waterdepth was set to 0.5 m (1.6 ft). This was done for numerical stability reasons which can be improved in future studies so that the actual minimum water depth as measured can be used.

The mesh used in the hydrodynamic calculations for the case with one makaha is shown in Fig. 14. The mesh was refined near the makaha. A close up of the mesh near the southern makaha can be found in Fig. 15. The width of the opening is 11.87 m (38.9 ft) instead of the 2.5 m (8.2 ft) width measured at the site. This adjustment also needed to be made for numerical reasons which are related to the fact that a very small opening causes a very strong jet around the makaha which in turn causes very large velocity gradients or spatial accelerations that stalls the simulations unless very small finite elements and time-step size are used. Such small finite elements could not have been used in this preliminary study.

In Fig. 16, the mesh for the case with two sluice gates is shown. To obtain this mesh, the mesh of the single makaha case was taken as the starting mesh and elements are added, and

some nodes are shifted interactively with the mesh generation program TRIGRID. Thus the meshes used in two different cases were practically the same except for the obvious difference of the presence of one and two makahas. A close-up of the area near the makaha on the western side of the fishpond is shown in Fig. 17. In this mesh, the makaha has a width of 10.0 m (32.8 ft) instead of 2.5 m (8.2 ft) as measured. The western makaha could be made smaller because the jet there is weaker as will be seen later in Chapter 5.

Other general information about the two meshes are given in Table 3.

	Number of elements	Number of nodes	Number of boundary nodes	Bandwidth
Fishpond with single makaha	557	1228	226	122
Fishpond with double makaha	587	1287	226	122

Table 4.1: Mesh and matrix parameters

2 Other numerical considerations and parameters

The boundary conditions are shown in Fig. 18. The tide was imposed on the nodes on the southern boundary. This boundary is called the entrance boundary. At the eastern and western lateral boundaries, a free slip condition was used. Physically, there is then no flow across these boundaries while water particles can slide along the boundary. This assumption might not be perfectly valid, however, the calculated values near the makahas and inside the fishpond are not expected to be affected by this assumption, and indeed, the results presented later support this point. This boundary condition provides an effective way of handling the problem. Nevertheless, the validity of this assumption need to be further investigated. The wall of the fishpond as well as the shore are both no-slip boundaries and, therefore, the no-slip condition was imposed there (as well as on the sea floor by theory) since the flow is assumed to be viscous.

The tide used in the computations was the predicted tide for Kaunakakai on April 4, 1996. Kaunakakai is located on the south shore of Molokai, close to One Alii fishpond. The surface elevation on the entrance boundary is specified by the tidal elevations. The direction of the tide is assumed perpendicular to the shore. The tide used in the calculations for a period of slightly more than 24 hours is presented in Fig. 19.

In order to start the computations, the initial conditions for the surface elevation and velocities must be input to the model. Usually, these values are not known unless they are

Numerical wave Gauge	X-Coordinate	Y-Coordinate
No. 1	108.72 m (356.7 ft)	-355.70 m (-1,167 ft)
No. 2	109.37 m (358.8 ft)	-176.14 m (-577.9 ft)
No. 3	4.28 m (14 ft)	-28.92 m (-92.6 ft)
No. 4	114.60 m(376 ft)	-88. 31 m (-289.8 ft)
No. 5	63.04 m 206.8 ft)	-31.08 m (-102 ft)

Table 4.2: Location of numerical wave gauges used in the calculations

measured on site. However, starting the calculations either at the crest or the trough of the tide elevation provides a reasonable assumption of zero or near zero velocities in the entire computational domain since tidal waves are very long waves. Physically, at these near zero velocities, the tide is reversing. In this study, the calculations were started at the crest of the tidal wave. To do this, a continuous time series of the tidal elevation was obtained by repeating the predicted tide, and the highest crest point was chosen as the starting point. This means that the next stage of the tide was assumed to be the ebb tide.

Numerical wave gauges were placed in different positions inside and outside the fishpond to measure the calculated surface elevation and water particle velocities. The coordinates of the locations of the gauges used in both the single and double makaha models are given in Table 4 (also see Figs. 20-21):

The time stepping was done by using a leap-frog time stepping scheme which facilitates an semi- implicit treatment of tidal gradient and bottom-friction terms with an explicit treatment of the viscosity scheme. The convection terms were handled by using a Lagrangian particle tracking algorithm (see Sundararaghavan (1992) for details).

The other parameters used in this study are as follows: time step $\Delta t = 5s$ (which is found to be small enough for our calculations); eddy viscosities $E_x = E_y = 5.0\ m^2/s$ (53.8 ft^2/s); Chezy coefficient $C = 50m^{[1/2]}/s$ (90.6 ft1/2/s) (see for example, Wang et al., 1975, and Niemeyer, 1978) so that the bottom friction coefficient given by 3.7 becomes C_f =0.0039.

3 Filtering

Initial test runs indicated that sharply turning high currents near the sluice gate entrance caused a jet near the narrow gates and induced spikes in the surface elevations which gradually grew and resulted in numerical instability. It is anticipated that a carefully hand-crafted mesh may eliminate this emergence of spikes. Another way of eliminating these spikes is by

using a filtering scheme.

We developed, in this study, a novel, simple filtering scheme based on a weighted averaging technique. To perform this filtering, all the six interior nodes neighboring a particular node is considered. The weights are given by the inverse of the distance between the particular node and the neighboring node. This can be expressed as follows:

$$a_i^f = wa_i + (1-w)\ (\sum_{j=1}^{N_b} \frac{a_j}{\Delta s_j})/(\sum_{j=1}^{N_b} \frac{1}{\Delta s_j}) \tag{4.3}$$

where a_i is the value of the parameter at the ith node that is being filtered, a_j is the value at the jth neighboring node, Δs_j is the distance between nodes i and j, N_b is the total neighboring nodes, w is the weight used to represent the significance of neighboring-node values of velocity and surface elevation compared to their values at node i, and a_i^f is the filtered value at node i. In the calculations performed in this study, w was taken as 0.4, i.e. 40% weight was given to the center node and 60% was given to all the neighboring nodes, because when w ¿ 0.4 the filtering was not effective, resulting in the eventual stalling of the computer program due to excessively large velocity values. Both the surface elevation and velocities were filtered at every time step inside the domain, i.e. the boundary values were not filtered.

Chapter 5

Results

Figures 22-26 show the variation of surface elevation and velocity components at the five numerical gauge locations given in Table 4 for the single makaha case. Figures 36-40 show similar results for the double makaha case. It can be seen from these figures that the surface elevations vary only negligibly inside the domain. The velocities at the makahas reach up to 25 cm/sec and are quite high when compared with velocities elsewhere. Such high velocities are a direct result of the fact that the surface elevations do not spatially vary significantly. It may be noted that the velocities and surface elevations are out of phase, i.e., the surface elevation reaches its maxima or minima while velocities are close to zero and vice versa.

Even though the surface elevations vary smoothly in time, the velocities have secondary oscillations. Note that these secondary oscillations could be made smaller by using a smaller value for the weight function in 4.3. However, we could have then overfiltered the results. And since no current measurements are available for this fishpond, a verification cannot be made at this time.

The calculations were carried out for a period lasting a little more than 24 hours. It can be seen from Figs. 22-26 and 36-40 that velocities and surface elevations repeat themselves after 24 hours. This proves that the initial condition assumption (that the velocities are almost zero at reversing tide) is justified.

Figures 22-26 and 36-40 can be compared to signify the differences between the single and double makaha cases. It can be observed from Figs. 23 and 37 that the velocities at the southern makaha are greater for one makaha case than for the two makaha case. When there are two makahas available for mass transfer between the fishpond and open water, the mass transfer is shared by the two makahas unlike that in the one makaha case where all the

mass transfer has to take place through only one makaha. This results in lesser velocities at the southern makaha for the double makaha case. Figure 24 shows that the velocity near the western makaha is close to zero for the one makaha case. Fig. 38 shows velocities up to 6 cm/sec through the western makaha while reduction at the southern makaha case is also about 5 cm/sec. Thus, by opening the western makaha, the net mass transfer remains the same but the mass transfer occurs at different locations of the fishpond.

The water at the western makaha is stagnant when the makaha is closed while it takes up about one fourth of the mass transfer when it is open. While in the former case, there is little chance of outside water presence near the western makaha, there is active exchange between the waters outside and inside the fishpond in the latter case.

Figures 27-35 and 41-49 present the velocity vectors for the ebb, flood, and reversing tides for the single and double makaha cases. These figures show the spatial variation of velocities with different lengths and directions. The most striking feature in these figures is the high velocities at the makahas compared to elsewhere. It can be noticed that the velocities at reversing tides are almost zero throughout the entire domain. The velocities inside the fishpond drops as we move away from the makahas. Comparisons of Figs. 27-35 for one makaha case with the corresponding Figs. 41-49 for the two makaha case show that, during the ebb and flood tides, the circulation in the northern part of One Alii fishpond is significantly enhanced by the presence of the western makaha. Such increases in circulation due to tidal currents would clearly decrease the residence time of the suspended sediment inside the fishpond, thereby slowing down the process of silt accumulation.

Figures 50-51 show the presence of two stagnation points in the single makaha case at the flood and ebb tides and Figs. 52-53 show the presence of five stagnation points in the double makaha case. Figures 50 and 52 are the snapshots of the velocities during the flood tide at t=20 hours and 2 minutes, and Figs. 51 and 53 are the snapshots of the velocities during the ebb tide at t=26 hours and 26 minutes. At the stagnation points inside the fluid, all velocity components are zero. It is interesting to note that there are no stagnation points inside the fishpond in the single makaha case while there are three stagnation points inside the fishpond in the double makaha case. Although it is early to say, this may be a function of pond bottom morphology.

Chapter 6

Conclusions and Recommendations

A number of fishponds on the island of Molokai were surveyed during two site visits. One of the fishponds, namely One Alii fishpond, was chosen for the tidal circulation study undertaken in this preliminary project. During the second site visit, the fishpond geometry, water depth variation inside and outside the fishpond and tide elevations were measured. The measured tide is found to be in good agreement with the predicted tide.

To simulate the tidal circulation, the conservation equations of mass and momentum were solved numerically using the finite-element method. The computational domain was discretized into small, quadratic triangular elements with six nodes each. These elements were generated by an automatic mesh generation program. The measured data were used in the calculations to simulate the currents generated by the tide inside and outside the fishpond. The rigid boundaries, namely the shore and the fishpond wall boundaries, were assumed to be no-slip boundaries with zero water particle velocity components. On the lateral boundaries, a free-slip condition was used.

Two different fishpond makaha cases were considered. In the first case, only the southern makaha was assumed to be open. In the second case, both the southern and the western makahas were opened in the computer calculations. The results show that there is significant improvement in the circulation in the northern part of the fishpond when both makahas are open. This fact leads to the conclusion that the number and locations of makahas are very important parameters in the circulation characteristics of a fishpond as one might expect. It is expected that the experience of the Hawaiian people in designing ponds has resulted in good locations for makahas. This is certainly true in One Alii fishpond case when the western makaha, which is currently closed, is restored in the future to its original structure.

The methodology developed here for obtaining the circulation characteristics of a fishpond is applicable to any other fishpond. However, we have encountered a number of difficulties in this preliminary study. These difficulties may be overcome in a full-fledged study and we can also improve a number of techniques used in this study in the future. These difficulties and the proposed solutions are listed as follows:

- Domain size is rather large forcing us to use large finite elements. As a result, the accuracy suffers, especially around the makahas where the current velocities are very large, resembling a jet. In no previous study of the circulation characteristics of a partially-open basin can one find very small openings, such as represented by the makahas or sluice gates of a fishpond. For example, when one studies the circulation patterns inside a harbor or an estuary, the openings are very large and, therefore, one would not encounter the difficulties that we have had in analyzing a fishpond. Also, note that when one uses smaller finite elements, the computational time increases dramatically since we must also reduce the time step-size to have numerically stable results. In this study, for example, each run took about 24 hours of central processing unit (CPU) time on a rather powerful, UNIX based IBM/RS/6000/550 workstation. The turnaround time is of course longer. One solution to this problem is to recode the program in a parallel structure and use the parallel programming facilities of the Maui Super Computer Center. This way the CPU time required will be considerably less. Also note that the stability of the numerical method used here depends on the water depth through Eqs. 4.1 and 4.2, and that is why the minimum water depth was set to 0.5 m (1.6 ft) as indicated in Section 4.1. Once the CPU time problem is solved, smaller water depths can be considered in the future.

- As the results show, because of the very small makaha openings, the water particle velocity gradients become excessively large, resulting in the saw-tooth behavior of the velocity components. If these high- frequency oscillations are not treated by means of a filtering scheme, we have seen that the calculations cannot be continued. The novel filtering scheme devised here proved to be very effective, however, we have no way of knowing how much we need to filter unless we can directly compare the calculated current velocities with the observed ones. There is definitely a need to verify the calculations by direct comparisons with measurements.

- The mesh generation program used here, although very useful, proved to have some draw backs. For example, especially around the small makaha openings, the elements

are distorted. These distortions may cause accuracy problems. It is necessary to modify the current program to have a better mesh generation capability applicable to fishpond geometries.

- We have used the free-slip condition on the lateral boundaries on the eastern and western parts of the computational domain. Although the boundary condition used here appears to work effectively, it is expected that the use of a non-reflective boundary condition on these boundaries will further increase the accuracy of the calculations. At this point, we cannot verify in a definite sense how much tidal wave reflection reaches these boundaries without measured values. It is possible to minimize the reflections on these boundaries by using an open boundary condition like the modified Orlanski condition (see for example, Yang and Ertekin, 1992).

As mentioned above, a number of improvements can be made to the calculation method introduced here and observational data can be gathered to verify the calculations and to adjust some of the parameters used to have a better accuracy in predictions. Furthermore, because the final goal is to devise a method that can accurately simulate the sediment transport in a fishpond and ways to minimize silt accumulation, a number of additional calculations must be done. Our recommendations for these additional work are as follows:

- Include the shear stresses due to wind. Wind shear stresses on water surface induce surge which may account for damage to walls. To do this, it is necessary to measure the wind velocities near the fishpond. The measured velocities can then be used in the computer program.

- Include wave action. We have not considered the low period wave action in this study. However, the theoretical model is capable of including waves of shorter lengths superimposed on the tidal wave. Inclusion of shallow water waves will allow us to determine the wave set-up due to the onshore mass transport. These studies are necessary to determine the best design for the fishpond wall slope and height.

- Sediment transport. Once we have the current velocities, we can calculate the sediment transport inside the fishpond after we develop computer programs to model this. Such simulations can be done for long periods of time to predict the movement of sediment within the fishpond and to locate areas of significant sediment accumulation. Residence time can also be calculated to estimate the amount of time the water particles remain inside the fishpond. This is important to know because the amount of flushing of the

water out of the fishpond affects a number of parameters, such as nutrient content of the water and silt accumulation. Although we have observed the circulation patterns in One Alii fishpond for the one and two makaha cases and compared them visually (see Sundararaghavan and Ertekin, 1996), we can define the circulation around a closed contour as the integrated value of the tangential component of the velocity vector on the closed contour. It is possible to calculate this circulation for different contours inside the fishpond and do a direct comparison. Similarly, the flux out of or into the fishpond can be calculated.

- It is also possible to consider the run-off into the fishpond. We can include run-off at given nodes in our model and treat it as a "source" of water flow into the fishpond. This model should also include the sediment transported into the fishpond.

- We have stressed that on-site measurements of, for example, the current velocities are necessary to verify the predictions. In Chapter 3, we have seen that there are a number of empirical coefficients that we used in our model. These coefficients, e.g. Chezy coefficient, can be varied to determine how much they affect the results and the ones that provide the best fit to the ones derived from measurements can be used in the numerical model. The same is true for the wind shear stresses. It is important that we note here that One Alii fishpond is not necessarily the best fishpond to undertake a measurement program because, as pointed out in the video of Van Stiphout and Ferier (1996), at high tide, parts of the walls of the fishpond allow water passage over them. Because we will not be able to simulate this condition in our calculations, it is expected that, depending on the amount of water that goes over the walls, there will always be differences in the predictions and measurements no matter how much various parameters in our model are adjusted.

- In this preliminary study, we have considered a total duration of 24 hours only. Numerical simulations of tidal currents for longer periods of durations will have to be done so that secondary oscillations in velocities may be studied more extensively. Also, the influence of different tidal patterns, highlighting seasonal variations, on the results may be studied.

- Additional calculations can answer the following questions raised by Helsley (1996): i) Is it possible to increase further the circulation within the pond by opening and closing the makahas during the simulations depending on whether we have a flood tide or ebb tide?, and ii) is it possible to divert the jet that occurs during the flood tide by placing

an angular plate near the makaha so that the jet will circulate the stagnant water that we have seen on the eastern part of One Alii fishpond? Doing both calculations are possible even with the present computational capabilities that we have, and they are very worthwhile tasks to complete since they may indeed show that circulation within a fishpond can further be increased. The opening and closing of the makahas can be achieved by using a time- dependent finite-element mesh unlike the fixed (or time-independent) mesh used in this study. In practice, the makahas can either have manual or motorized gates made of stainless steel or aluminum plates that allow the flood tide to rush in the outside water or the ebb tide to flush out the stagnant inside water.

- Another worthwhile idea recently suggested by Minerbi (1996) that should be looked into is a comprehensive land and natural resource plan which integrates the solutions for the problems associated with deforestation, soil erosion and siltation of the fishponds. This plan would use the sediments removed from the fishponds to control soil erosion and also to enhance the forestation by supplying nutrient rich soil on the island of Molokai.

References

Brewer, W. (1993), Master conservation district use application form and draft environmental assessment for repair, reconstruction, maintenance and use of molokai fishponds, MBA International Report, January.

Ertekin, R. and M. Merrifield (1995), Report on molokai fishpond site visit, Memo submitted to UH Sea Grant College Program, November.

Farber, J. (1996), Community-based planning in the coastal zone, the case of molokai fishponds: Problems and potential, AOC Paper for Master of Urban and Regional Planning Degree, Dept. of Urban and Regional Planning, University of Hawaii at Manoa, Spring 1996.

Helsley, C. (1996), Personal communication.

Henry, R. and R. Walters (1993), Geometrically based, automatic generator for irregular triangular network, *Communications in Numerical Methods in Engineering*, 9:555-566.

Kashiyama, K. and T. Okada (1992), Automatic mesh generation method for shallow water flow analysis, *Int. J. of Num. Methods in Fluids*, 15:1037-1057.

Kikuchi, W. (1976), Prehistoric hawaiian fishponds, *Science*, 23 July, 193: PAGES =.

Kubato, G. (1996), Red tape stalls molokai pond revival, In Honolulu Star-Bulletin newspaper, Honolulu, January 29, p. A-3.

Mapworks, M. (1984), Molokai coastal resource atlas, Prepared for the US Army Corps of Engs., Pacific Ocean Div., Contract No. DACW-84-83-M-0660, Honolulu, HI, June.

Minerbi, L. (1996), Personal communication.

Minerbi, L. e. a. (1993), Molokai fishpond master cdua project, University of Hawaii, Department of Urban & Regional Planning, Practicum Class, December, 300 pp.

Niemeyer, G. (1978), Numerical methods for the simulation of hydrodynamic and ecological processes, Hawaii Institute of Geophysics, Report No. HIG-78-1, University of

Hawaii at Manoa.

Program), T. C. (1995), Channel Consulting Ltd., Canada.

Roache, P. (1972), Computational fluid dynamics, Hermosa Pub., Albuquerque, New Mexico, 446 pp.

Service, N. W. (1996), Personal Communication, Honolulu Office, HI.

Summers, C. (1971), Molokai: A site survey, Pacific Anthropological Records, No. 14, Bernice Pauahi Bishop Museum, Honolulu, 239 pp.

Sundararaghavan, H. (1992), Dispersion of wastewater in open coastal waters using finite element method, M.S. Plan B Paper, Dept. of Ocean Engineering, University of Hawaii at Manoa.

Sundararaghavan, H. and R. Ertekin (1996), Movie: Tidal circulation study of one alii fishpond, molokai, Video (VHS), Dept. of Ocean Engineering, University of Hawaii at Manoa.

Van Stiphout, A. and P. Ferier (1996), Movie: Molokai fishpond, Video (VHS) covering Keawanui, Ualapue, Nameless and One Alii fishponds, April 3-5, 25 min.

Wang, J. D. and J. J. Connor (1975), Mathematical modeling of near coastal circulation, Massachusetts Institute of Technology, MIT Sea Grant Program Report No. 75-13.

Yang, C. and R. Ertekin (1992), Numerical simulation of nonlinear wave diffraction by a vertical cylinder, Trans. of ASME, February, 114(1):34-44.

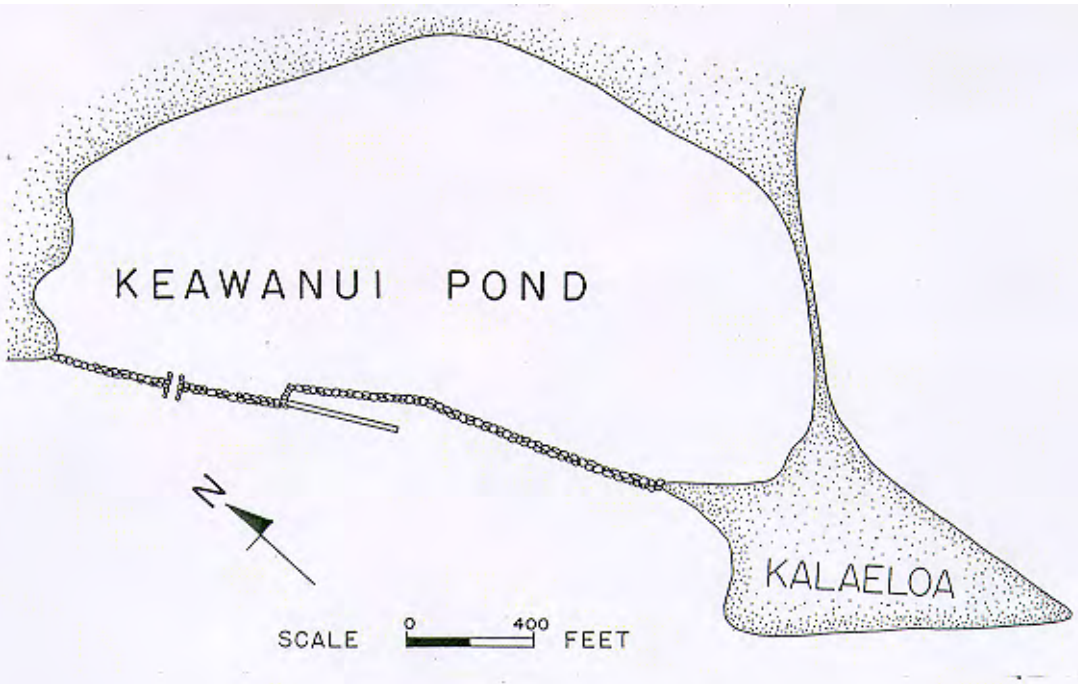

Fig. 1a Keawanui fishpond (site 163)

Fig. 1b Damaged wall of Keawaniu pond

Fig. 1c Mangrove encroachment in Keawanui pond.

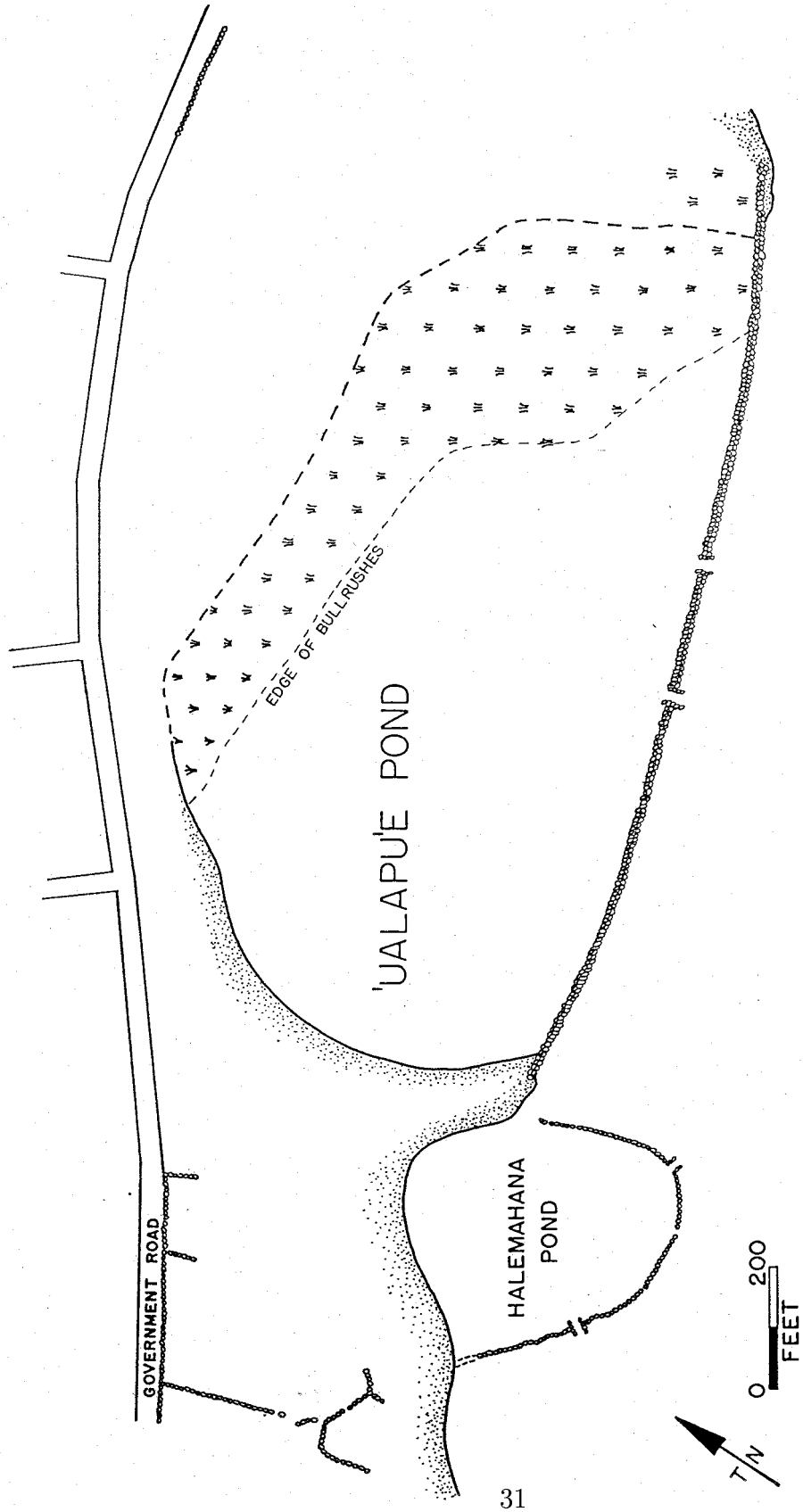

Fig. 2a Ualapue fishpond (site 185)

Fig. 2b Wall of Ualapue pond

Fig. 2c Makaha of Ualapue pond

Fig. 2d Mangrove encroachment in Ualapue pond

Fig. 2e Nursing tanks by Ualapue pond

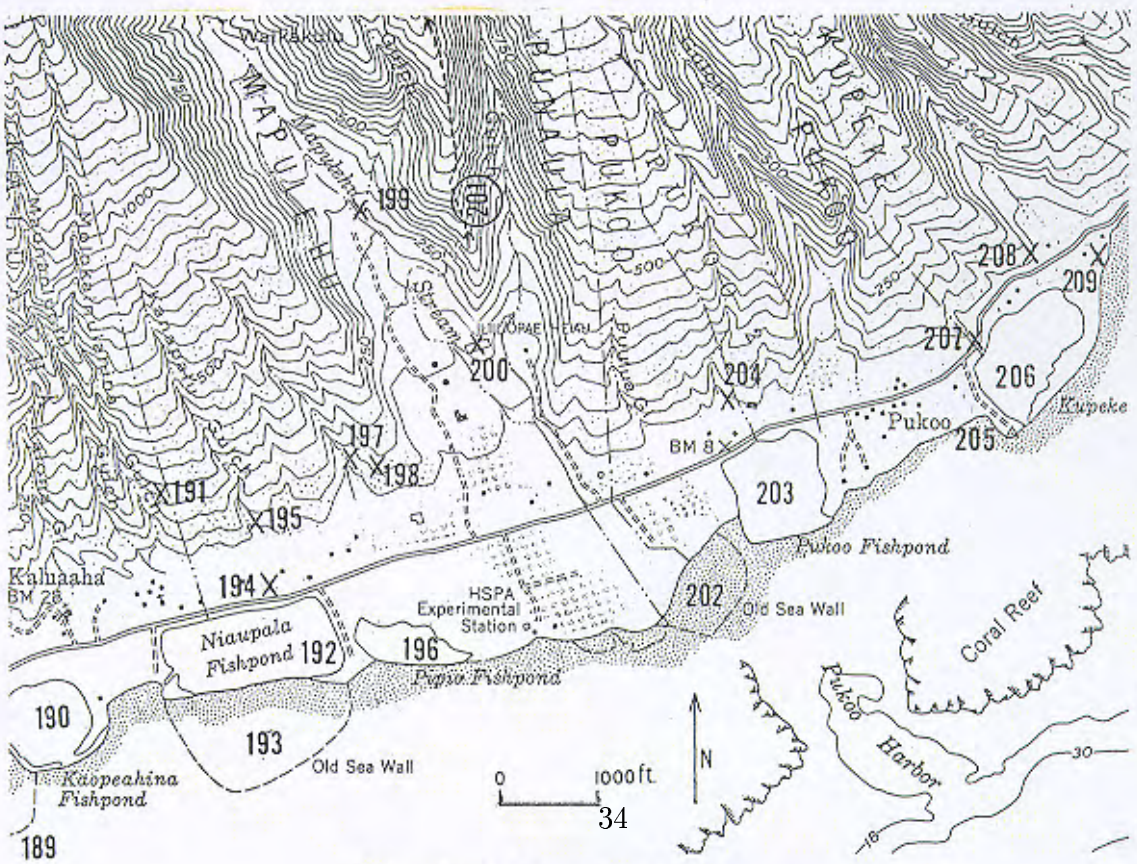

Fig. 3a Ni'aupala (site 192)

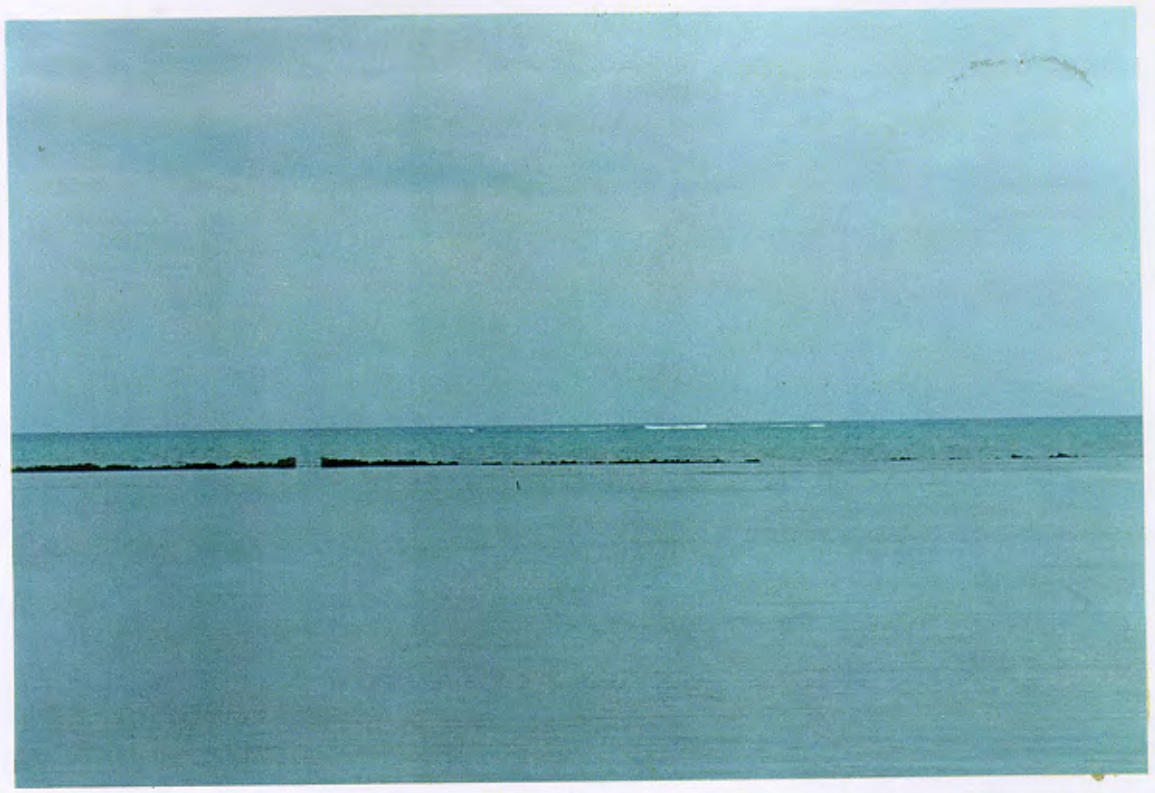

Fig. 3b Partially submerged wall of Ni'aupala pond

Fig. 3c Mangrove encroachment in Ni'aupala pond

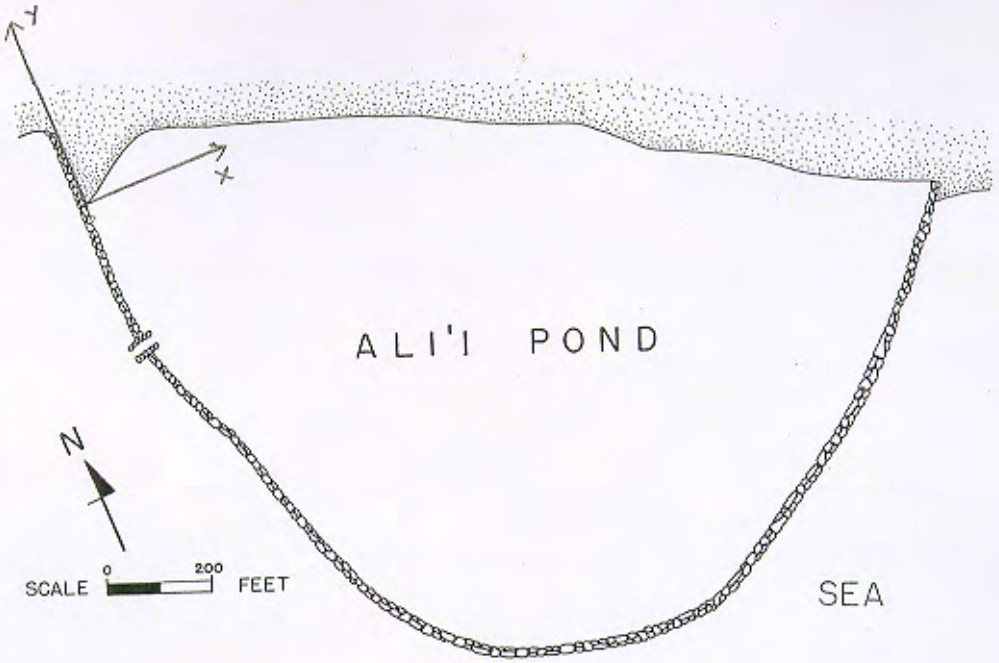

Fig. 4a One Ali'i fishpond (site 135)

Fig. 4b Mangrove encroachment on the wall in One Ali'i pond

Figure 4c Mangrove encroachment on the eastern part of One Ali'i fishpond

Fig. 4d Nursery fence in One Ali'i pond

Fig. 4e Rocks which closed the Western makaha in One Ali'i pond.

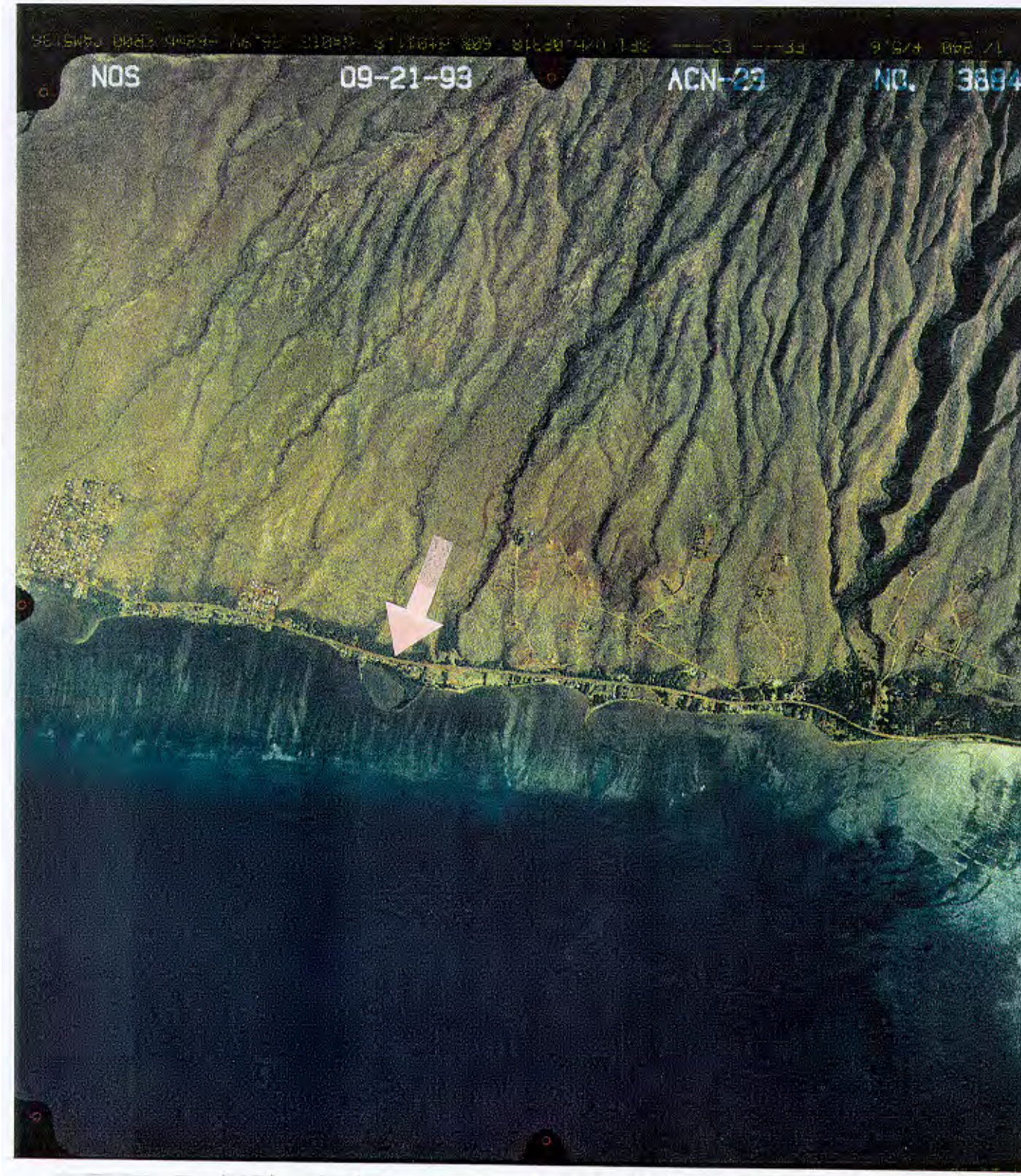

Figure 4f One Ali'i fishpond as seen from a NOAA airplane at 1,604 m (5,264 ft) altitude on September 21, 1993. Latitude: 21 deg 4.5 min North; Longitude: 156 deg 58.3 min West

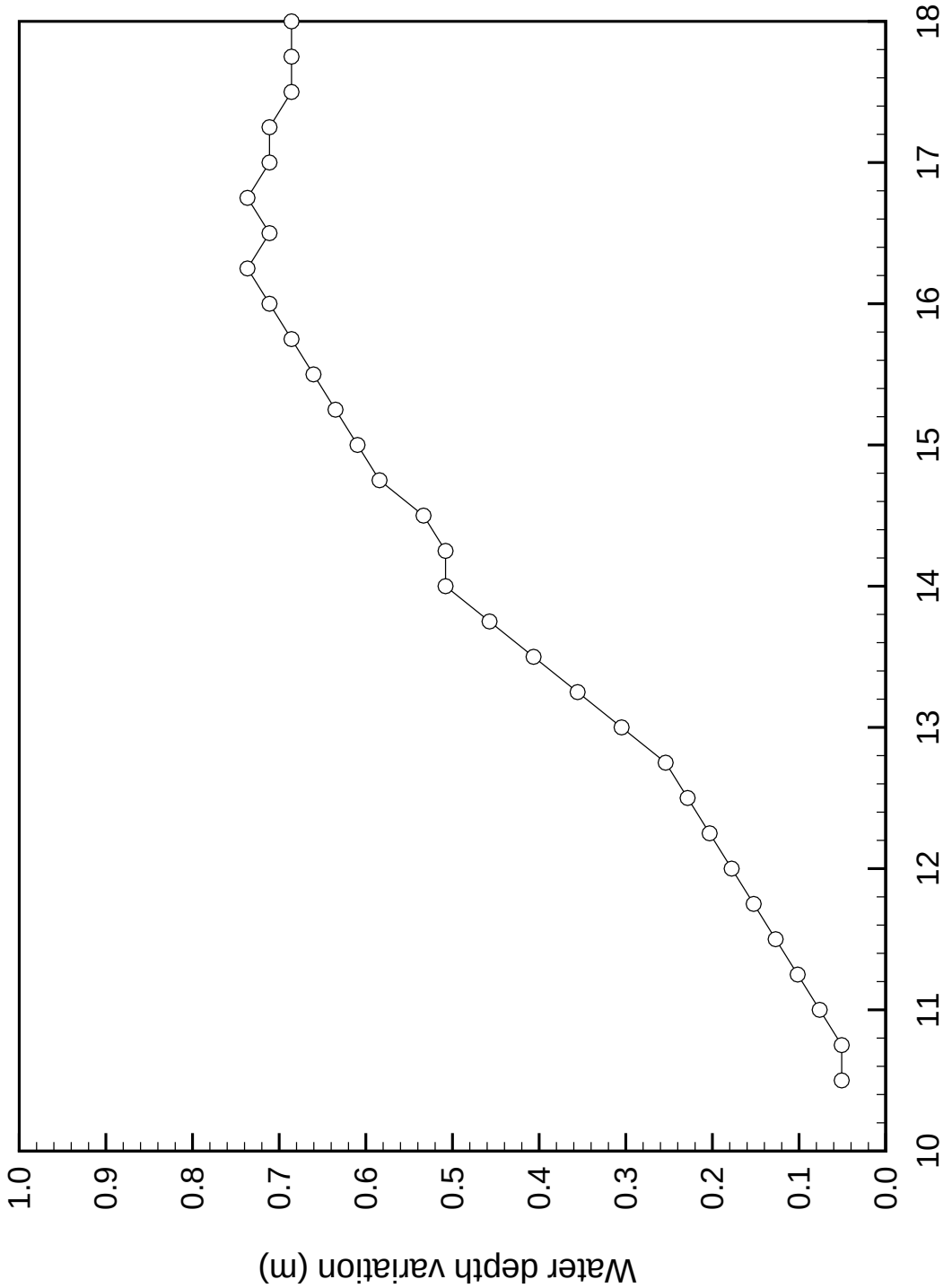

Fig. 5 Water depth variation inside One Ali'i fishpond (Apr 4, 1996)

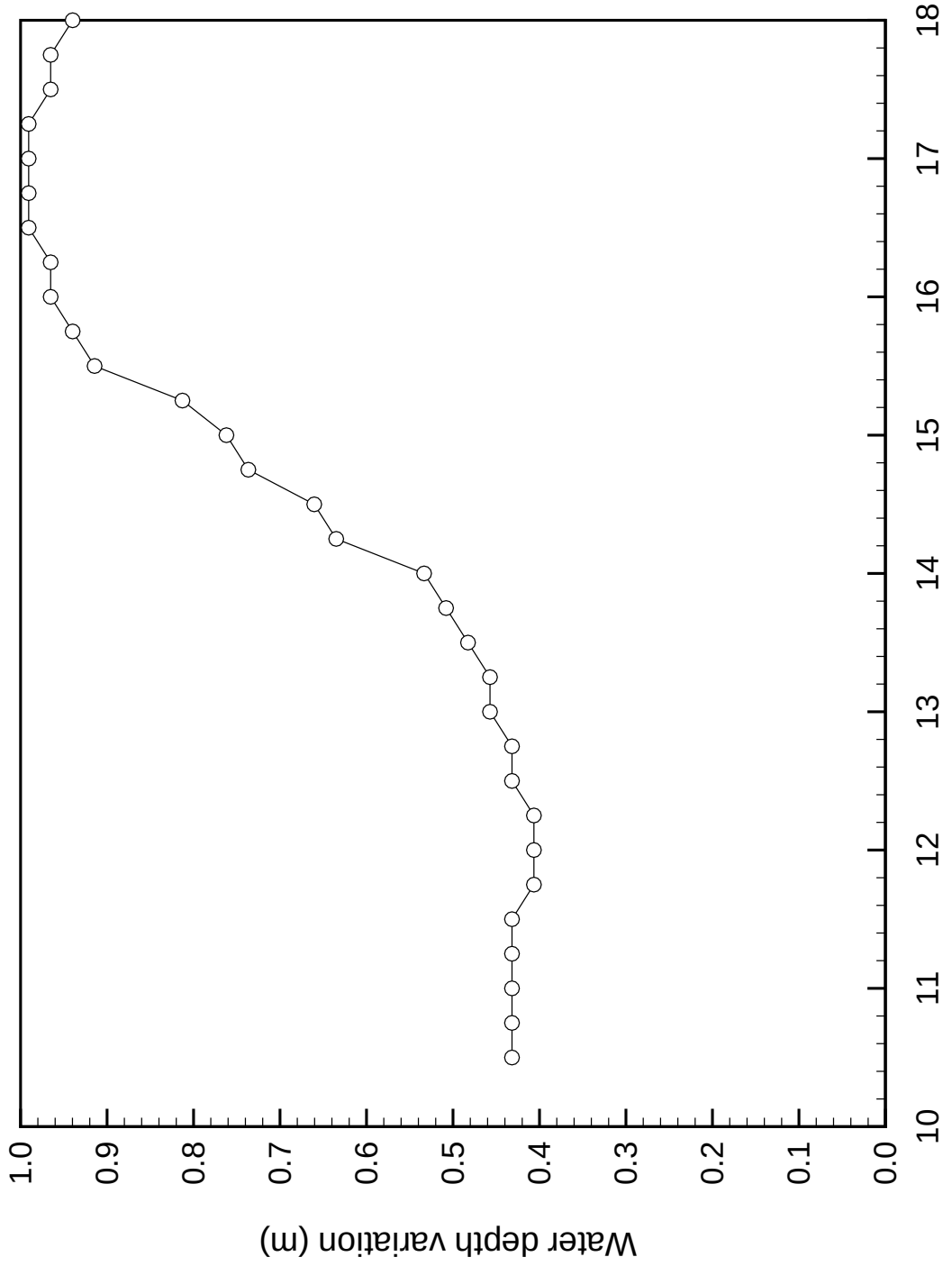

Fig. 6 Water depth variation outside One Ali'i fishpond (Apr 4, 1996)

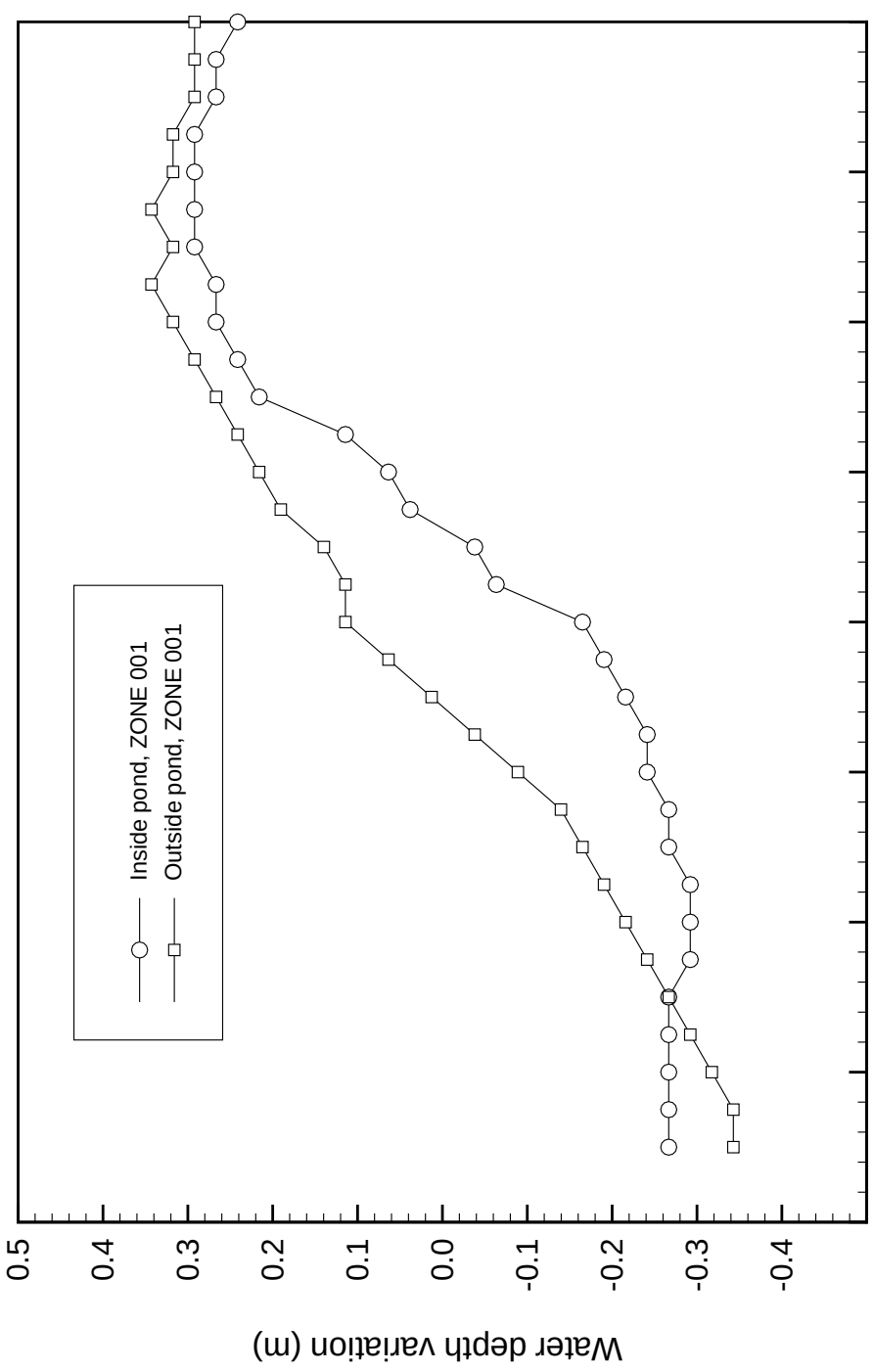

Fig. 7 Water depth variation inside and outside One Ali'i fishpond after subtracting mean depth (Apr 4, 1996)

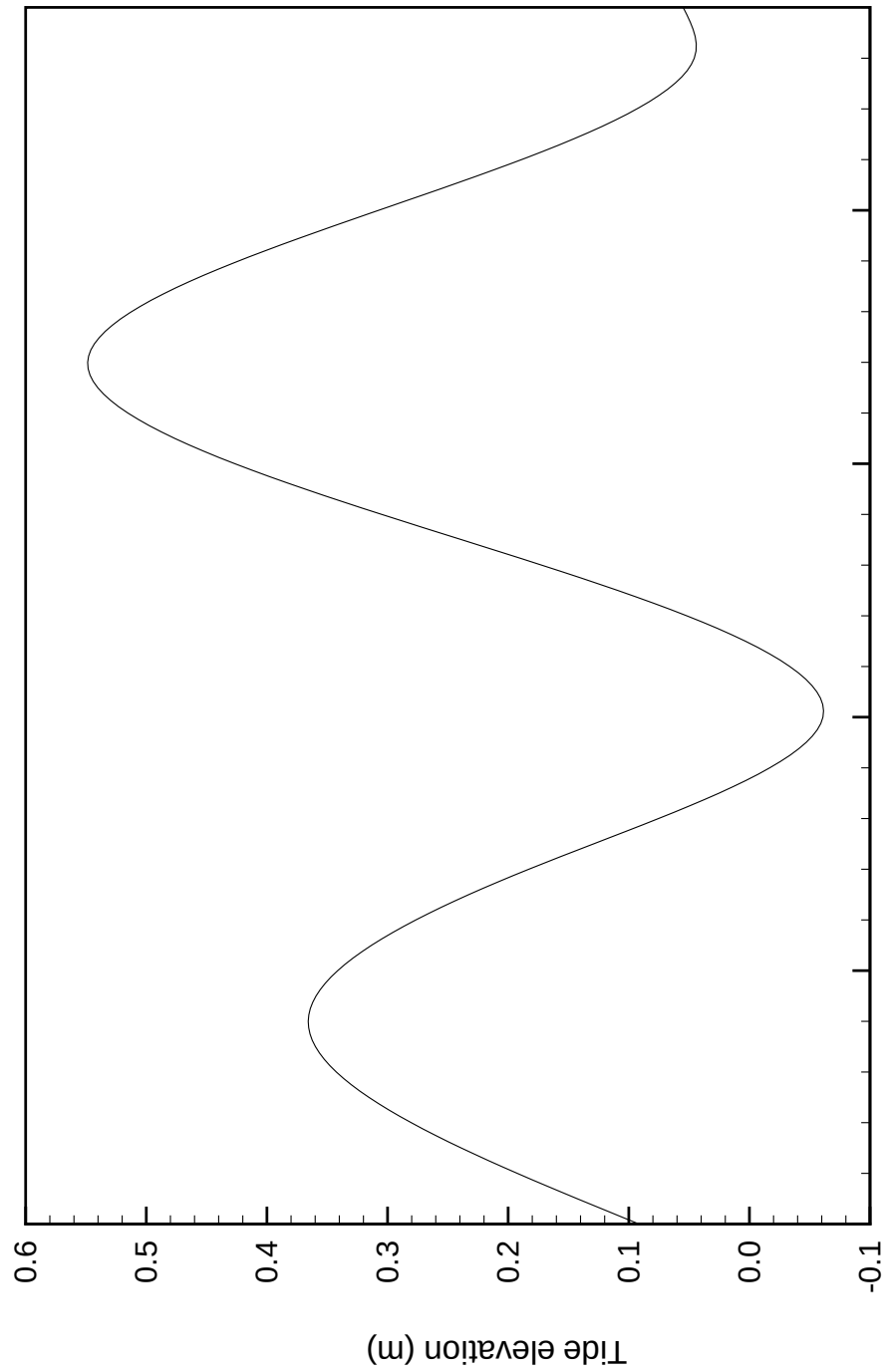

Fig. 8 Tide prediction for Kaunakakai (Molokai, Apr 4, 1996)

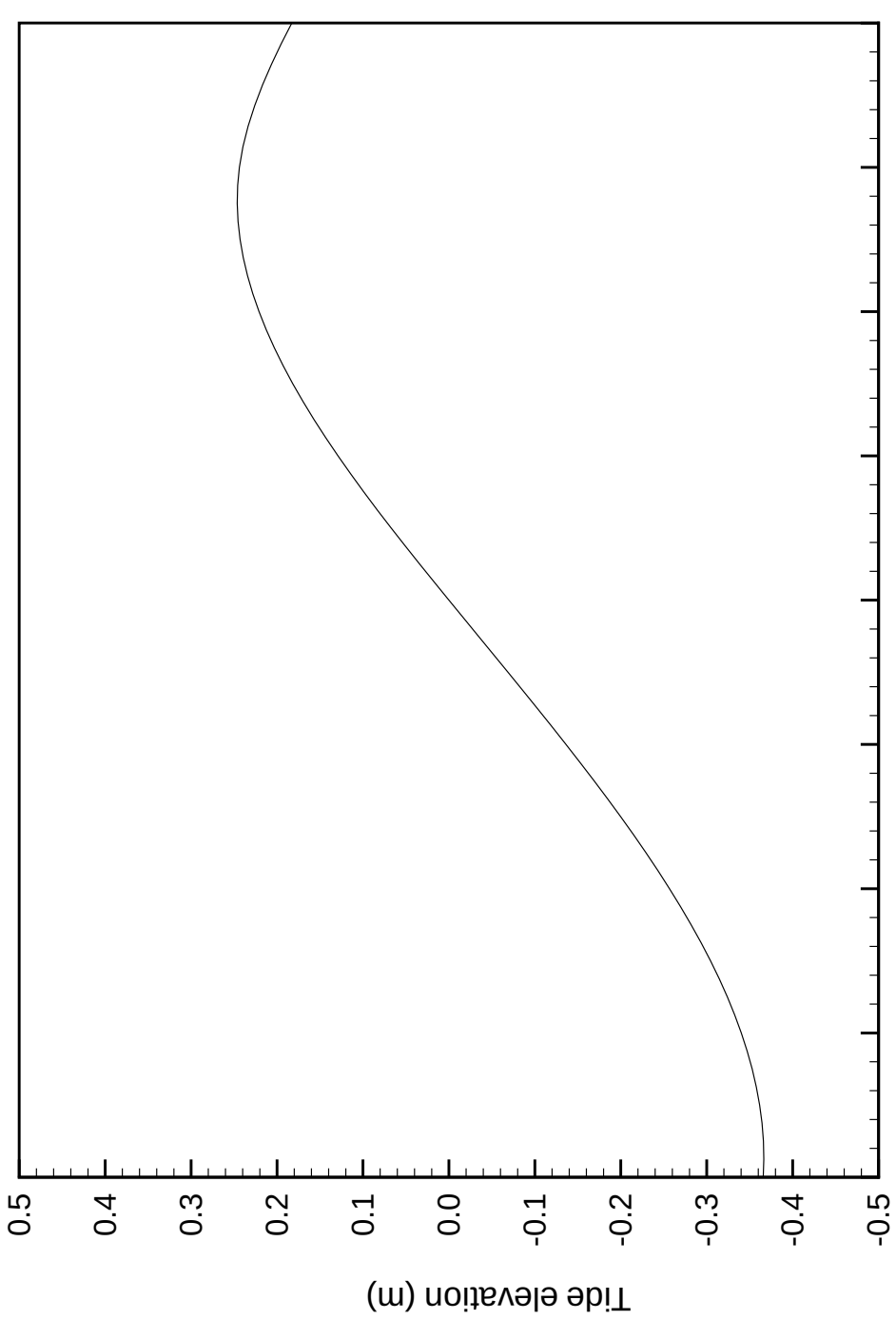

Fig. 9 Tide prediction for Kaunakakai after subtracting mean tide.
(Molokai, Apr 4, 1996)

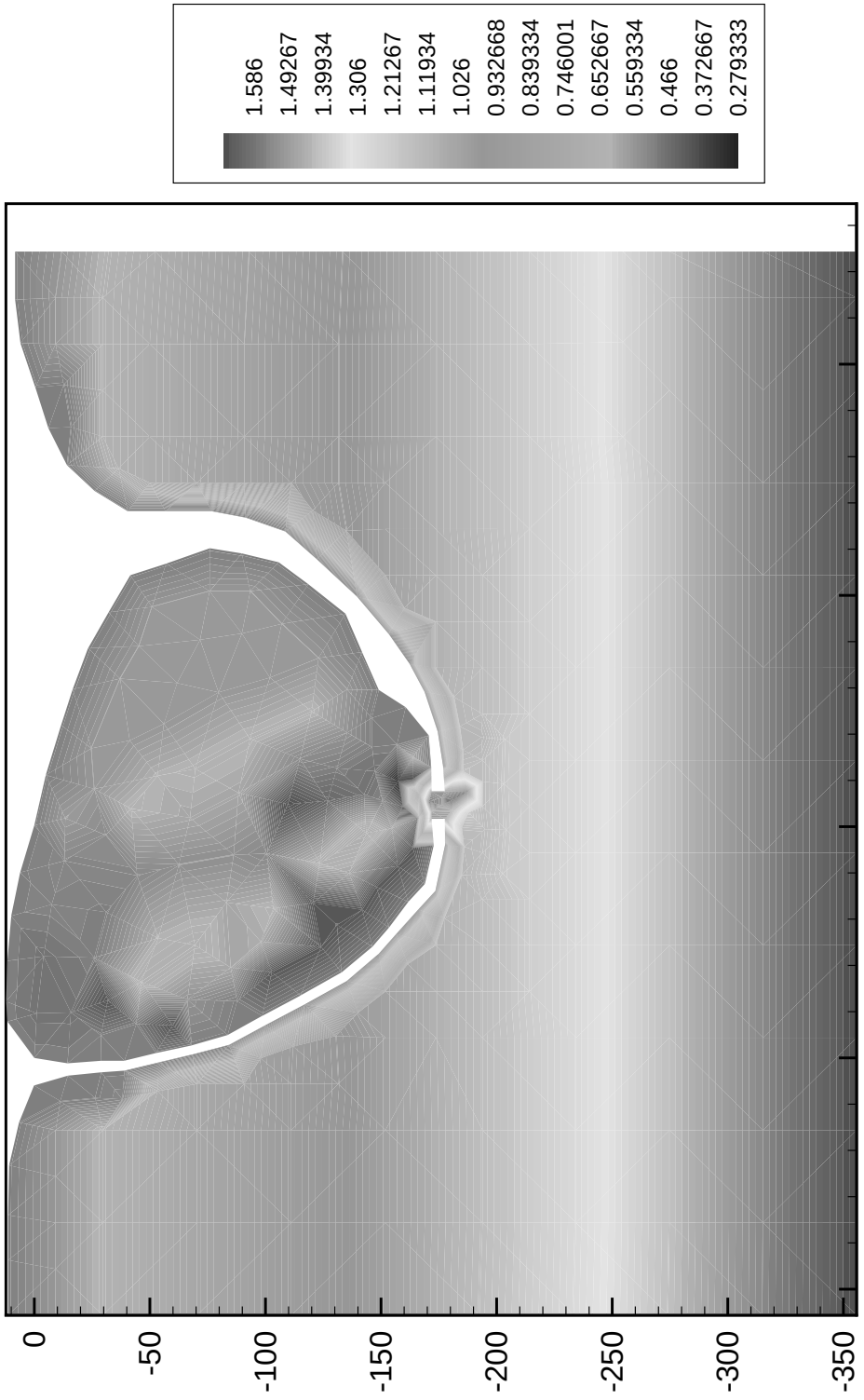

Fig. 10 Bathymetry of One Ali'i pond (m)

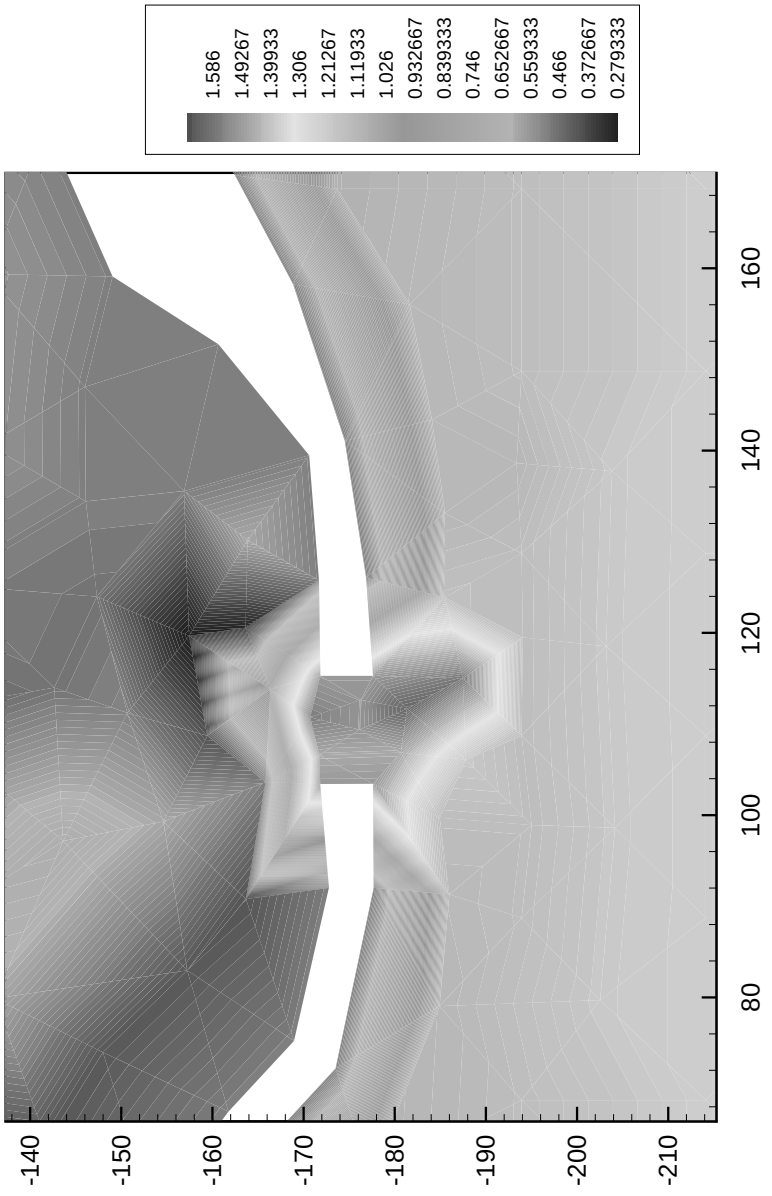

Fig. 11 Close up of bathymetry of One Ali'i pond (m)

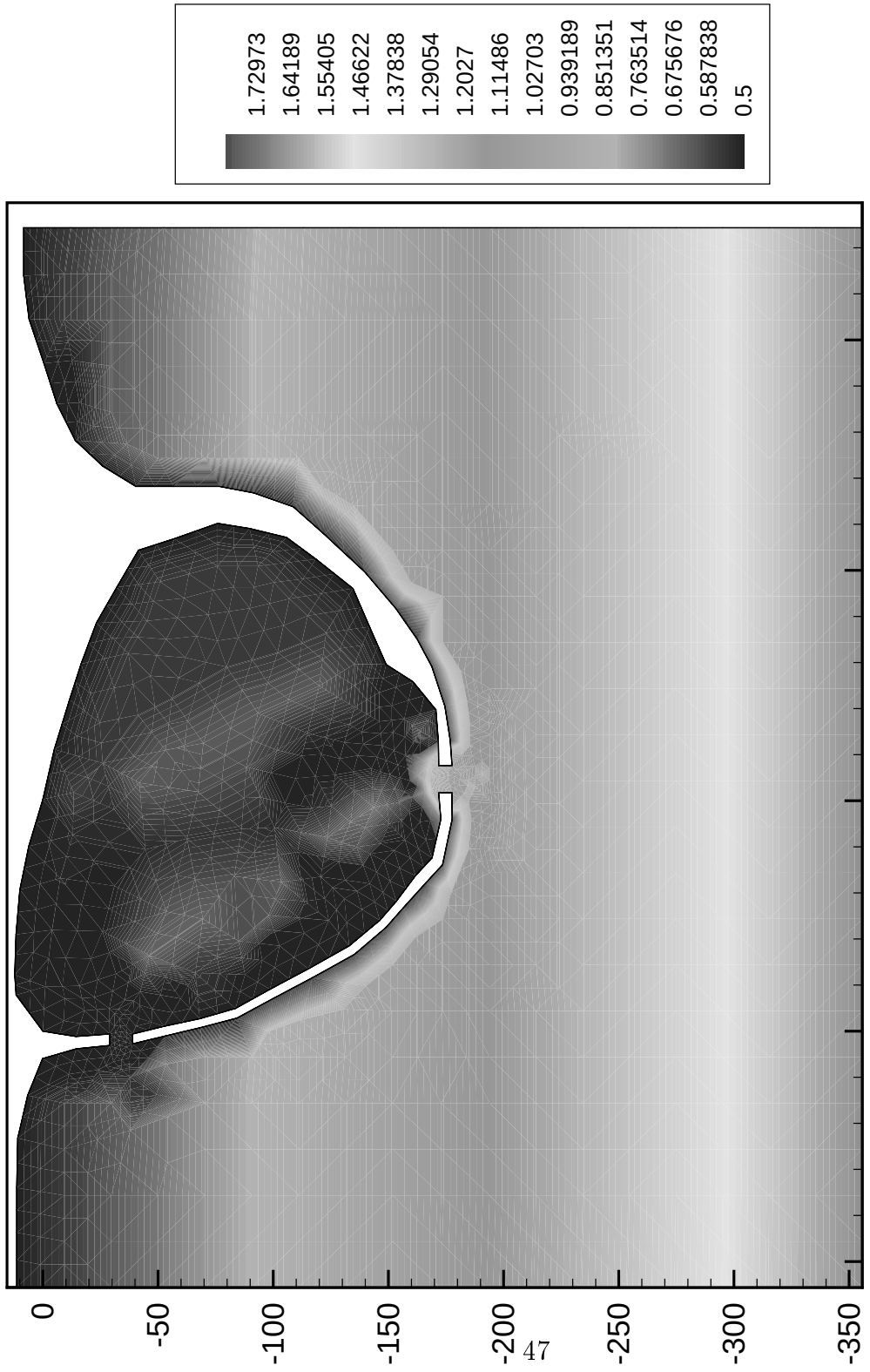

Fig. 12 Bathymetry of One Ali'i pond as used in computations (m)

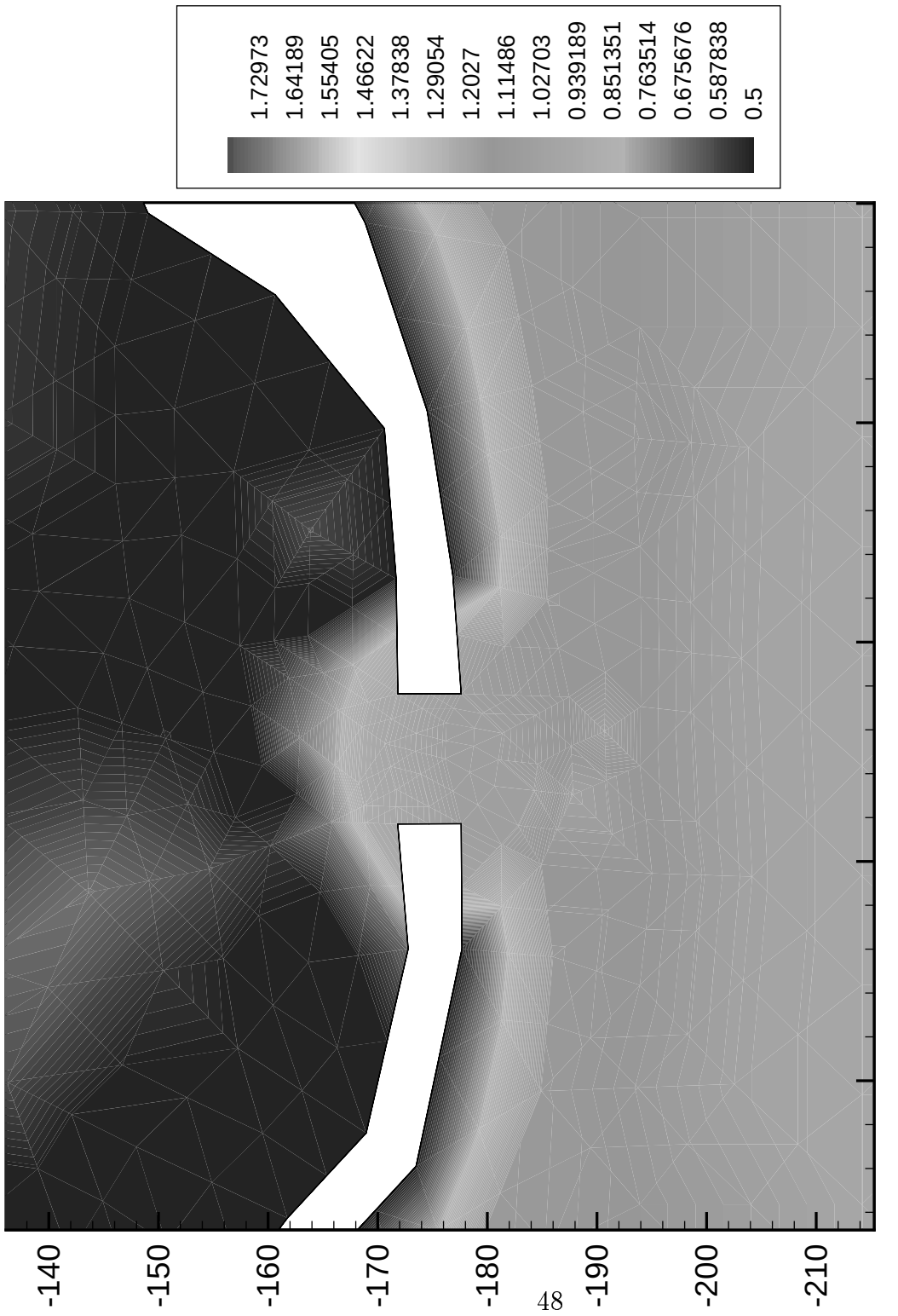

Fig. 13 Close up of bathymetry of One Ali'i pond as used in computations (m)

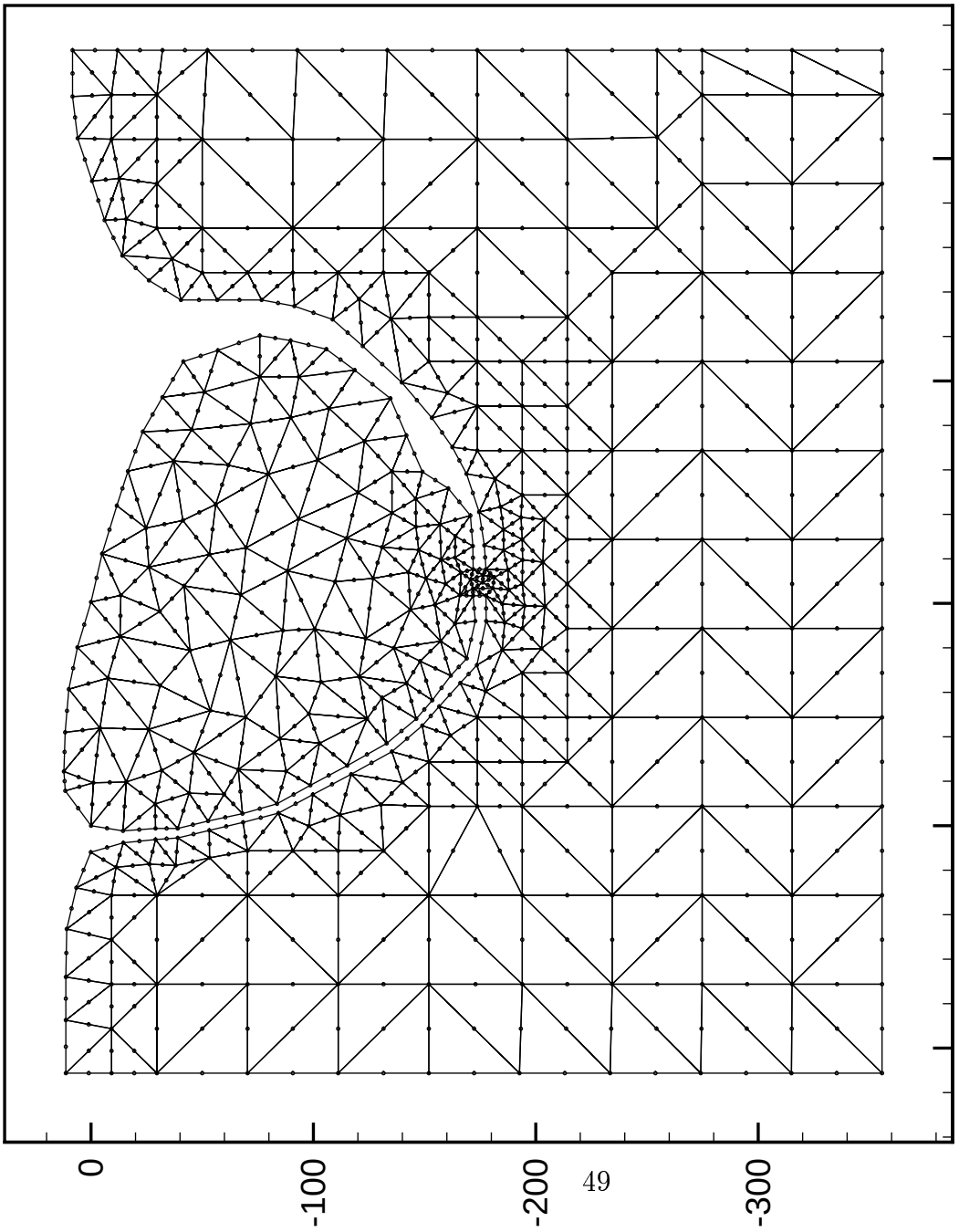

Fig. 14 Mesh of One Ali'i pond with one sluice gate

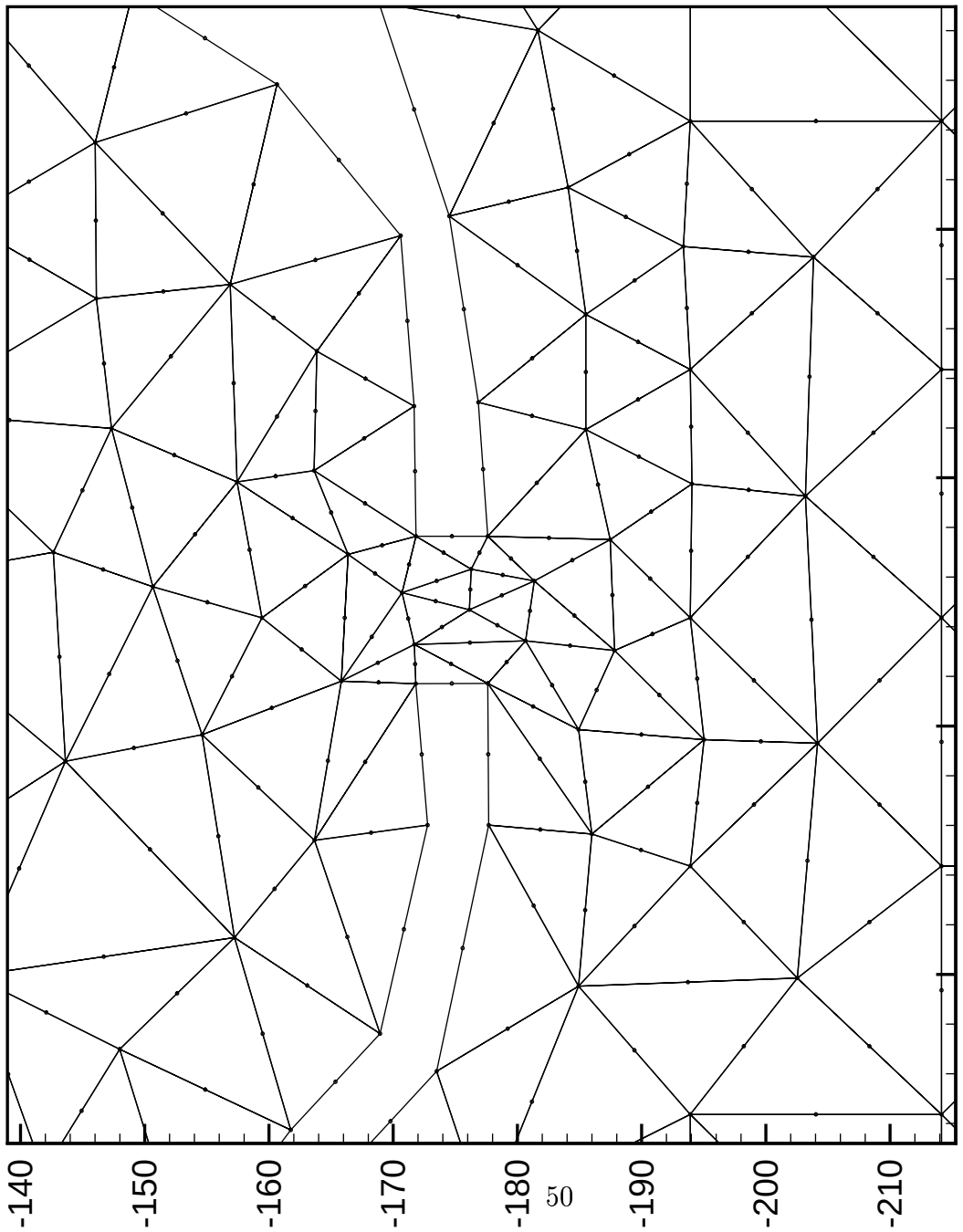

Fig. 15 Close up of mesh at sluice gate 1

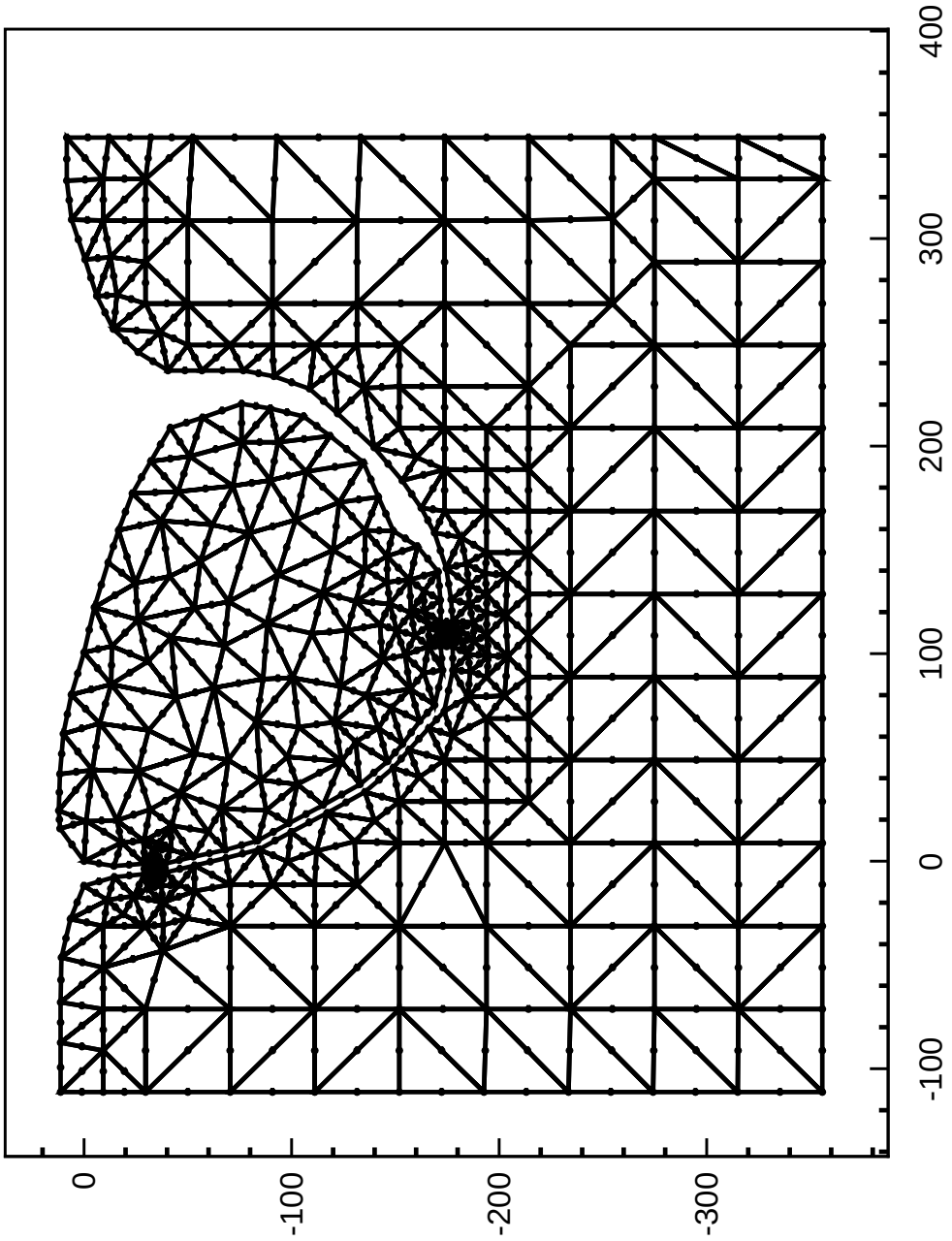

Fig. 16 Mesh of One Ali'i pond with two sluice gates

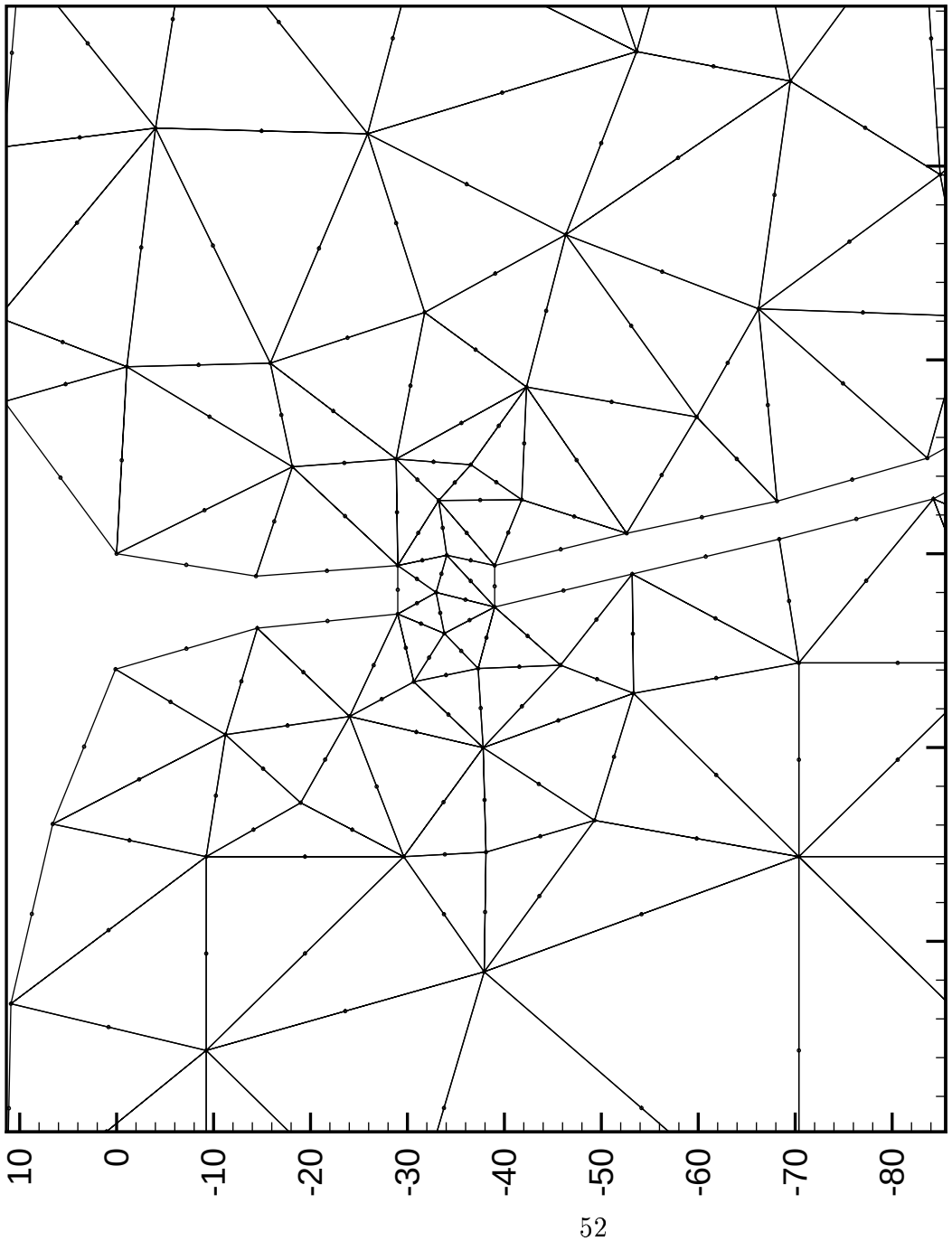

Fig. 17 Close up of sluice gate #2

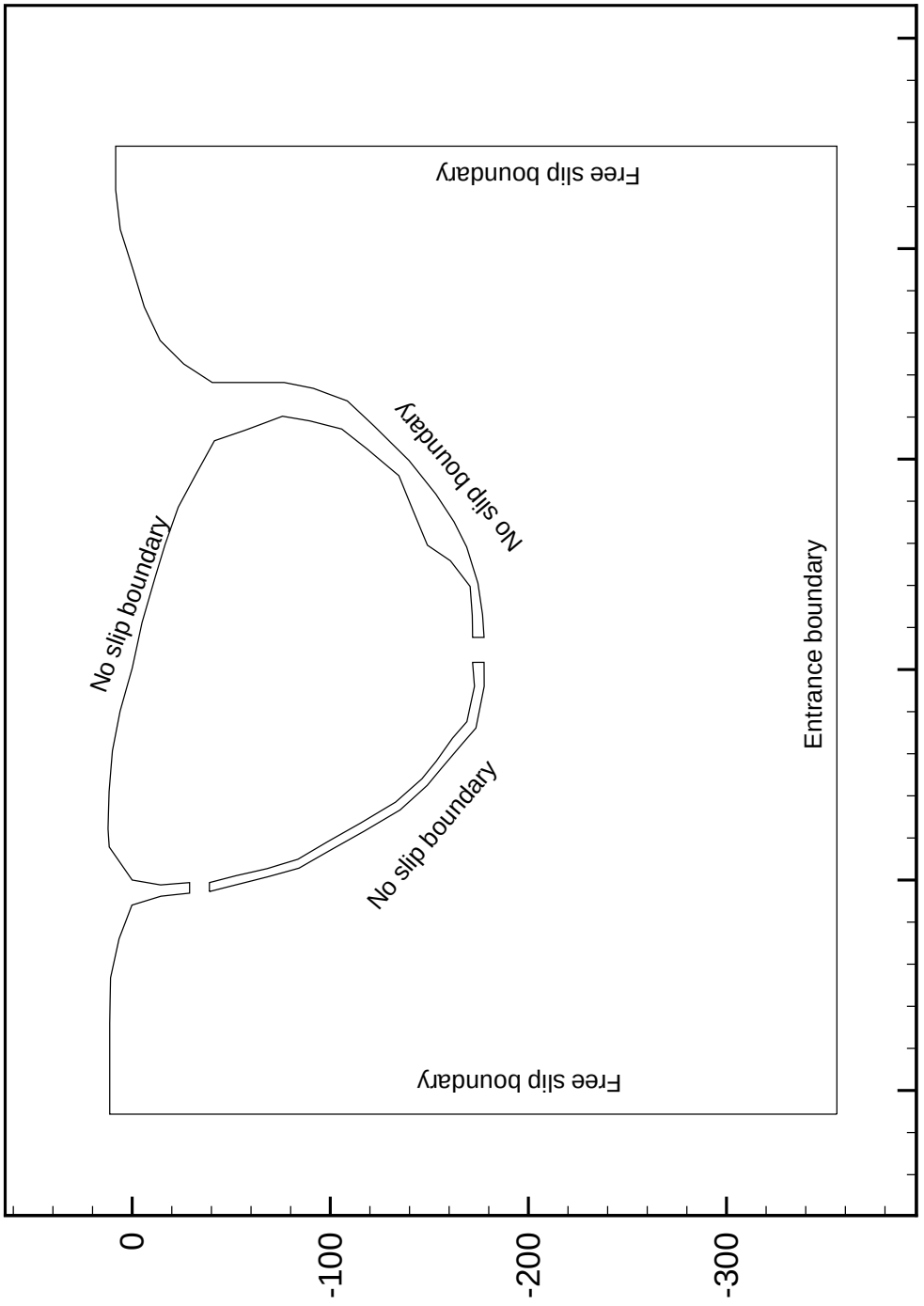

Fig. 18 Boundary conditions

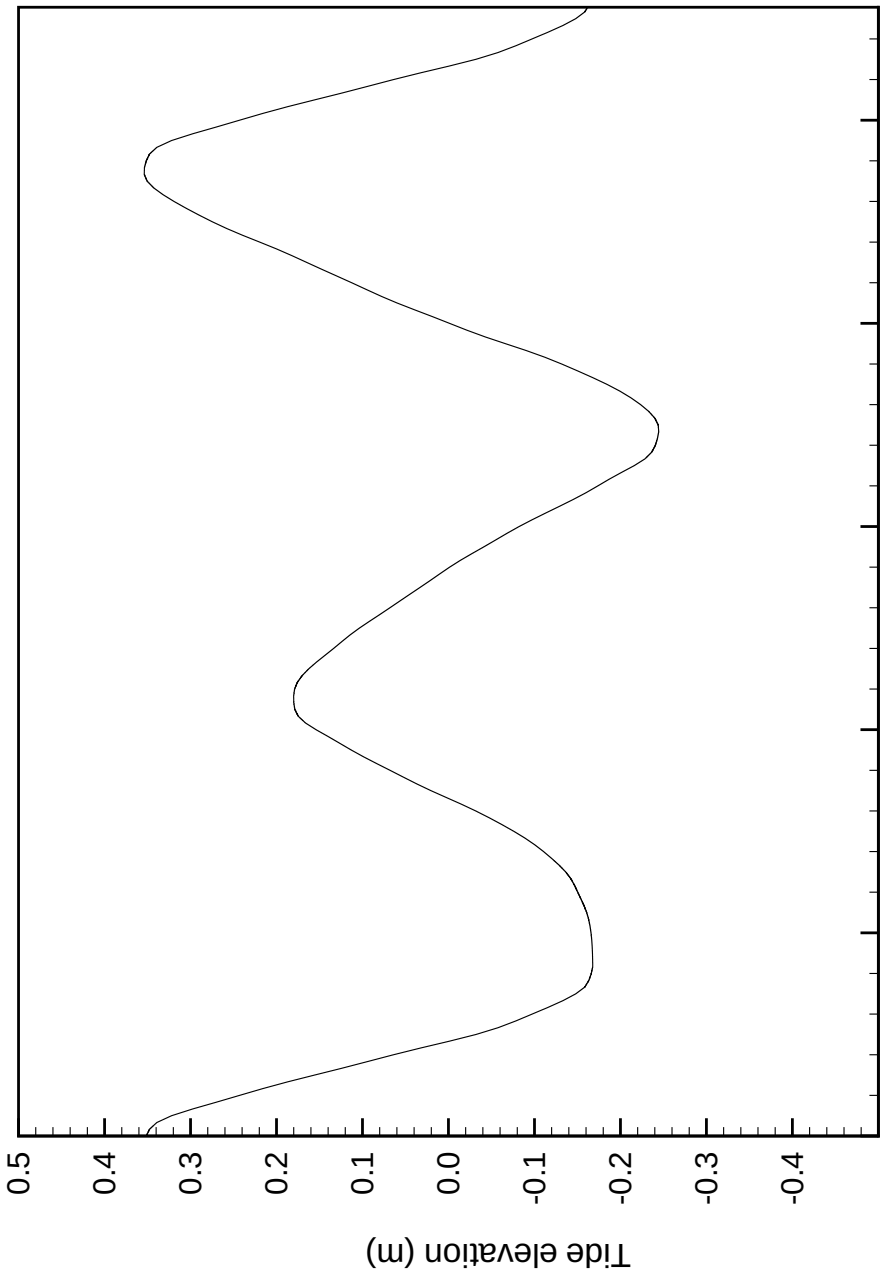

Fig. 19 Tidal elevations as used in computations

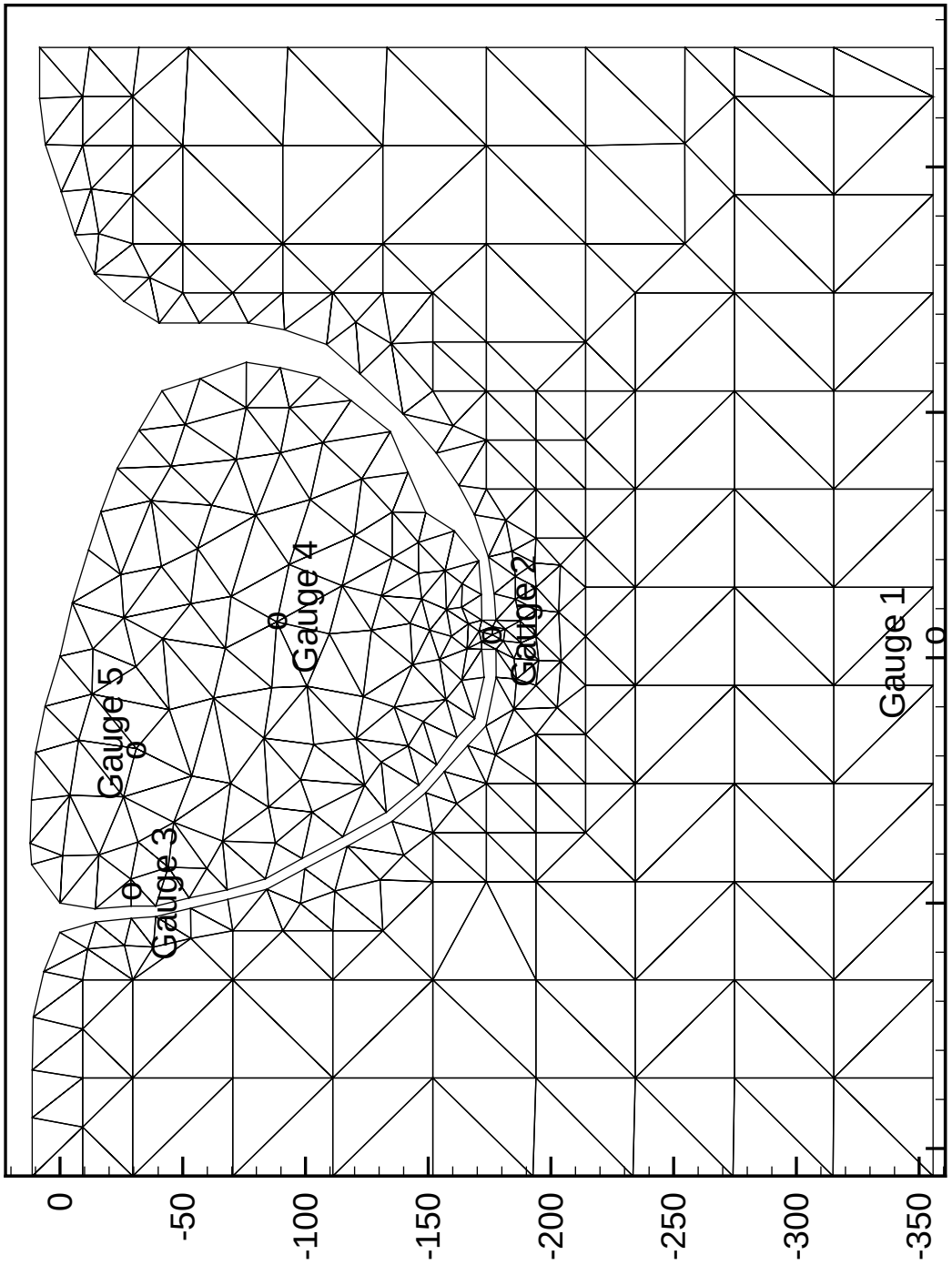

Fig 20. Location of numerical gauges (one gate case)

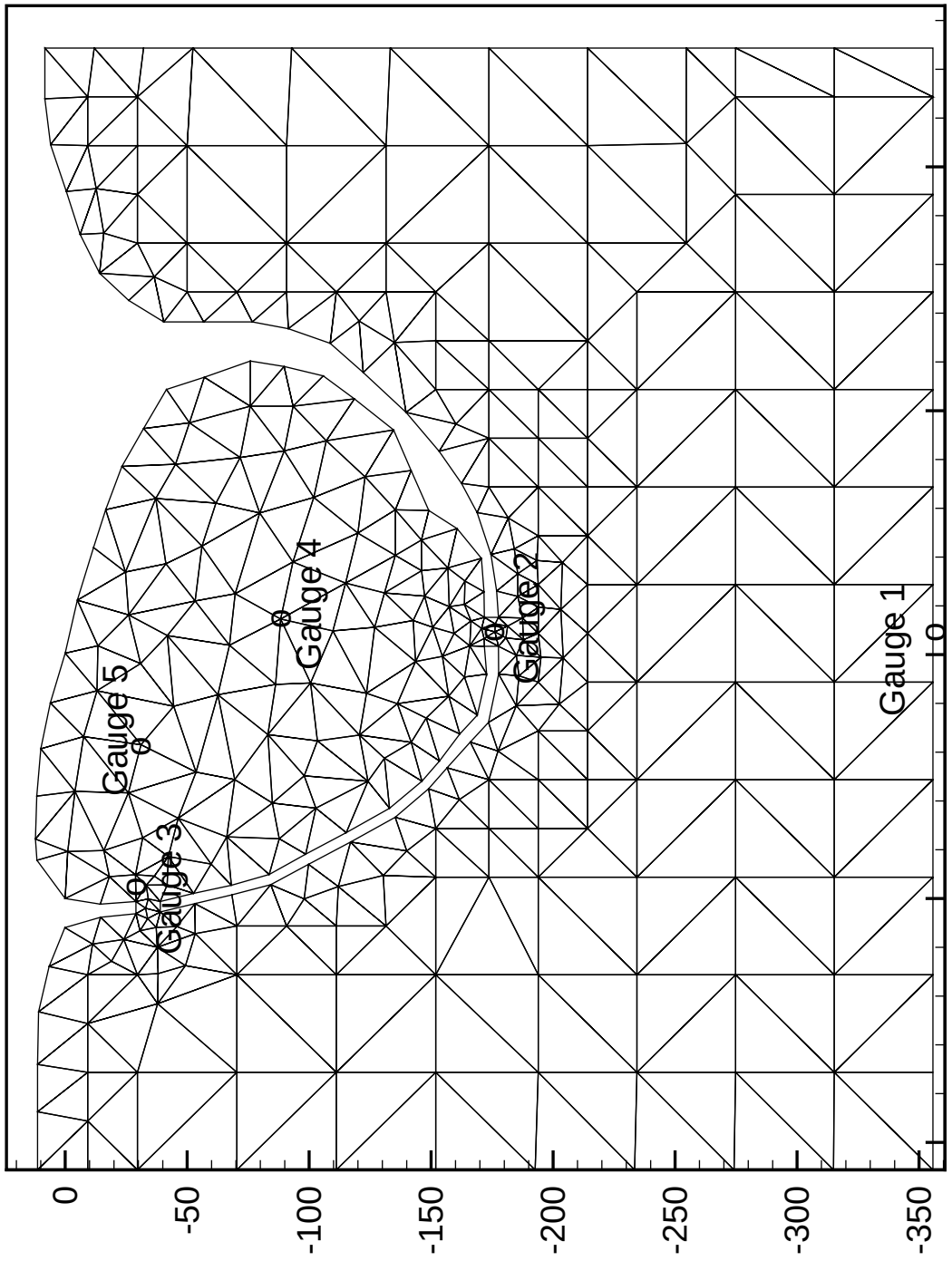

Fig 21. Location of numerical gauges (two gate case)

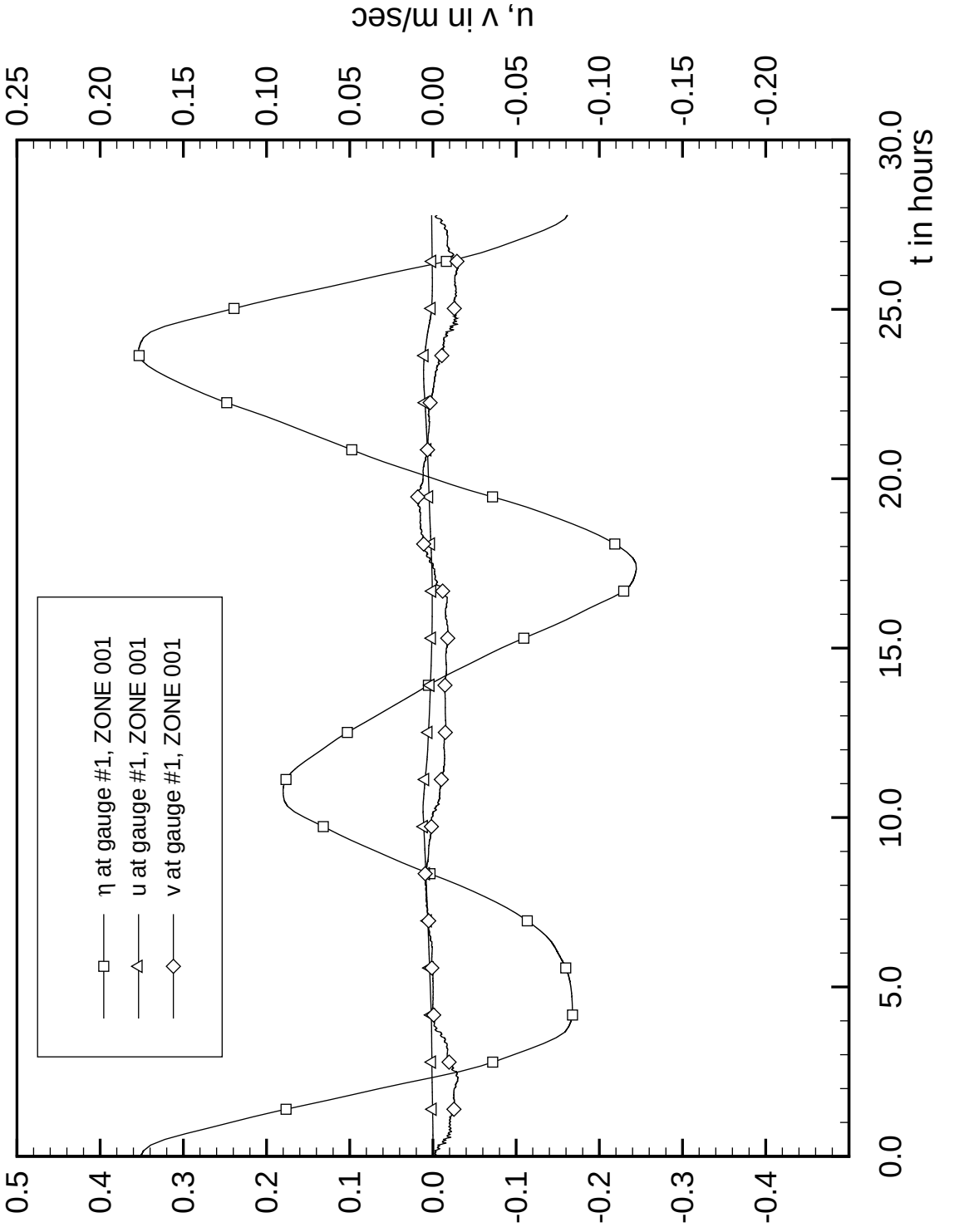

Fig. 22 Surface elevation and velocity components at gauge #1 (one sluice gate)

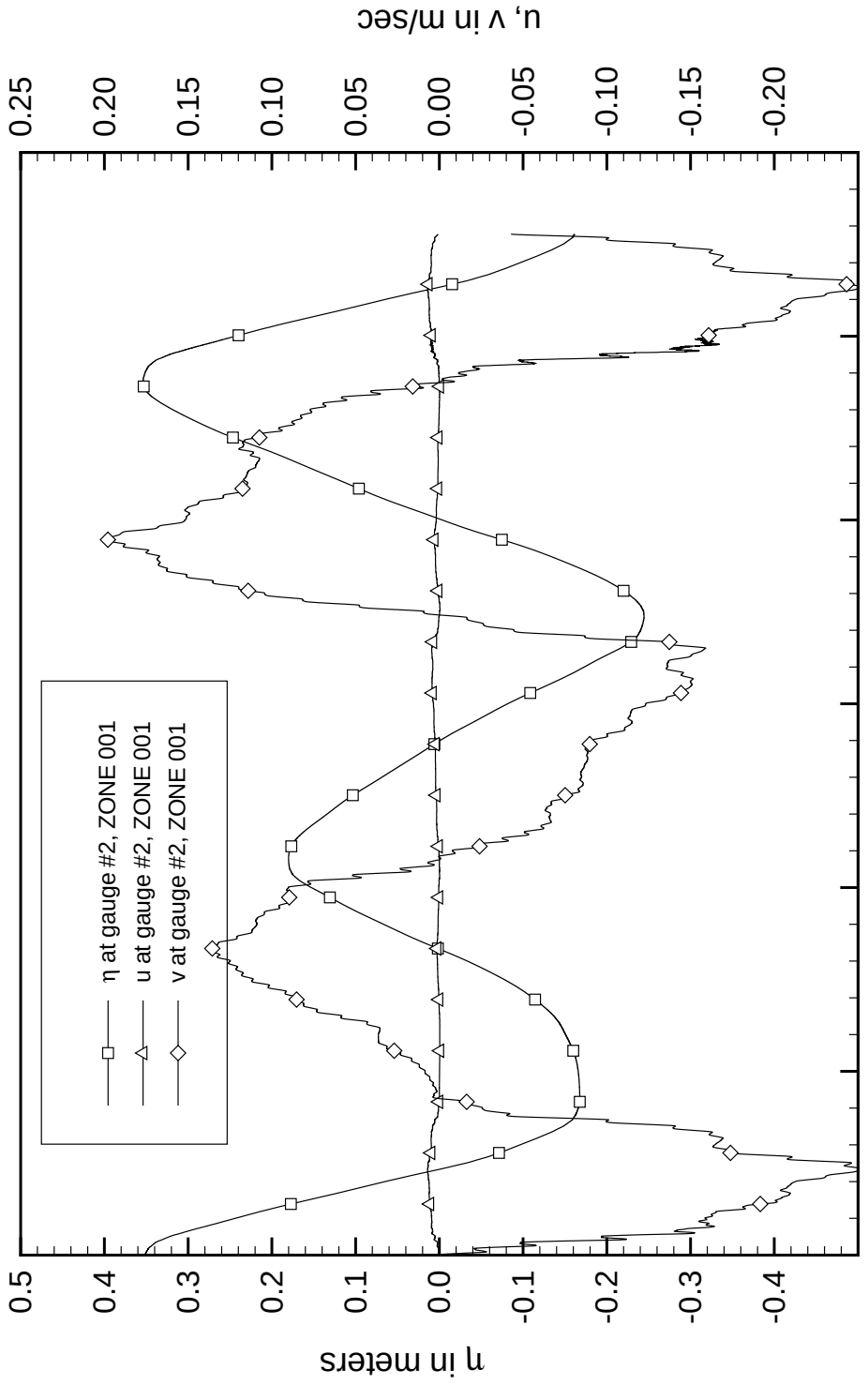

Fig. 23 Surface elevation and velocity components at gauge #2 (one sluice gate)

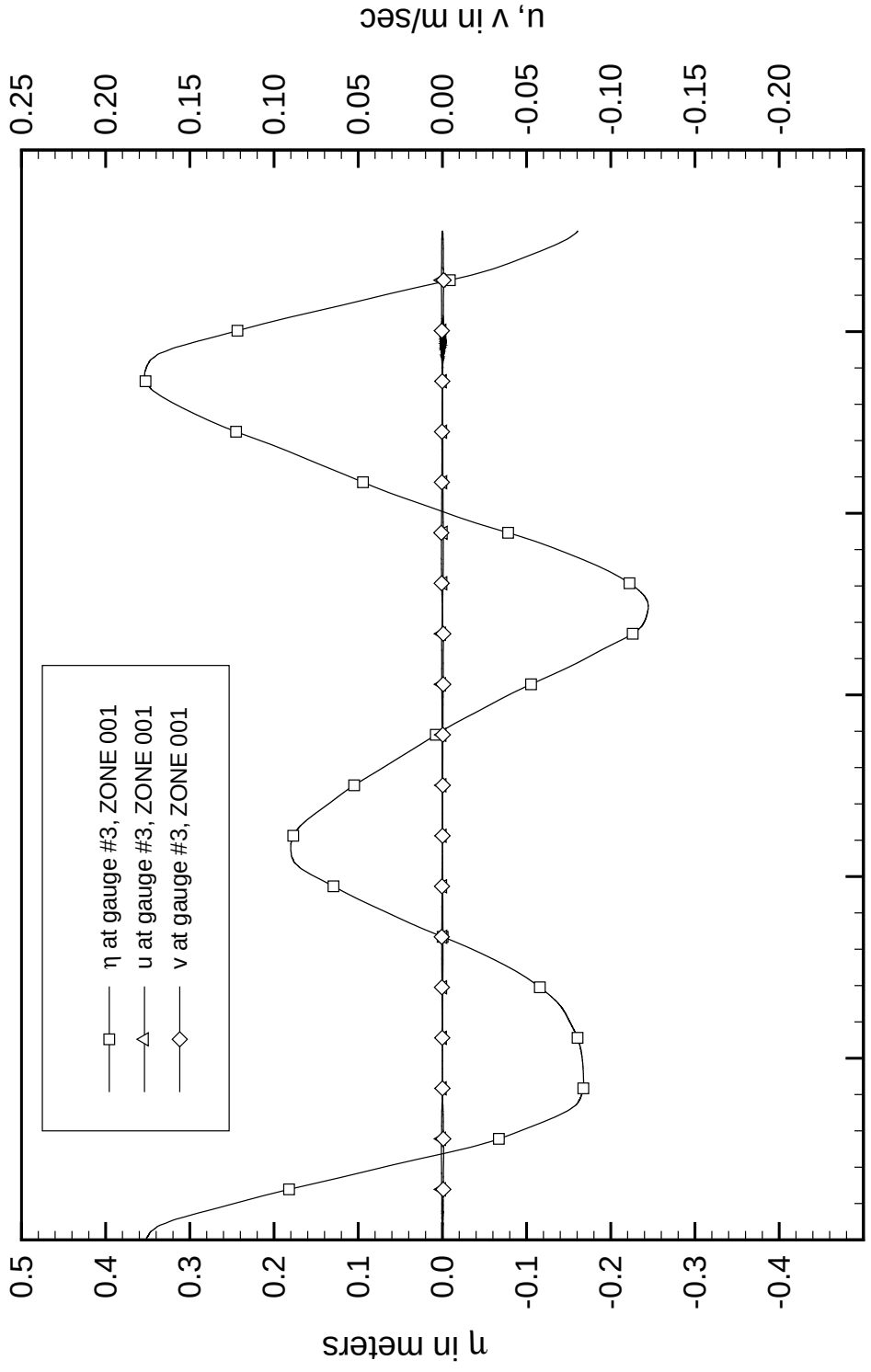

Fig. 24 Surface elevation and velocity components at gauge #3 (one sluice gate)

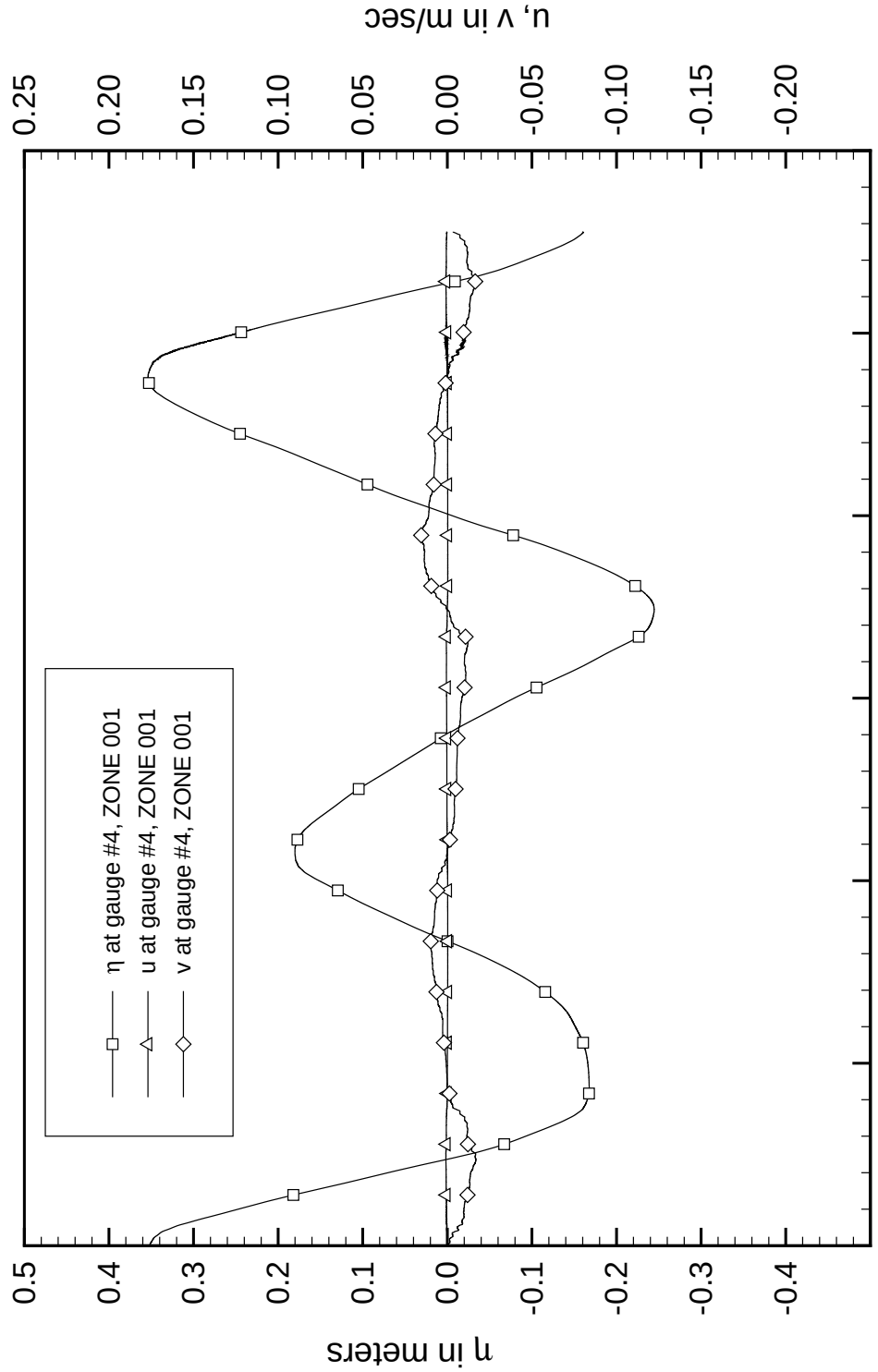

Fig. 25 Surface elevation and velocity components at gauge #4 (one sluice gate)

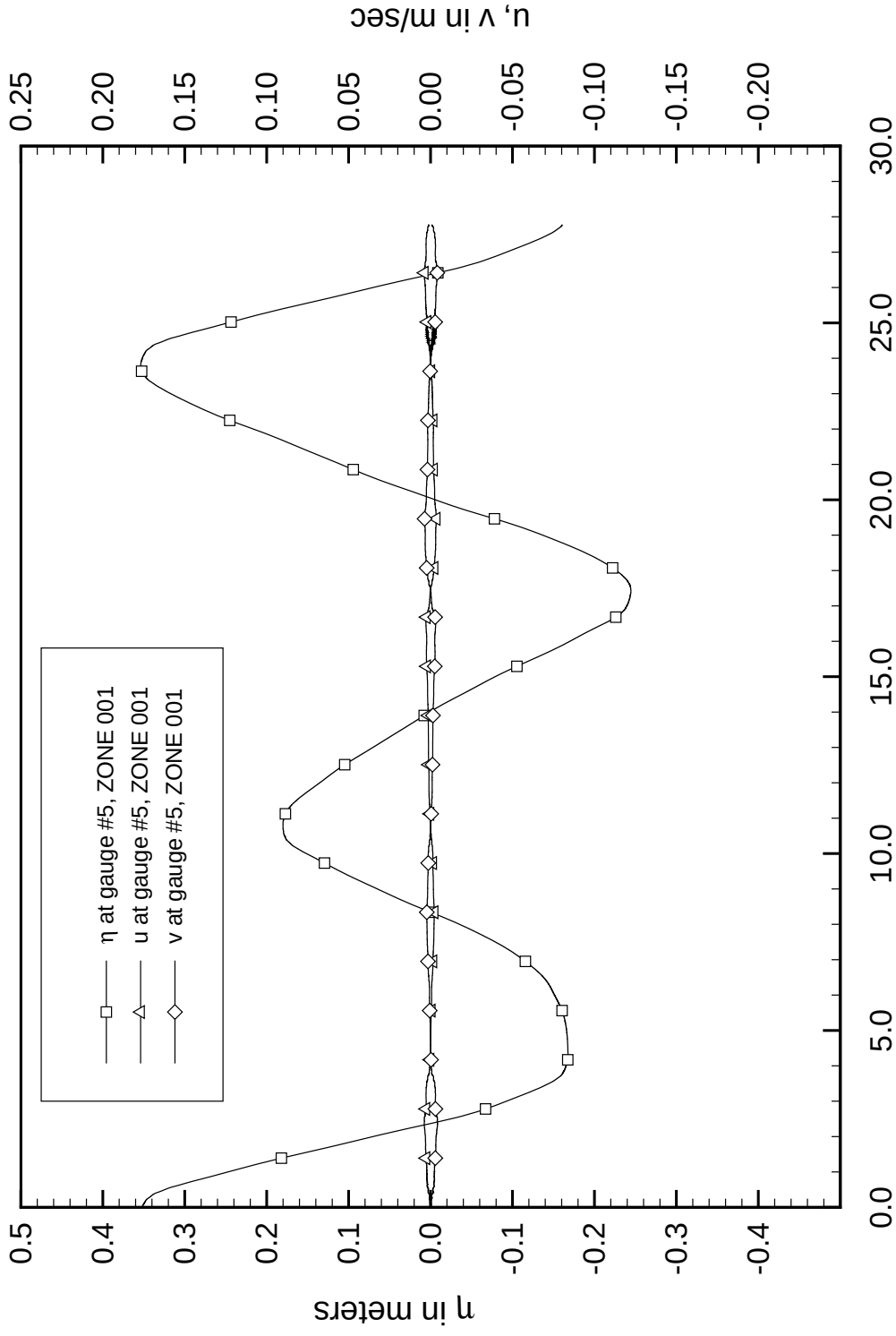

Fig. 26 Surface elevation and velocity components at gauge #5 (one sluice gate)

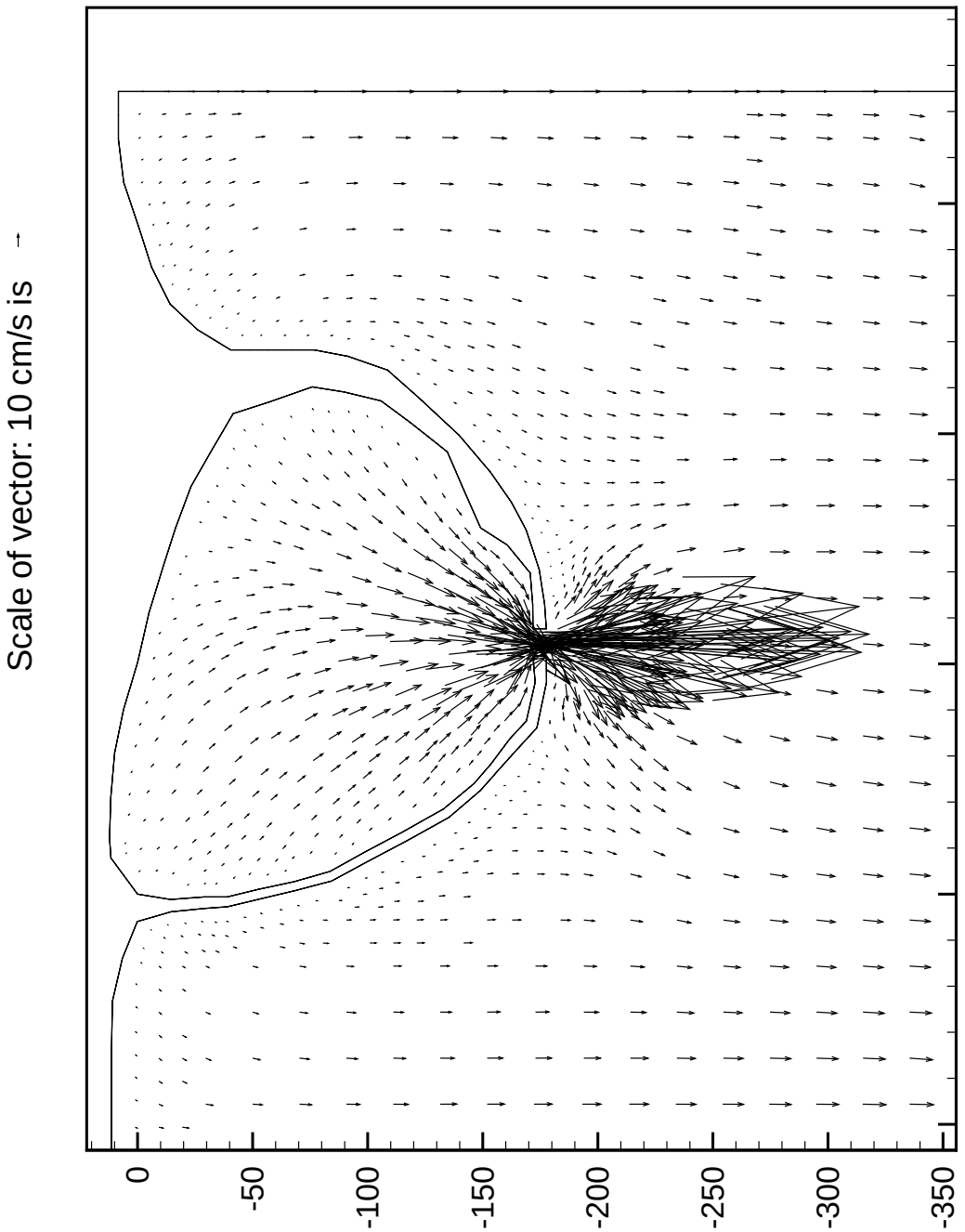

Fig. 27 Ebb tide, t=2 hrs 20 minutes

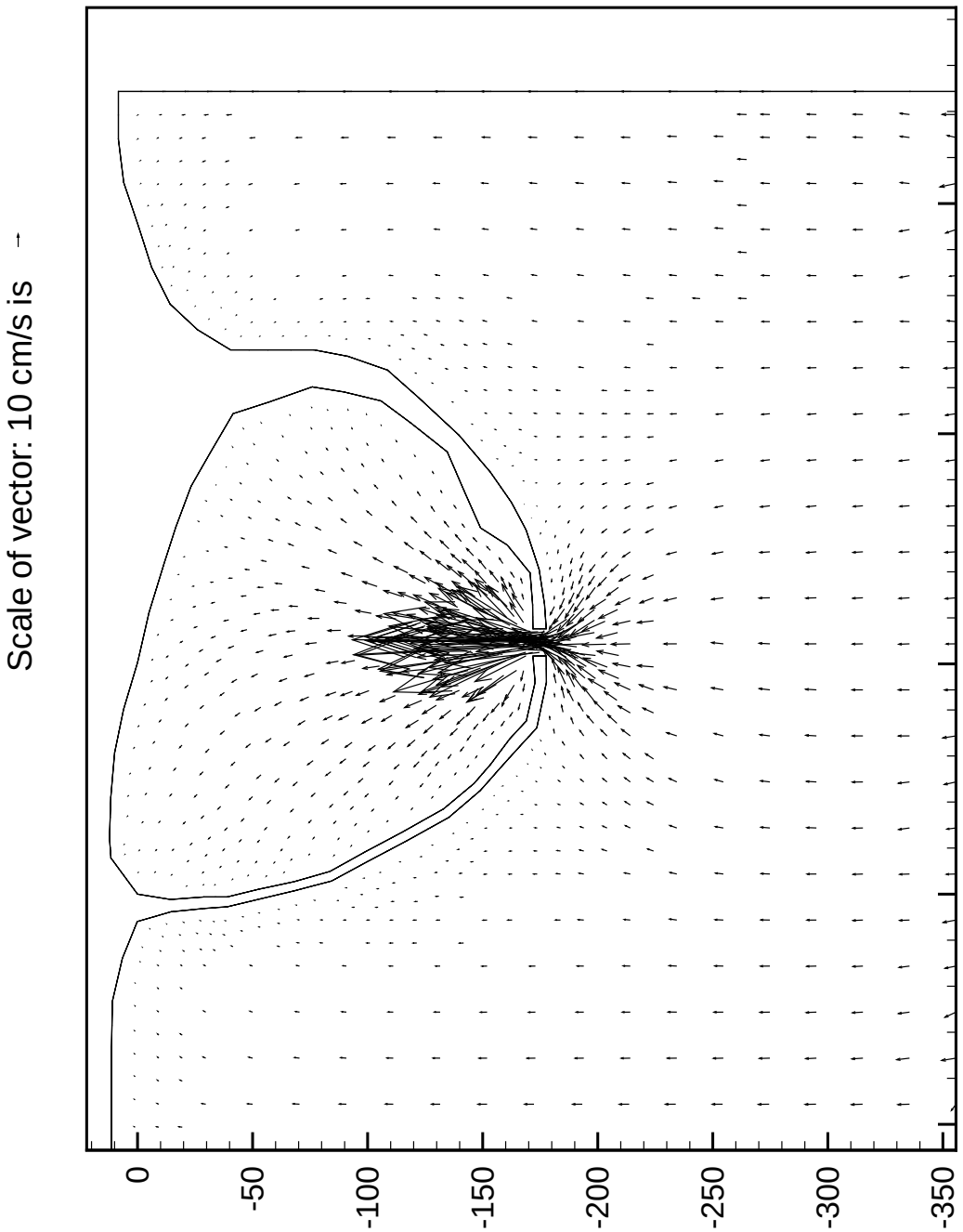

Fig. 29 Flood tide, t=8 hrs 17 minutes

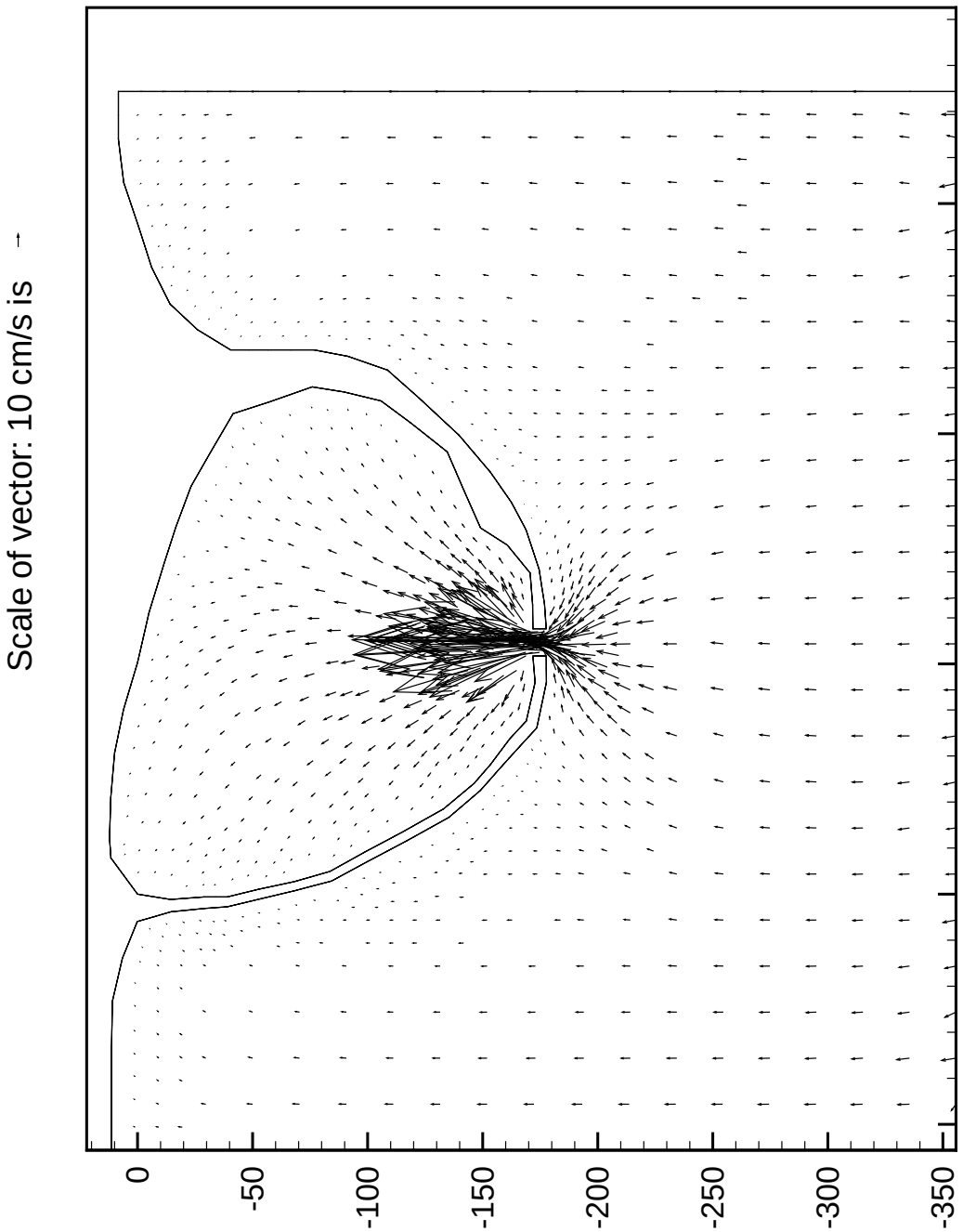

Fig. 29 Flood tide, t=8 hrs 17 minutes

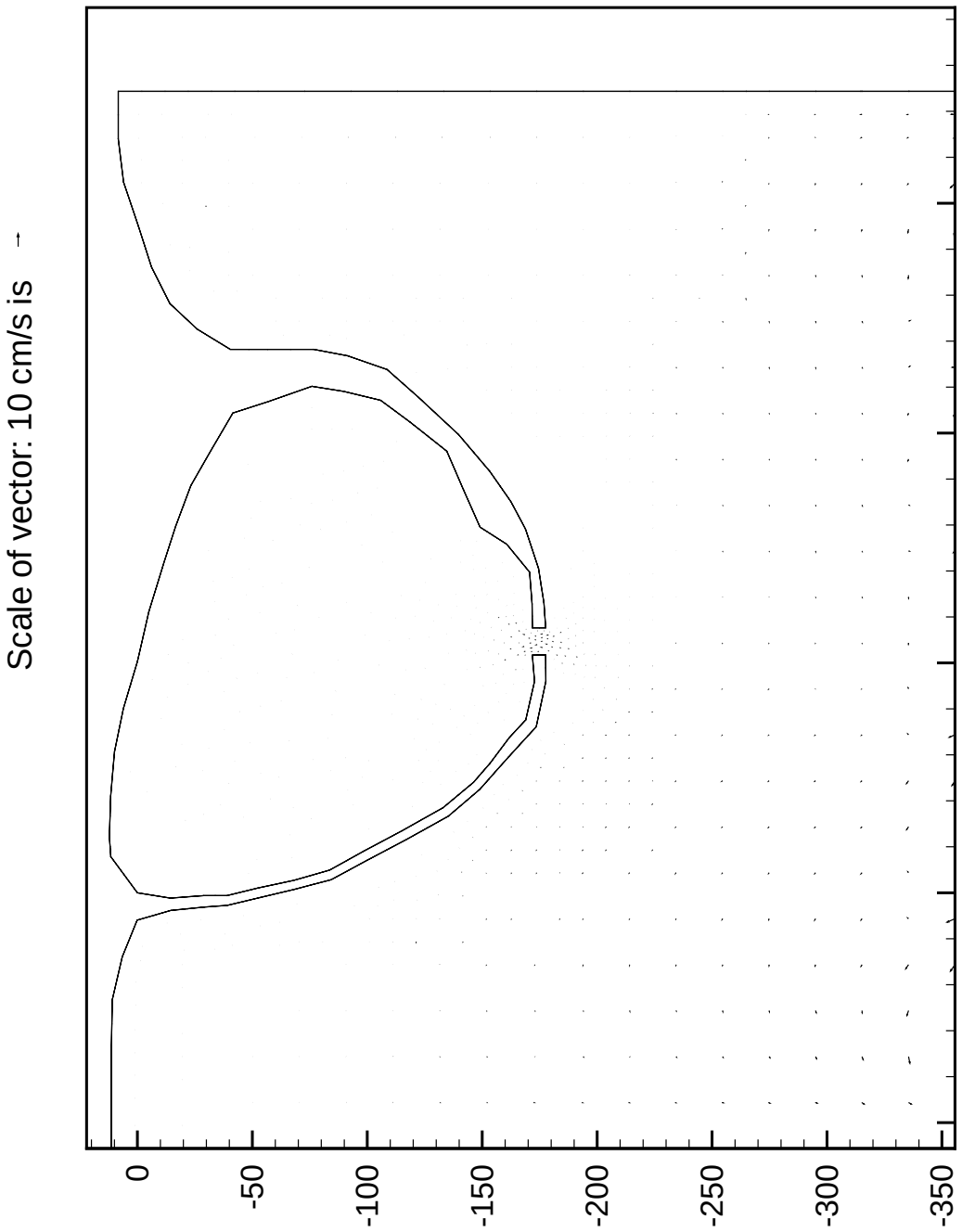

Fig. 30 Reversing tide, t=10 hrs 51 minutes

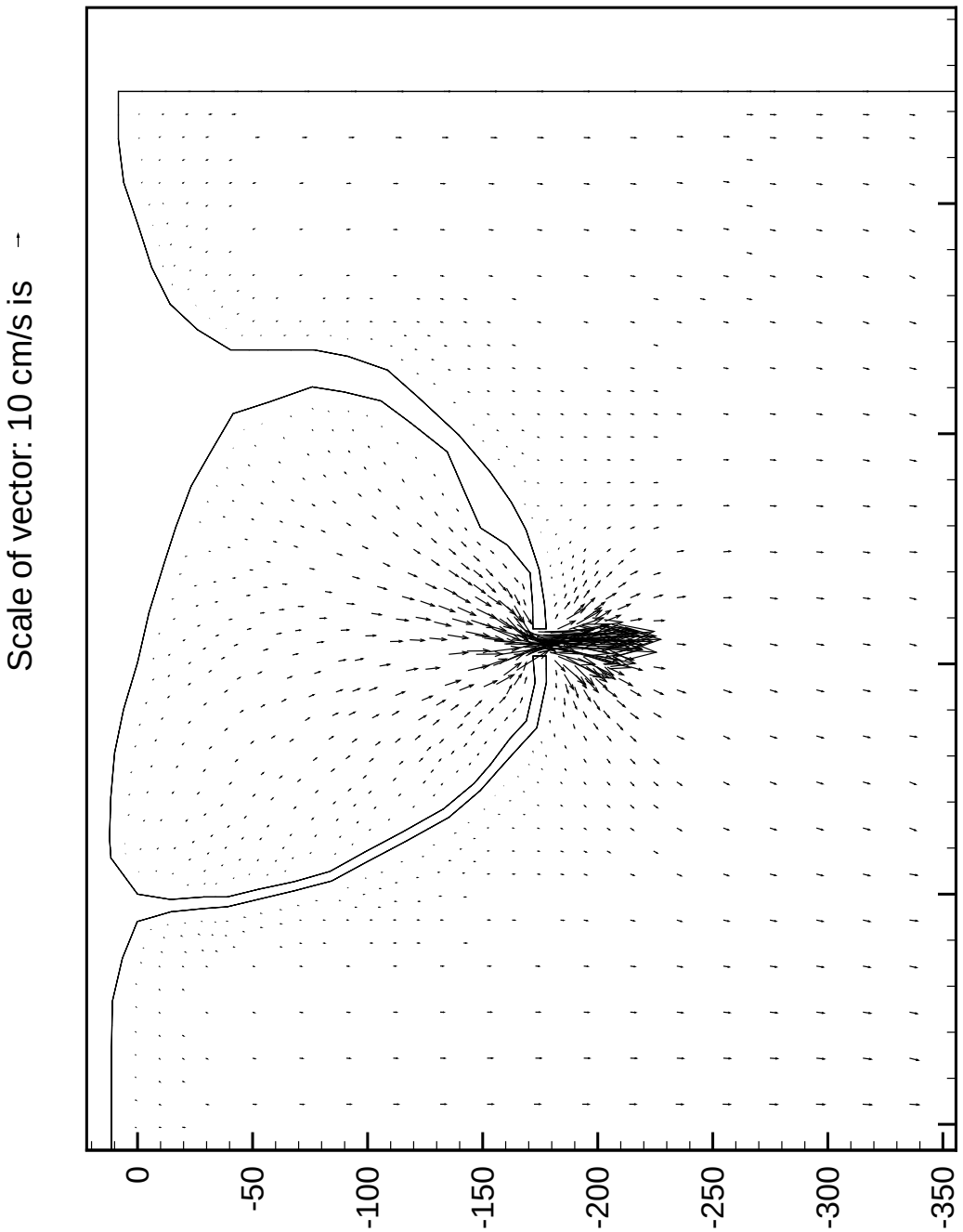

Fig. 31 Ebb tide, t=13 hrs 58 minutes

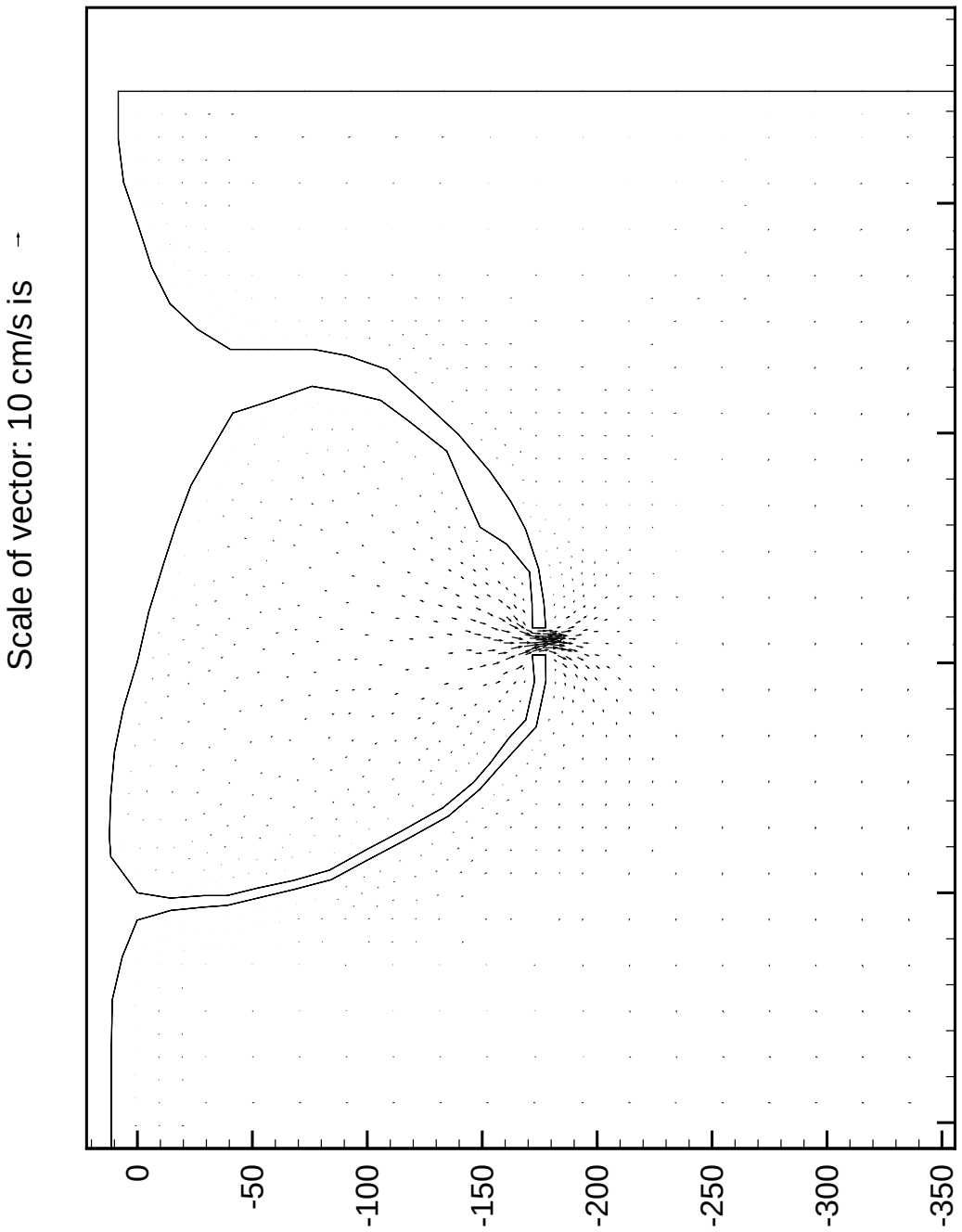

Fig. 32 Reversing tide, t=17 hrs 22 minutes

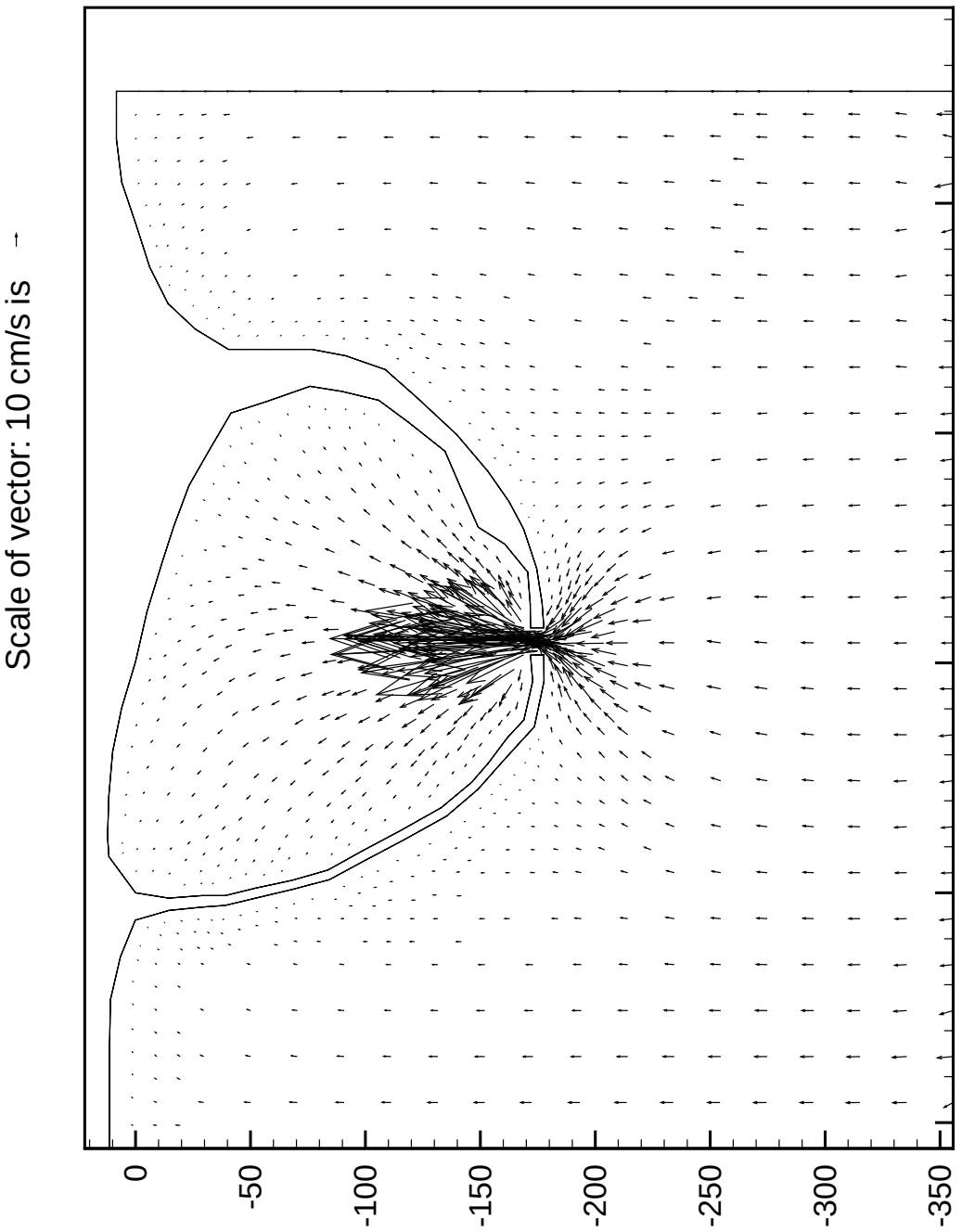

Fig. 33 Flood tide, t=20 hrs 2 minutes

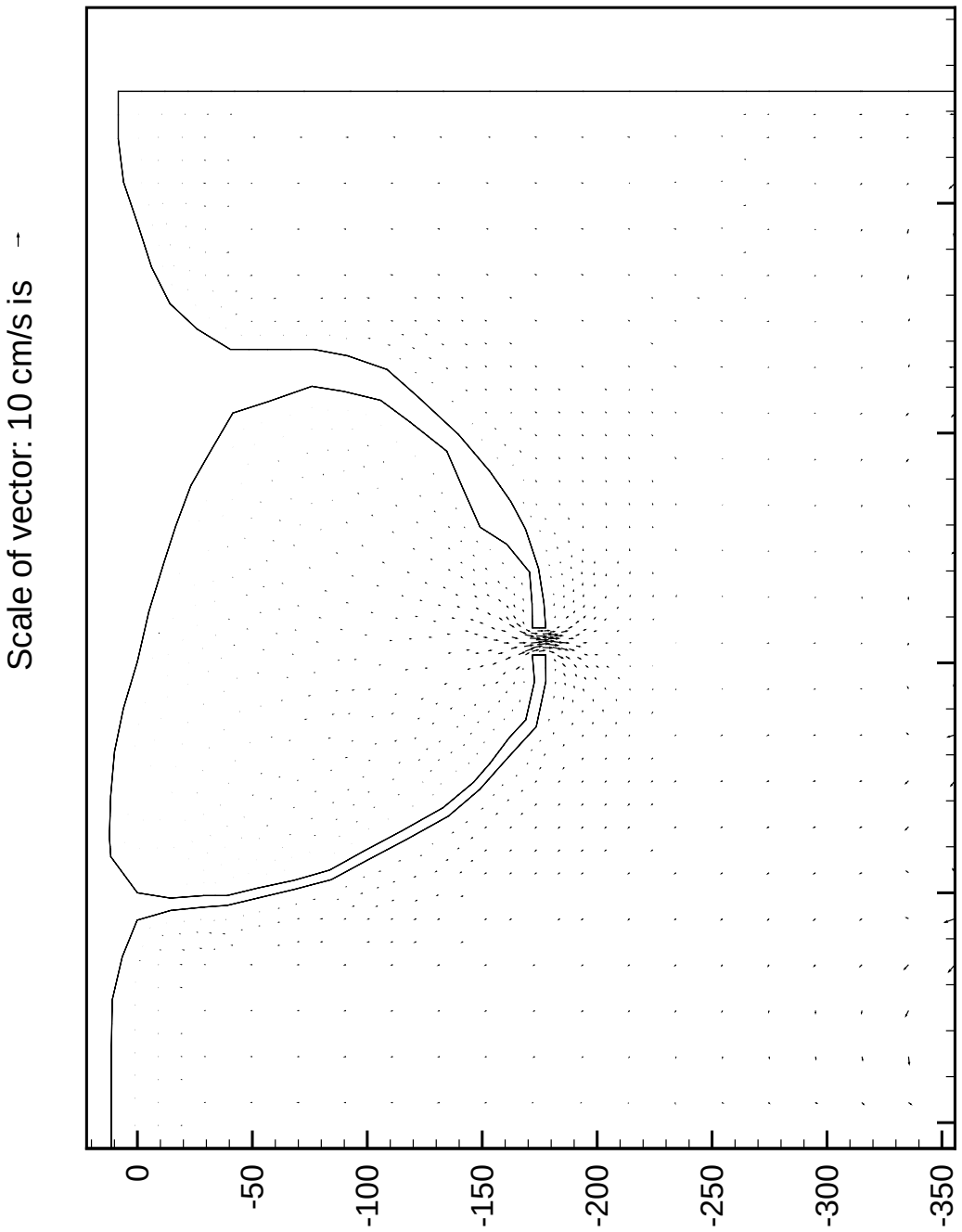

Fig. 34 Reversing tide, t=24 hrs 0 minutes

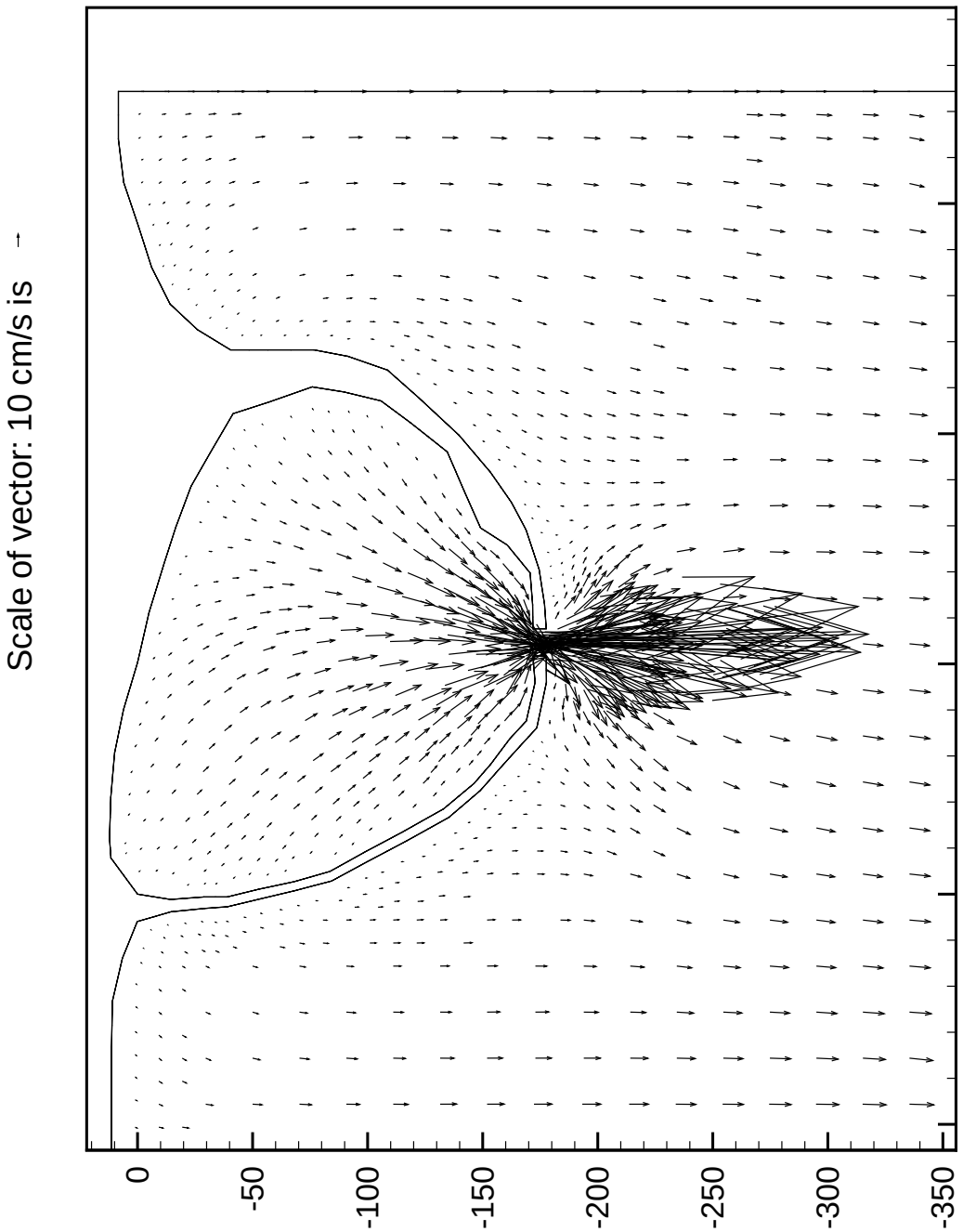

Fig. 35 Ebb tide, t=26 hrs 26 minutes

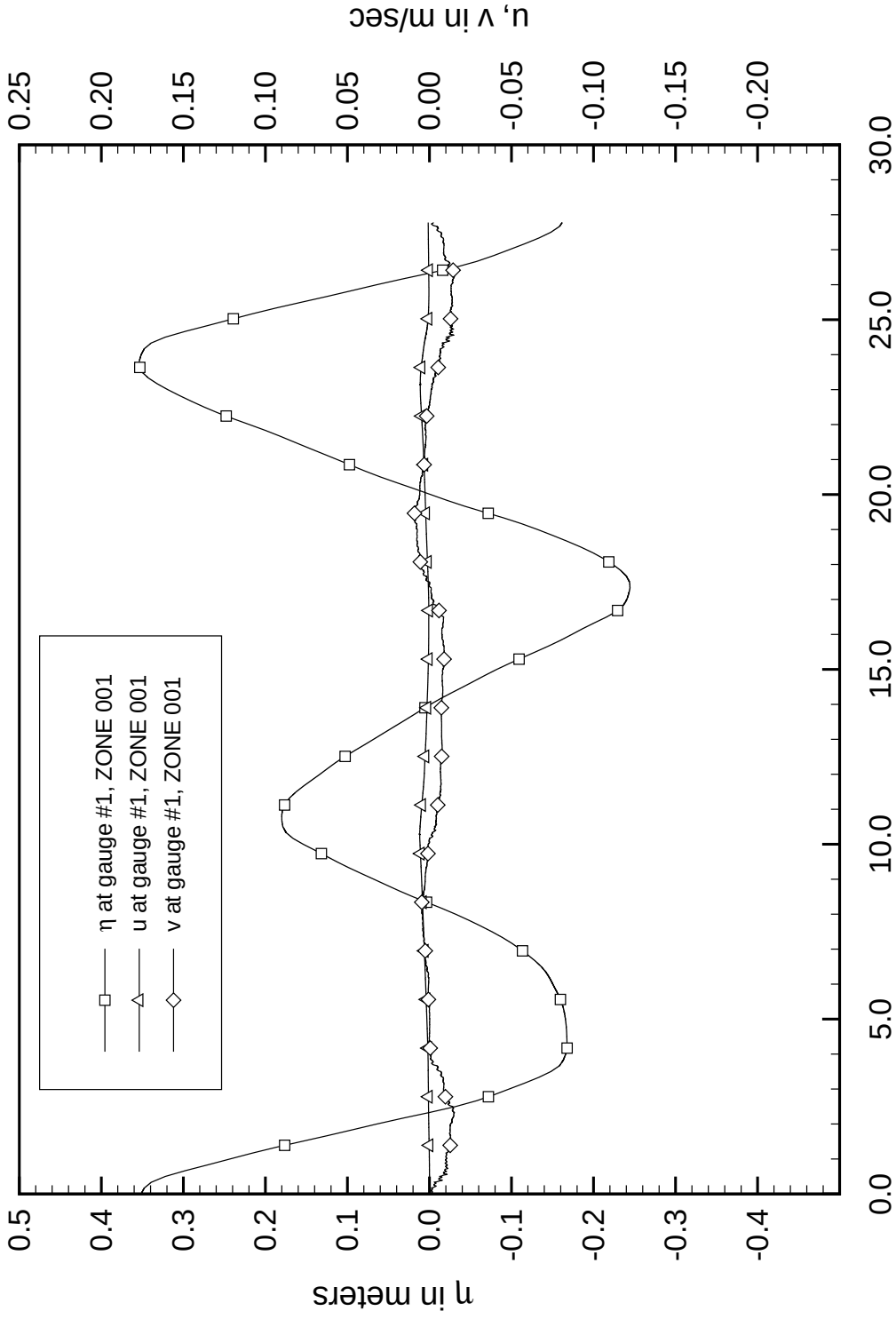

Fig. 36 Surface elevation and velocity components at gauge #1 (two sluice gates)

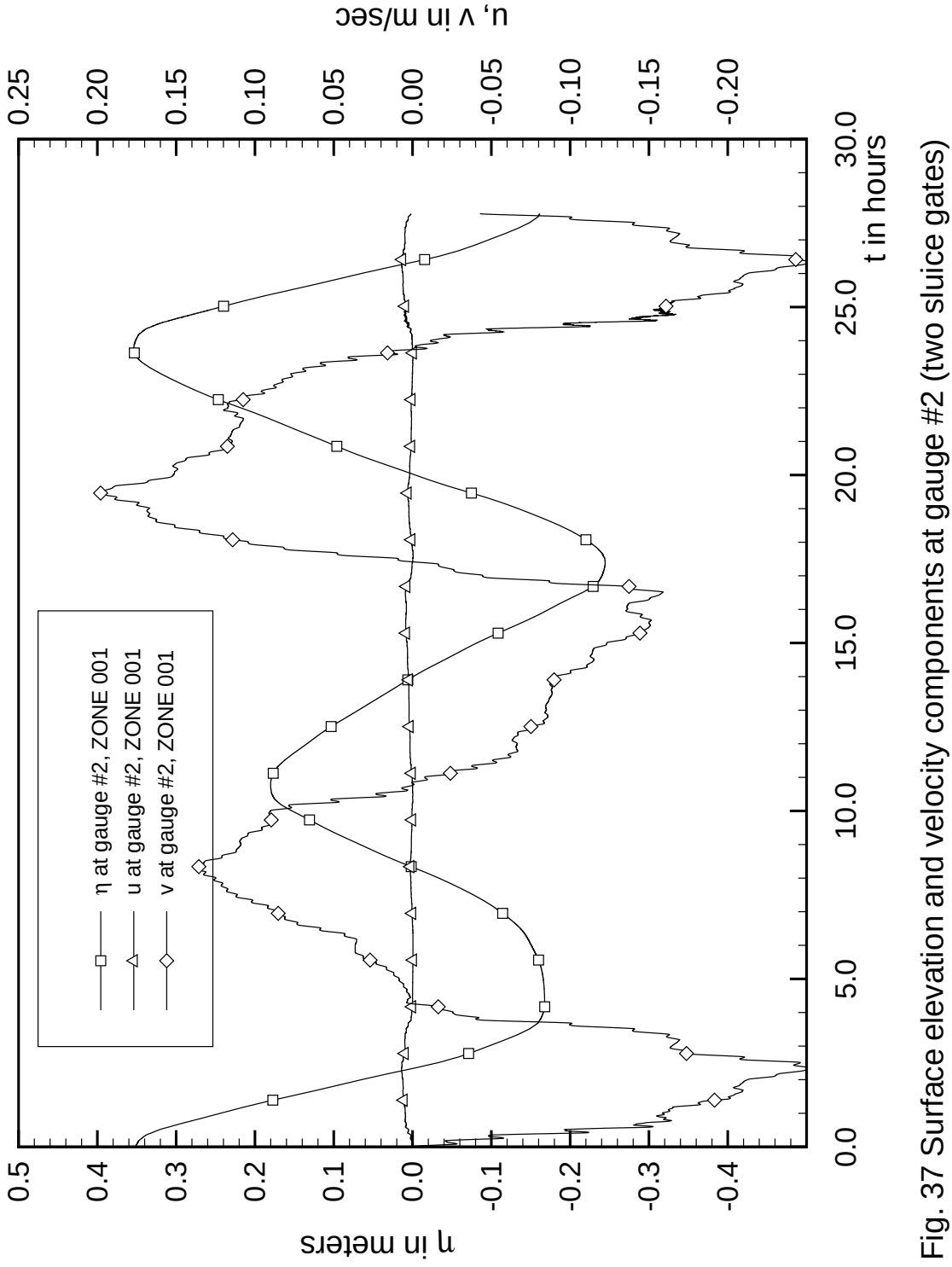

Fig. 37 Surface elevation and velocity components at gauge #2 (two sluice gates)

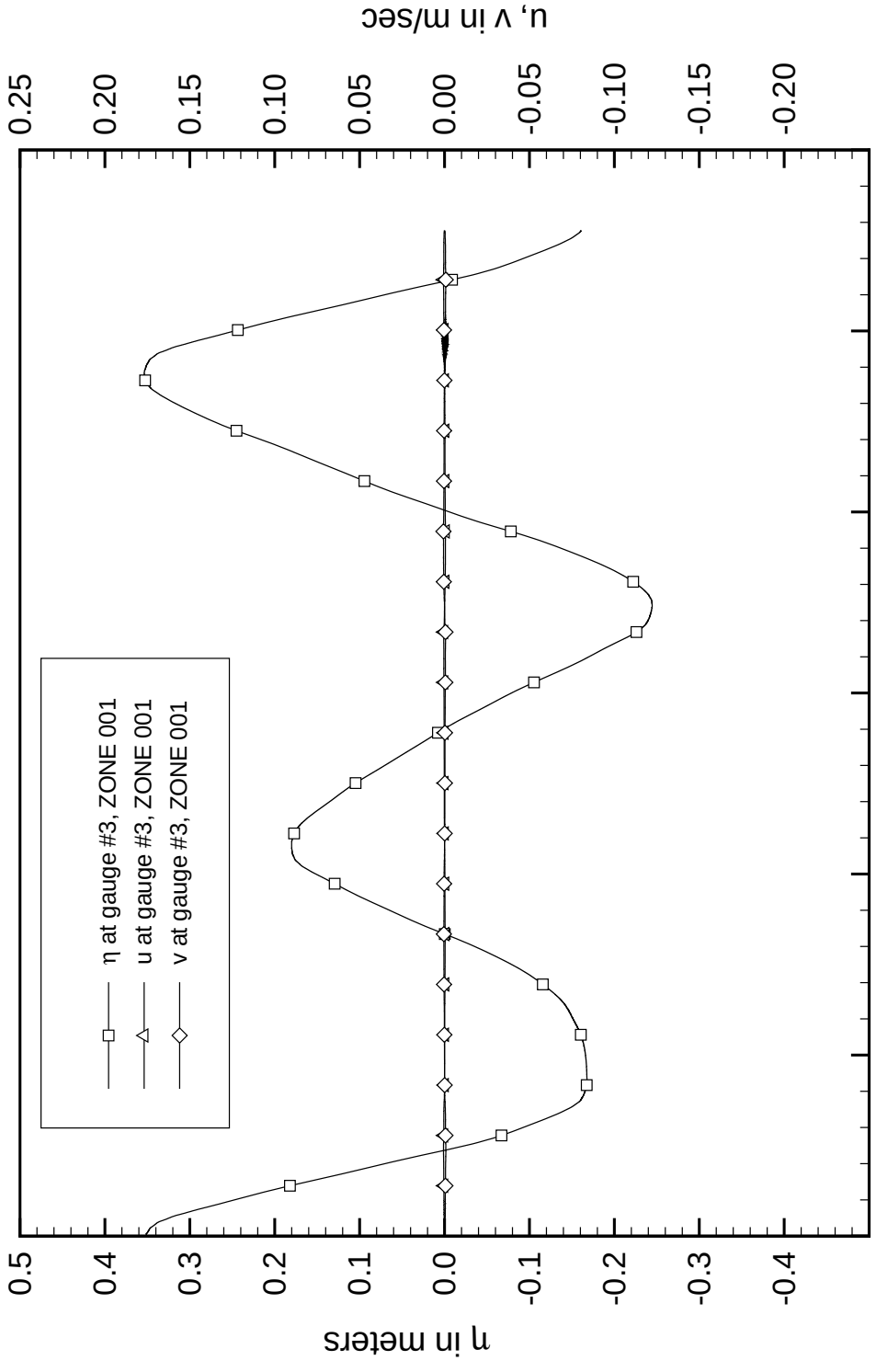

Fig. 38 Surface elevation and velocity components at gauge #3 (two sluice gates)

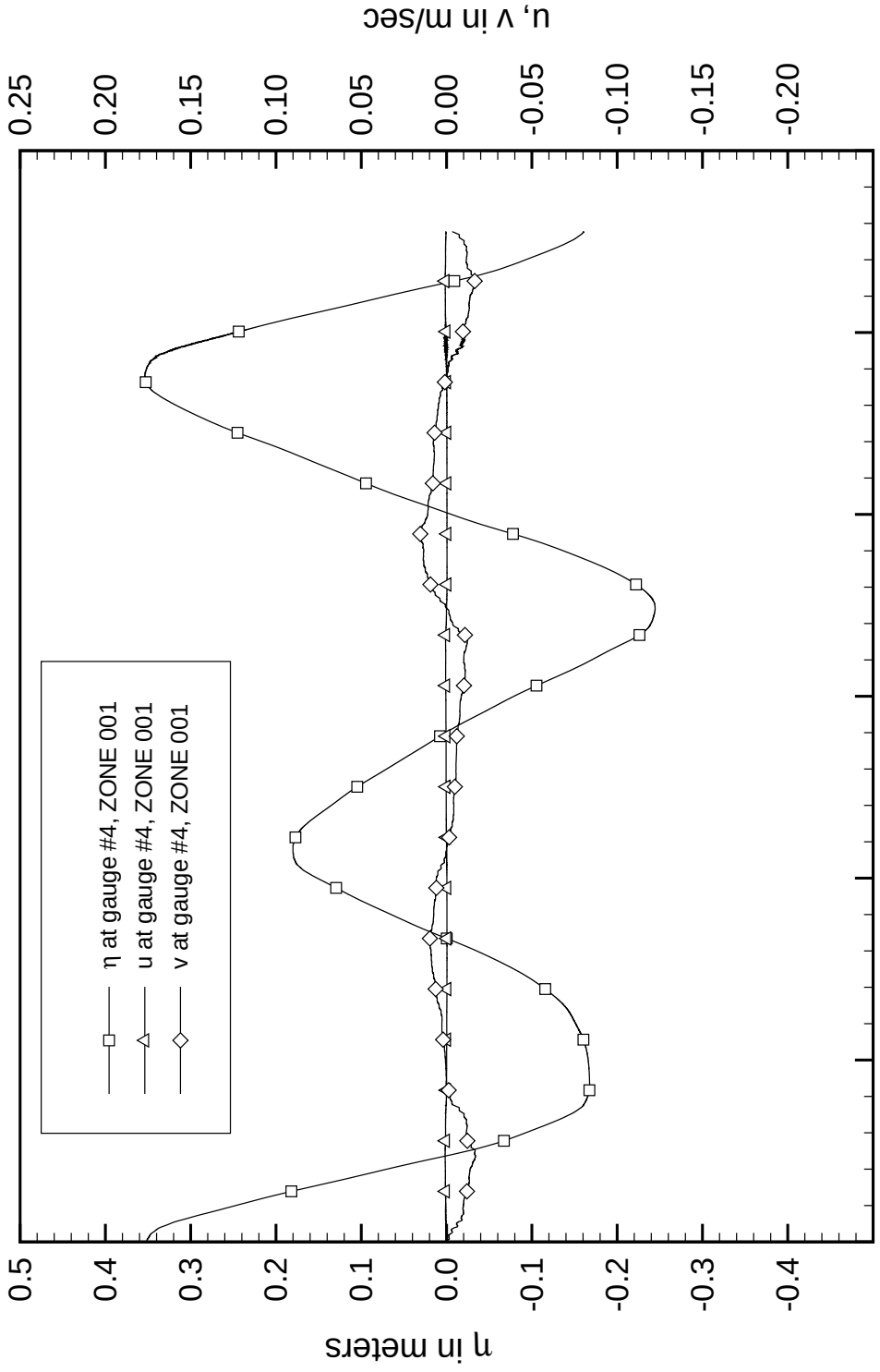

Fig. 39 Surface elevation and velocity components at gauge #4 (two sluice gates)

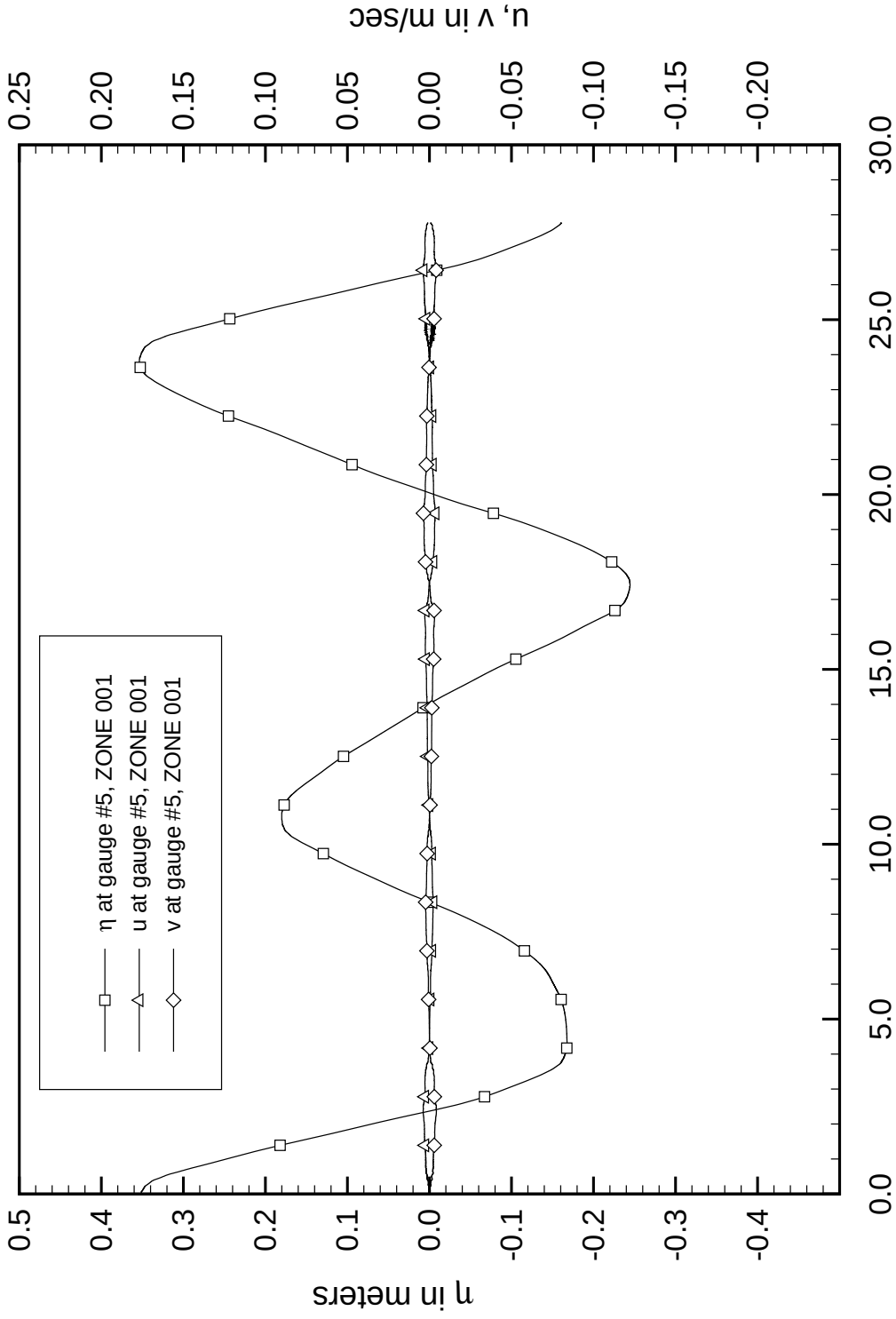

Fig. 40 Surface elevation and velocity components at gauge #5 (two sluice gates)

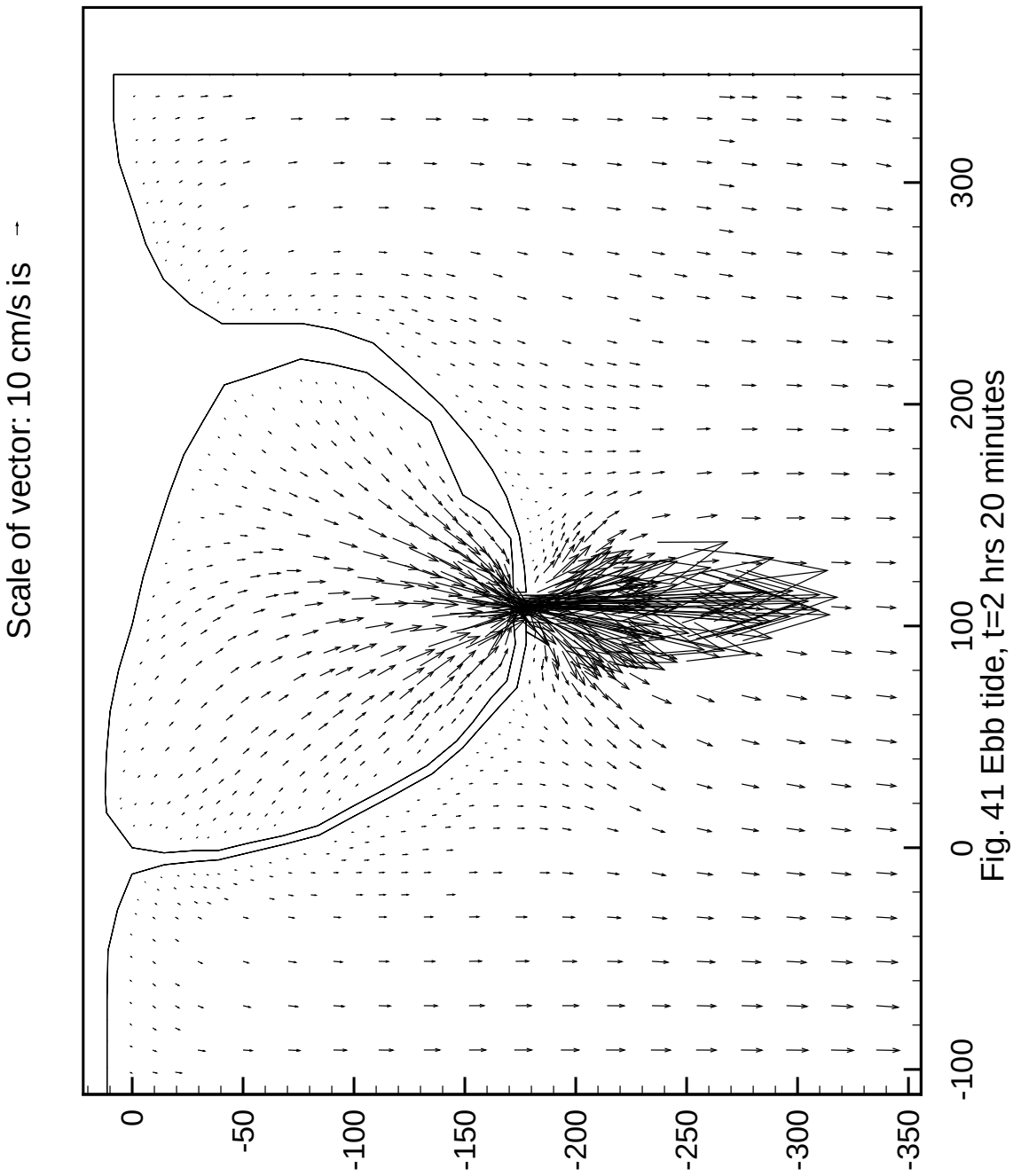

Fig. 41 Ebb tide, t=2 hrs 20 minutes

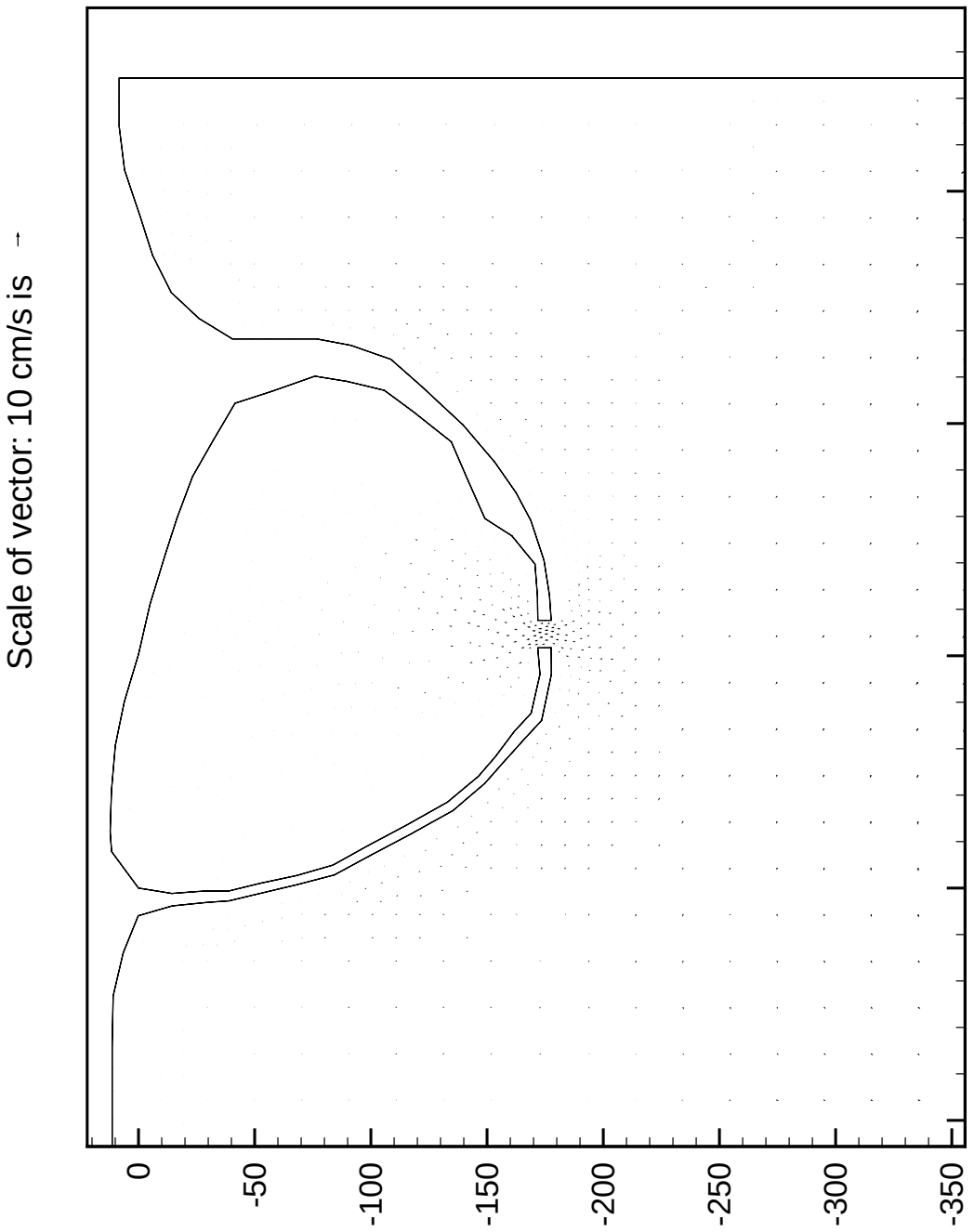

Fig. 42 Reversing tide, t=4 hrs 27 minutes

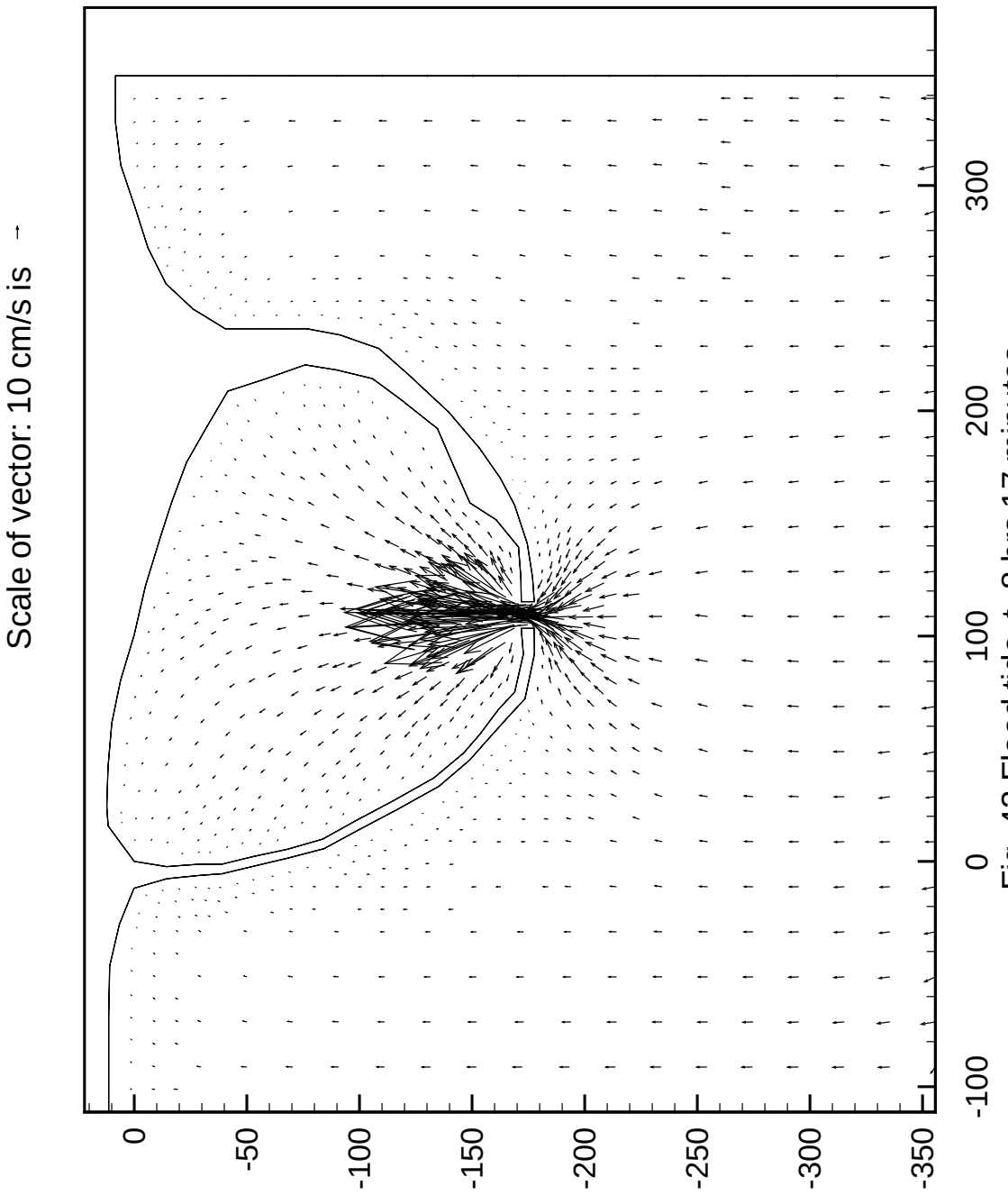

Fig. 43 Flood tide, t=8 hrs 17 minutes

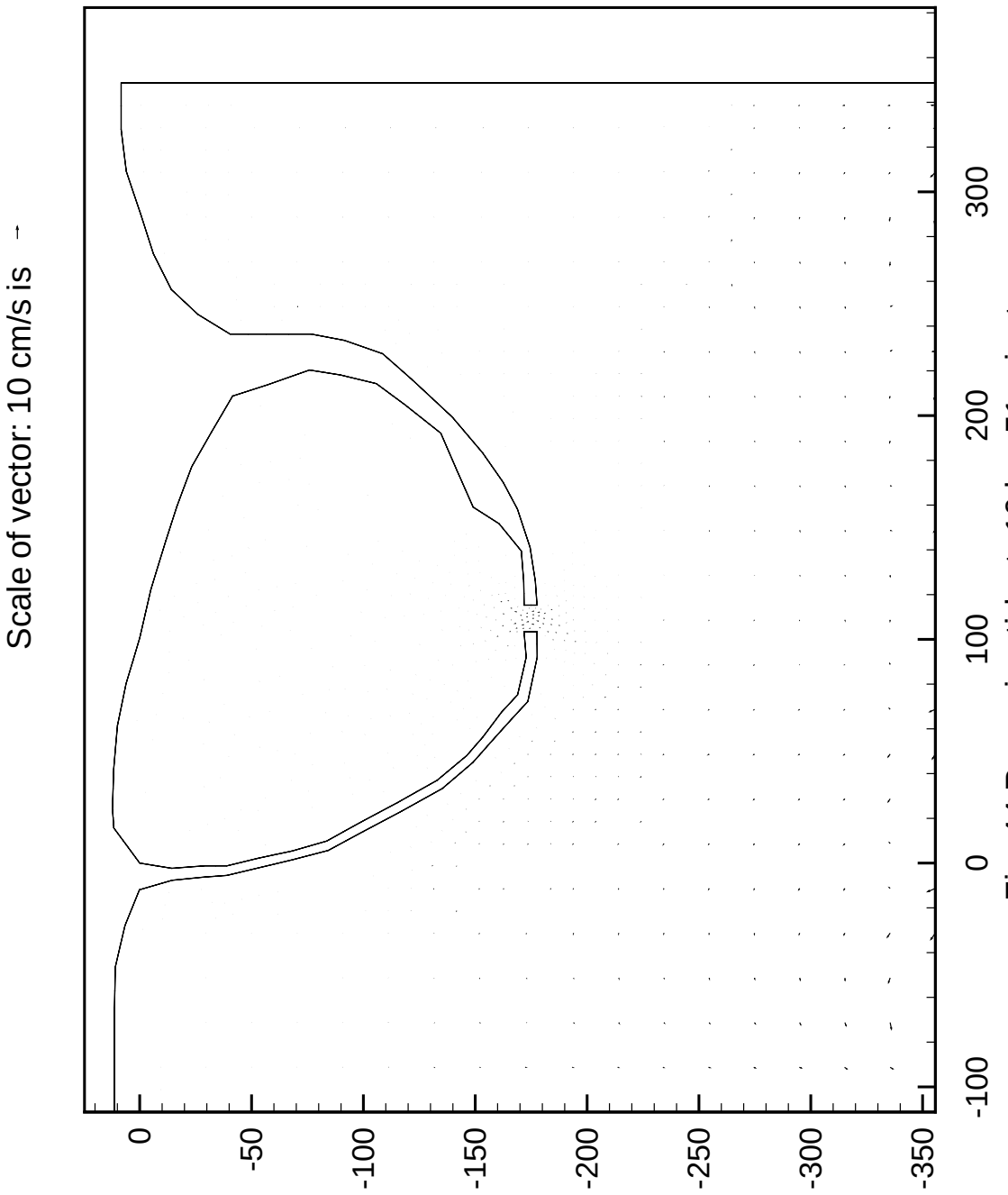

Fig. 44 Reversing tide, t=10 hrs 51 minutes

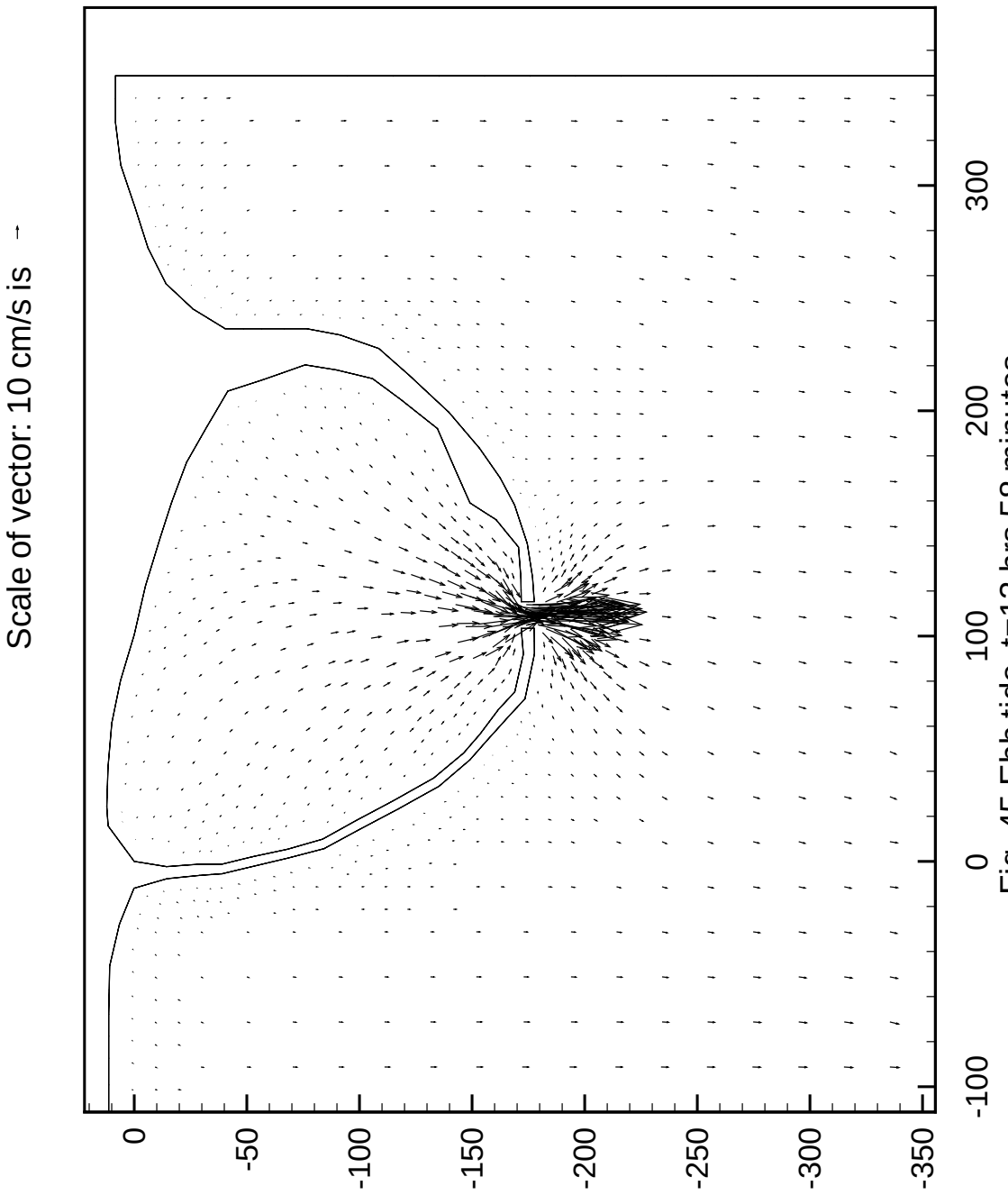

Fig. 45 Ebb tide, t=13 hrs 58 minutes

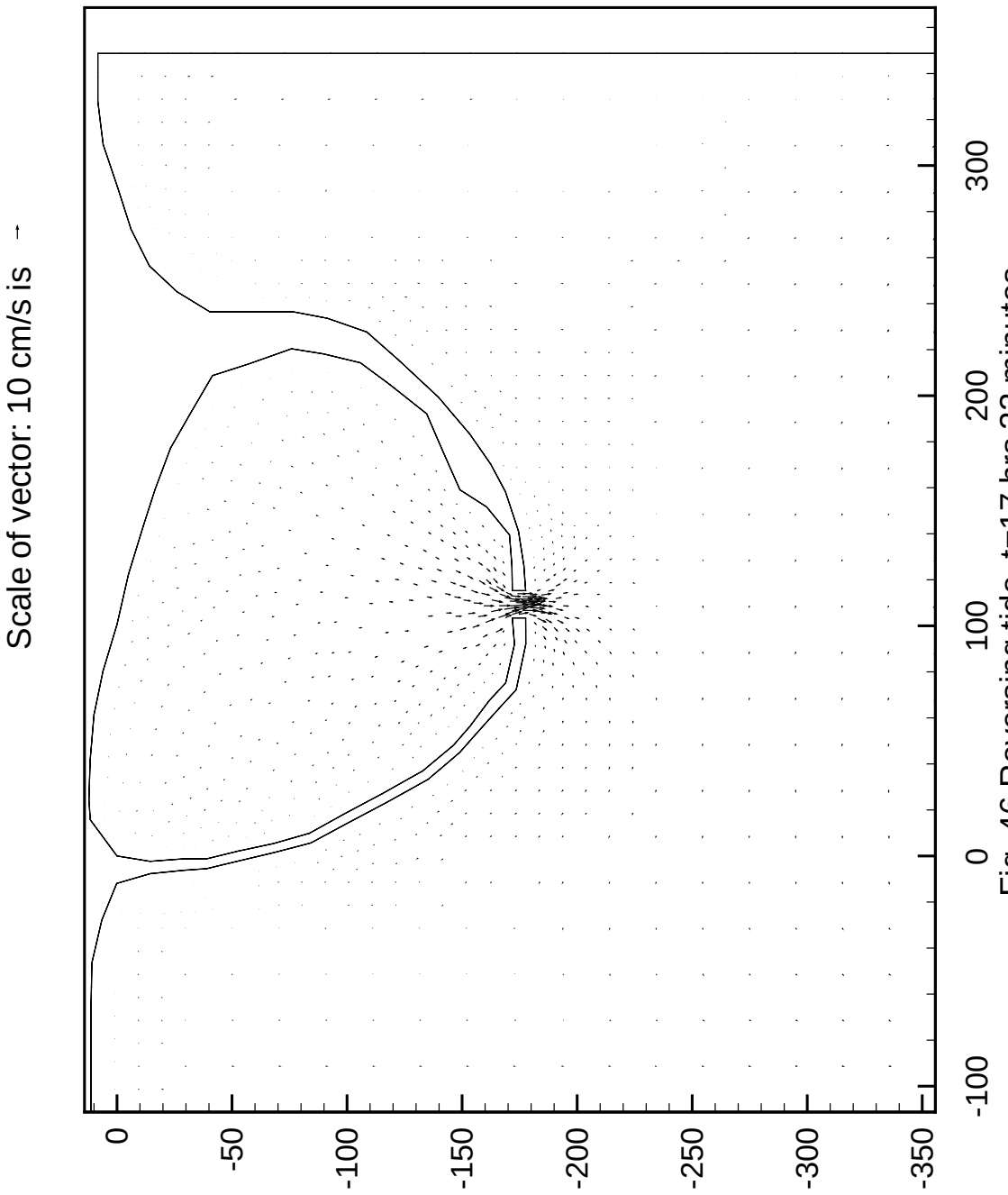

Fig. 46 Reversing tide, t=17 hrs 22 minutes

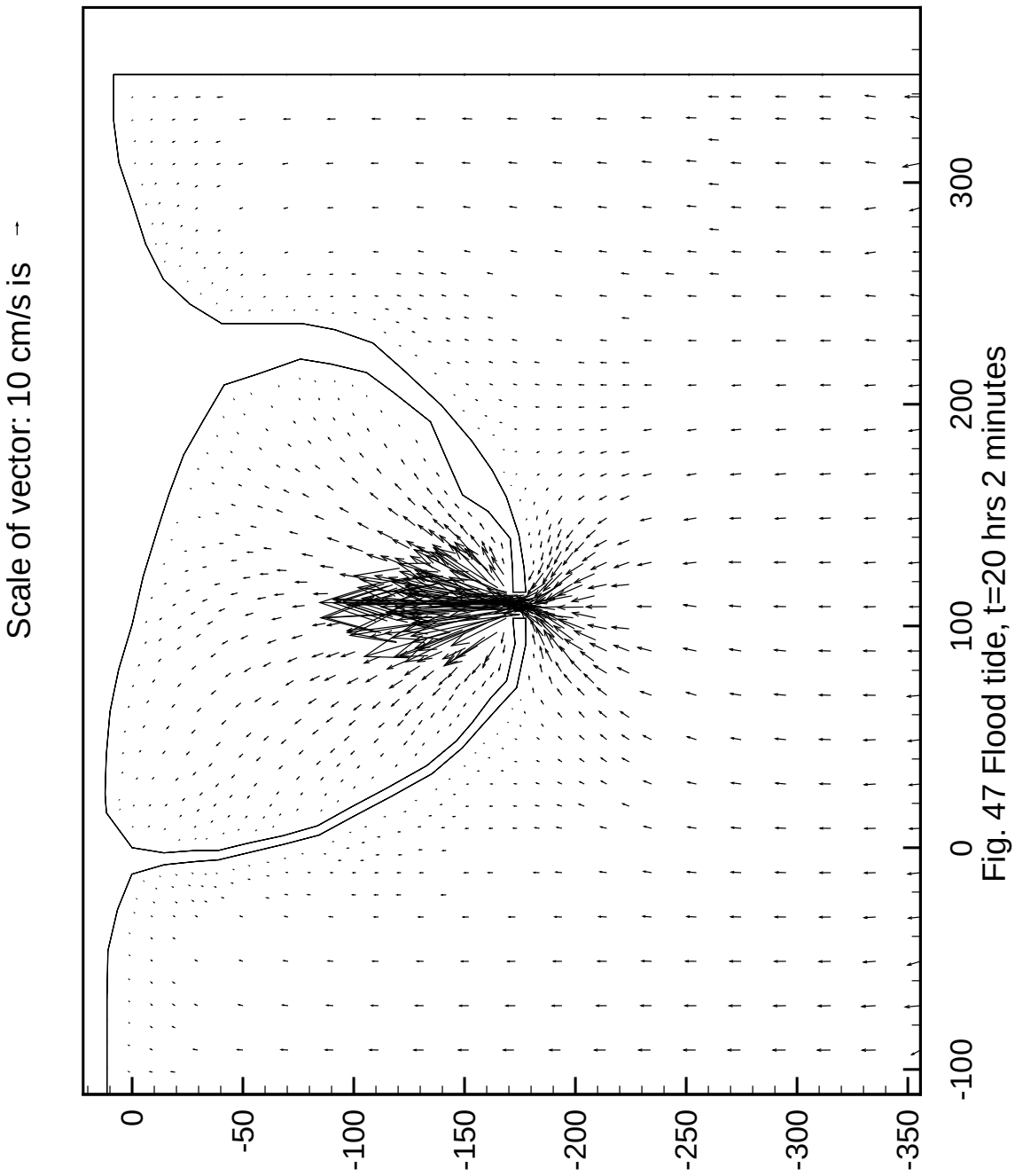

Fig. 47 Flood tide, t=20 hrs 2 minutes

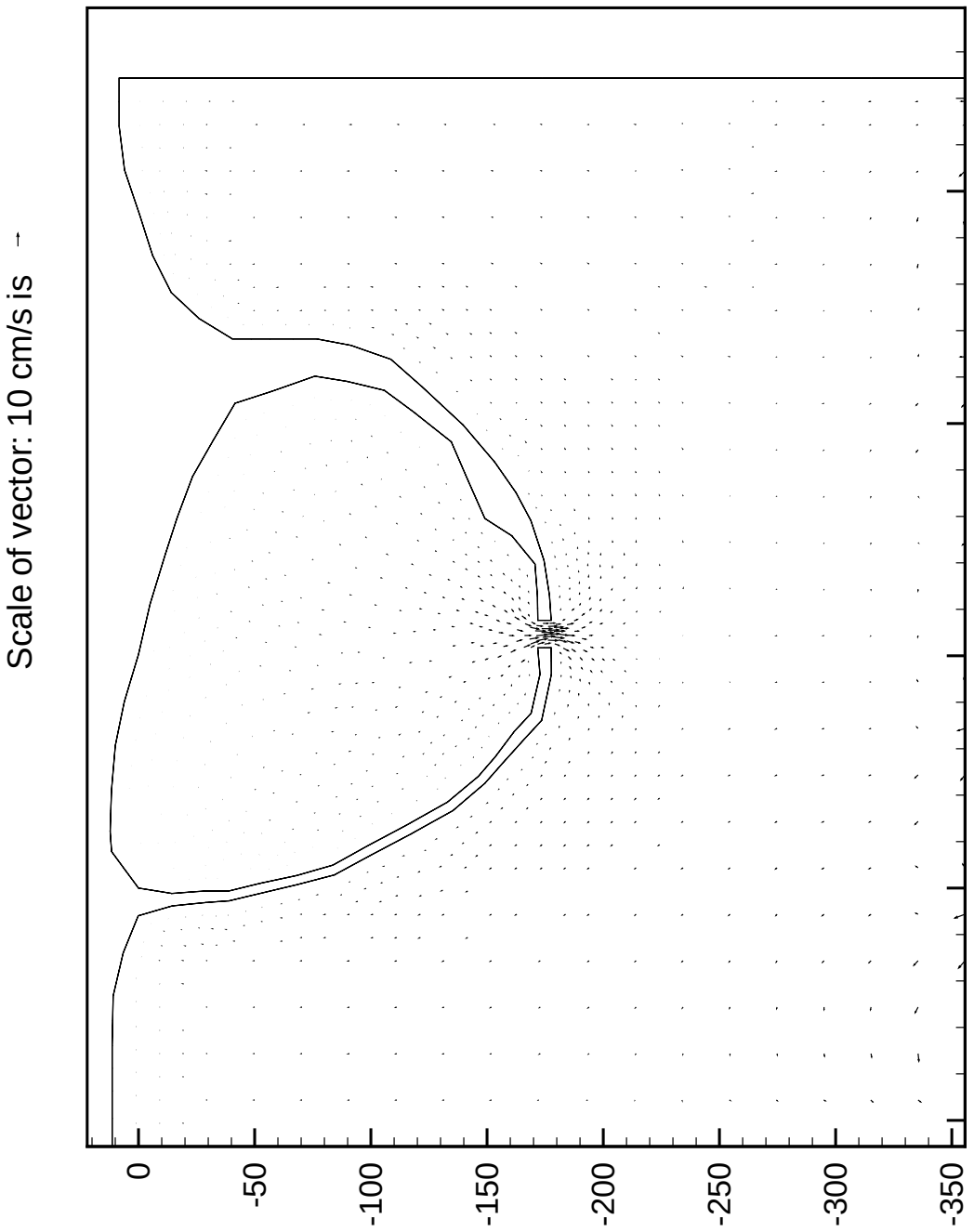

Fig. 48 Reversing tide, t=24 hrs 0 minutes

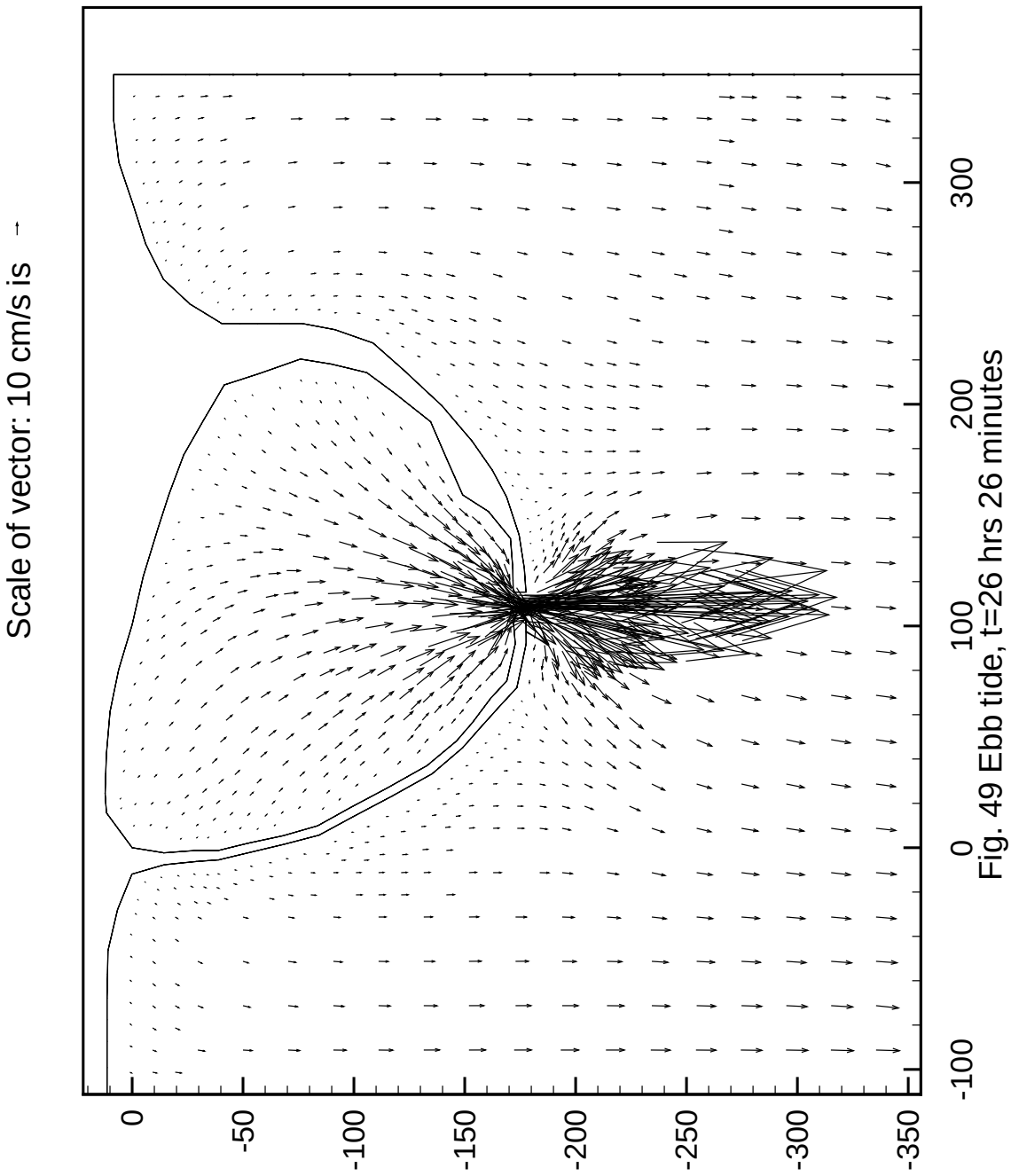

Fig. 49 Ebb tide, t=26 hrs 26 minutes

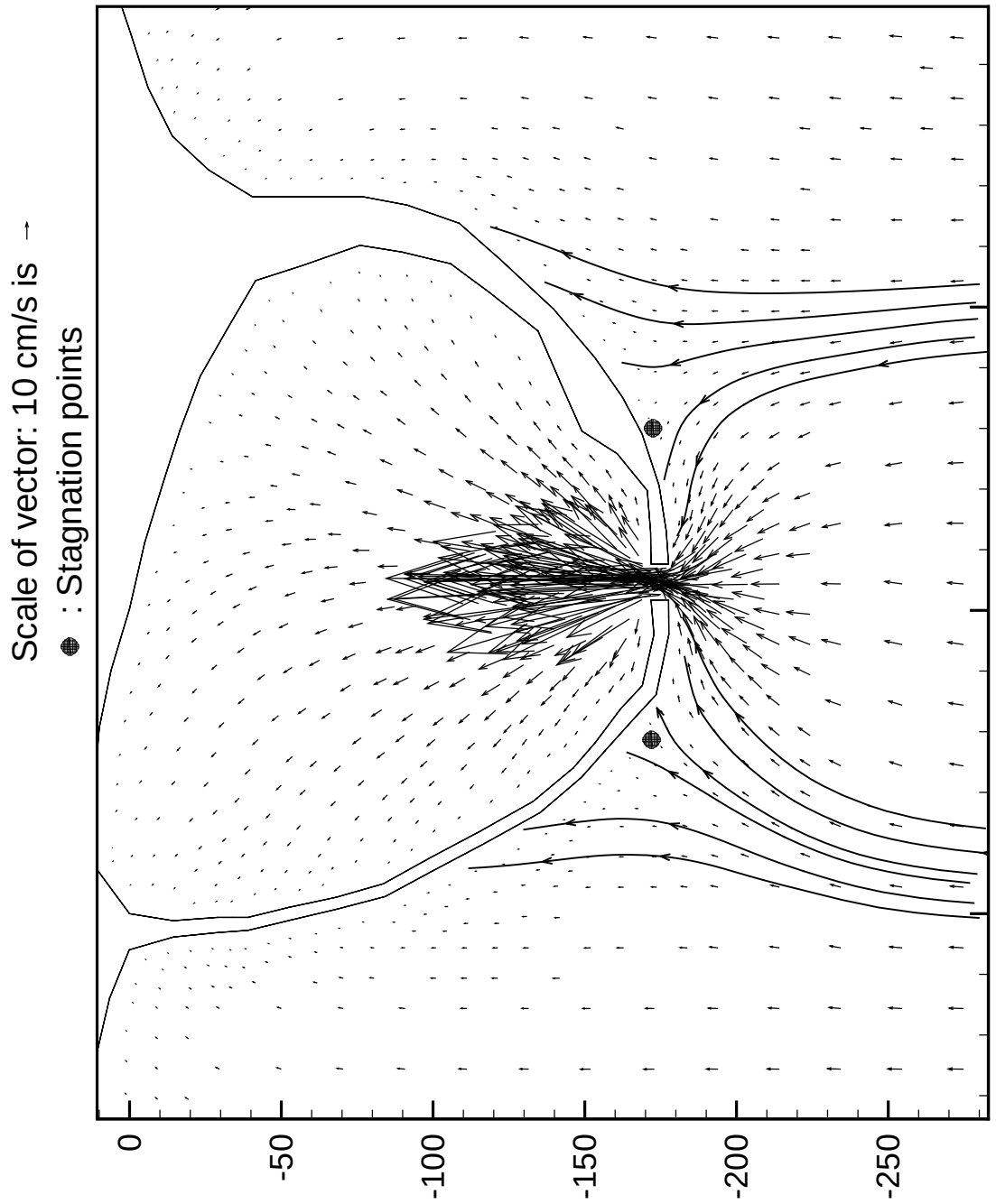

Fig. 50 Stagnation points at flood tide for one gate case

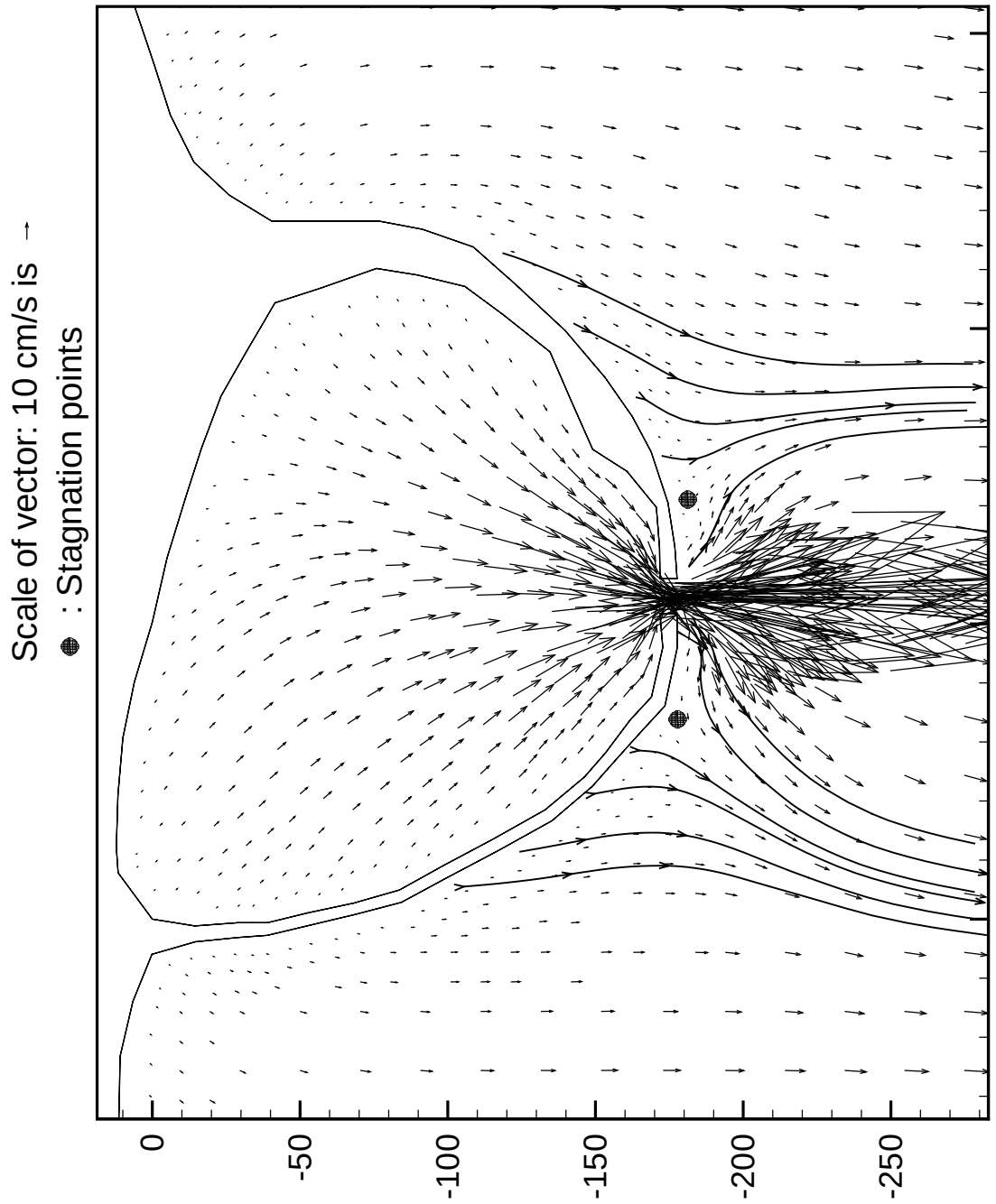

Fig. 51 Stagnation points at ebb tide for one gate case

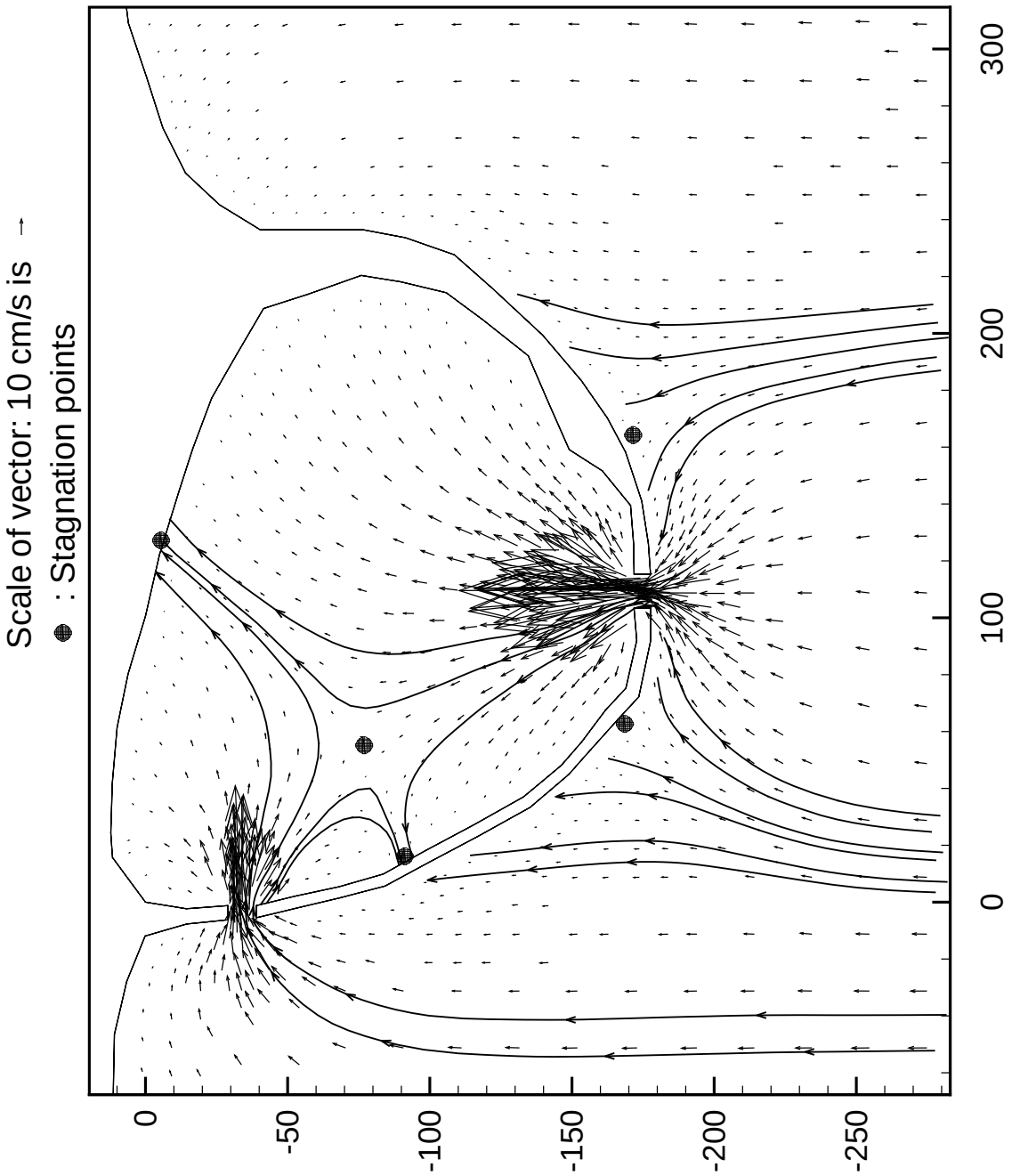

Fig. 52 Stagnation points at flood tide for two gate case

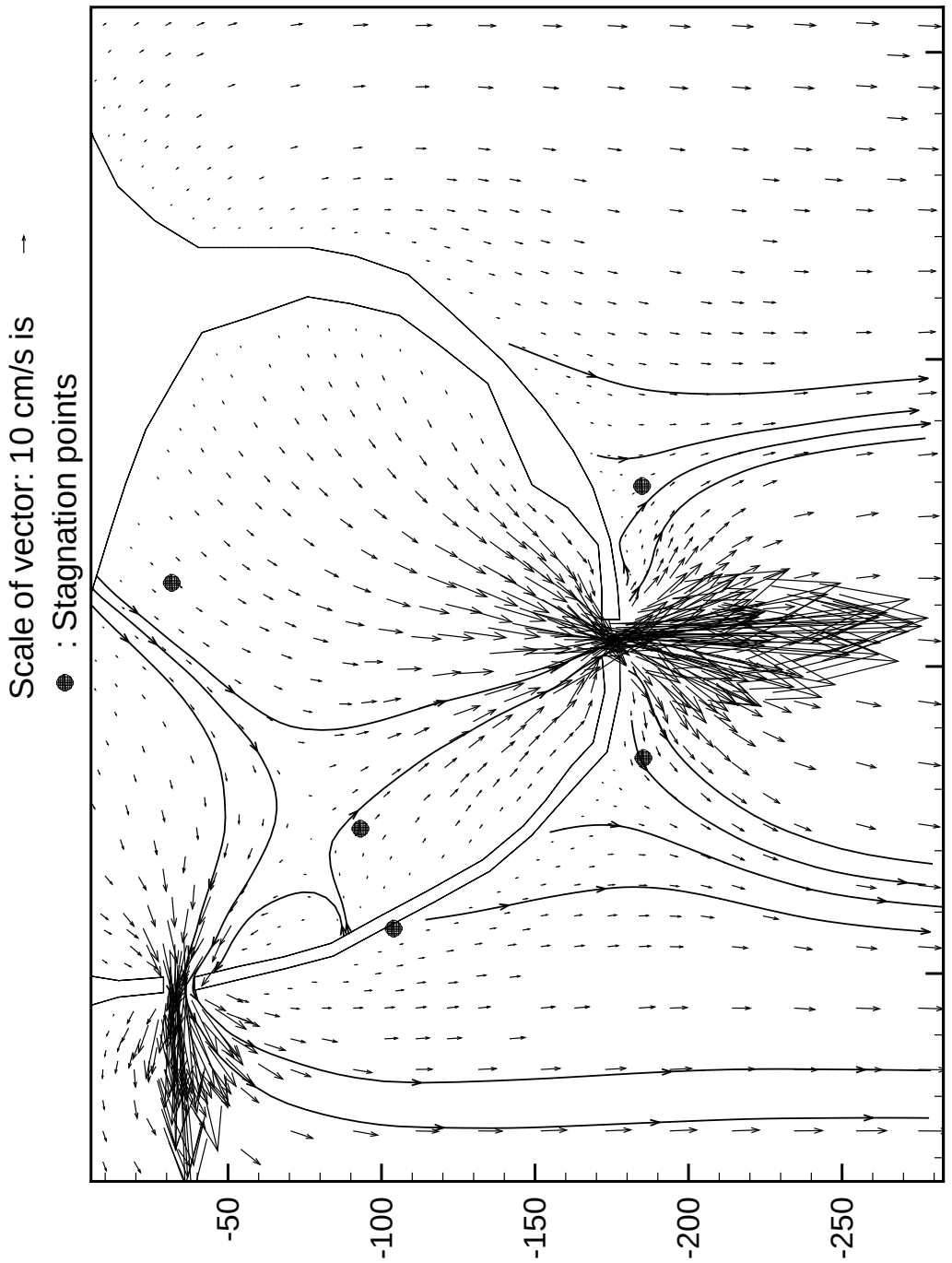

Fig. 53 Stagnation points at ebb tide for two gate case